EXPERIMENTATION AND INVESTIGATION OF OPTICAL-IRRADIATION-INDUCED SURFACE DAMAGE IN OPTICALLY NONLINEAR MATERIALS

Michael Bass, et al

Raytheon Company

Prepared for:

Air Force Cambridge Research Laboratories
Advanced Research Projects Agency

February 1973

AFCRL-72-0714

EXPERIMENTATION AND INVESTIGATION OF OPTICAL-IRRADIATION-INDUCED SURFACE DAMAGE IN OPTICALLY NONLINEAR MATERIALS

by
Michael Bass
David W. Fradin
Lowell H. Holway, Jr.

RAYTHEON COMPANY
RESEARCH DIVISION
WALTHAM, MASSACHUSETTS 02154

Contract No. F19628-70-C-0223

Project No. 4645
Task No. 464502
Work Unit No. 46450201

FINAL REPORT
FEBRUARY 1973

Contract Monitor: Dr. David Milam,
Optical Physics Laboratory

Sponsored by
Advanced Research Projects Agency
ARPA Order No. 1434 AMD #1

Monitored by
AIR FORCE CAMBRIDGE RESEARCH LABORATORIES
AIR FORCE SYSTEMS COMMAND
UNITED STATES AIR FORCE
BEDFORD, MASSACHUSETTS 01730

191R

ARPA Order No. 1434

Program Code No. 0D10

Contractor: Raytheon Company

Effective Date of Contract:
1 May 1970

Contract No. F19628-70-C-0223

Principal Investigator and Phone No.
Dr. Michael Bass/617 899-8400,
Ext. 2475

AFCRL Project Scientist and
Phone No. - Dr. David Milam
617 861-3898

Contract Expiration Date:
1 November 1972

Unclassified
Security Classification

DOCUMENT CONTROL DATA - R & D

(Security classification of title, body of abstract and indexing annotation must be entered when the overall report is classified)

1. ORIGINATING ACTIVITY (Corporate author)	2a. REPORT SECURITY CLASSIFICATION
Raytheon Co., Research Division 28 Seyon Street Waltham, Mass. 02154	Unclassified
	2b. GROUP N/A

3. REPORT TITLE

EXPERIMENTATION AND INVESTIGATION OF OPTICAL-IRRADIATION-INDUCED SURFACE DAMAGE IN OPTICALLY NONLINEAR MATERIALS

4. DESCRIPTIVE NOTES (Type of report and inclusive dates)

Final Report May 1, 1970 to October 31, 1972

5. AUTHOR(S) (First name, middle initial, last name)

Michael Bass
David W. Fradin
Lowell H. Holway, Jr.

6. REPORT DATE	7a. TOTAL NO. OF PAGES	7b. NO. OF REFS
February 1973	~~195~~ 191	101

8a. CONTRACT OR GRANT NO.	9a. ORIGINATOR'S REPORT NUMBER(S)
F19628-70-C-0223 ARPA Order No. 1434 b. PROJECT NO. 4645-02-01 c. DOD Element - 62403F d. DOD Subelement - 61101D	S-1505 9b. OTHER REPORT NO(S) (Any other numbers that may be assigned this report) AFCRL-72-0714

10. DISTRIBUTION STATEMENT

Approved for public release; distribution unlimited

Details of illustrations in this document may be better studied on microfiche.

11. SUPPLEMENTARY NOTES	12. SPONSORING MILITARY ACTIVITY
This research was supported by the Defense Advanced Research Projects Agency	Air Force Cambridge Research Laboratories (OP) L.G. Hanscom Field, Bedford, Mass.

13. ABSTRACT

Surface and unambiguous bulk damage to optically transparent materials have been studied both experimentally and theoretically. One of the most important conclusions reached to date is that the intrinsic laser-induced damage process is characterized by a probability for damage at each incident power density. This is in contrast to the previously held view that there was a threshold power density which divided damaging levels from those which would do no damage. A model for the damaging process, based on the probability measurements and electron avalanche breakdown, has been devised. In its simplest form, this model has successfully explained the most important properties of the measured damage probability in over 10 different materials. Electron avalanche breakdown, essentially in its dc limit, has been identified as the damaging interaction between 1.06 and 0.69 μm radiation and transparent alkali halide crystals. The first signs of deviation of the damage field from its dc value are found, however, at 0.69 μm. In general, the 0.69 μm damage field for a particular materials is greater than or equal to the damage field at longer wavelengths. Measurements of the distribution of breakdown starting times for several materials shown distinctly probabilistic characteristics. These properties are consistent with the computed distributions based on a model where an electron avalanche breakdown having statistical starting properties is the assumed damage process. Careful comparison of bulk and surface damage fields have shown them to be equal when the surface is free of polishing imperfections. When imperfections are present, the incident optical field is enhanced near the imperfections and so that measured surface damage field is reduced. Surface damage can be minimized, then, by obtaining imperfection-free finishes. Experimental techniques for making

DD FORM 1 NOV 65 1473 REPLACES DD FORM 1473, 1 JAN 64, WHICH IS OBSOLETE FOR ARMY USE.

I

Unclassified
Security Classification

14. KEY WORDS	LINK A		LINK B		LINK C	
	ROLE	WT	ROLE	WT	ROLE	WT
Laser damage Damage probability Electron avalanche breakdown Surface and bulk damage Inclusion damage Formative times Starting statistics						

Abstrast (Cont'd)

unambiguous bulk damage field measurements were developed where self-focusing and damage due to absorbing inclusions were eliminated. In developing these techniques an understanding of the experimental procedures, which led others to the erroneous conclusion that there is a damage threshold, was obtained. A theoretical treatment of the electron avalanche formation time, in which the Fokker-Planck equation in energy space was solved to find the electron distribution, was completed. The resulting estimates of the damage fields are in substantially better agreement with the experimental data than those obtained from "average electron energy" models.

AFCRL-72-0714 S-1505

EXPERIMENTATION AND INVESTIGATION OF OPTICAL-IRRADIATION-INDUCED SURFACE DAMAGE IN OPTICALLY NONLINEAR MATERIALS

by

Michael Bass, David W. Fradin and Lowell H. Holway, Jr.

Raytheon Company
Research Division
Waltham, Massachusetts 02154

Contract No. F19628-70-C-0223
Project No. 4645
Task No. 464502
Work Unit No. 46450201

Final Report

February 1973

Contract Monitor: David Milam,
Optical Physics Laboratory

Sponsored by
Advanced Research Projects Agency
ARPA Order No. 1434
Monitored by
Air Force Cambridge Research Laboratories
Air Force Systems Command
United States Air Force
Bedford, Massachusetts 01730

III

FOREWORD

This scientific report describes work performed under Contract No. F19628-70-C-0023 between 1 November 1971 and 31 October 1972. The report was assigned a Raytheon internal number S-1505.

Work was carried out at the Raytheon Research Division in Waltham, Massachusetts. The Principal Investigator was Dr. Michael Bass. David W. Fradin of Harvard University, working at Raytheon, was responsible for the studies of laser damage in alkali halide crystals. Dr. Lowell Holway contributed the theoretical analyses of electron distributions and avalanche formation times. The authors gratefully acknowledge the perserverance of D. Bua in designing the apparatus and in amassing the great quantities of data necessary for this work. The authors also wish to thank J. Geller of Photometrics, Inc., Lexington, Mass. for the excellent SEM micrographs. Useful discussions with Drs. Frank Horrigan and H.H. Barrett of Raytheon, Drs. David Milam and Erlan Bliss of AFCRL, and Dr. J. Khan of the Lawrence Livermore Laboratory are also acknowledged.

This report was submitted by the authors on 30 November 1972.

TABLE OF CONTENTS

TABLE OF CONTENTS (CONT'D)

TABLE OF CONTENTS (CONT'D)

TABLE OF CONTENTS(CONT'D)

LIST OF ILLUSTRATIONS

LIST OF ILLUSTRATIONS (CONT'D)

LIST OF ILLUSTRATIONS (CONT'D)

LIST OF ILLUSTRATIONS(CONT'D)

LIST OF TABLES

I. GENERAL INTRODUCTION

This program has been concerned with the problem of catastrophic damage to transparent optically nonlinear materials when irradiated with intense beams of light. In the course of these studies, however, several transparent materials which do not show second-order optical nonlinearities were also studied. The importance of the laser's transverse mode, of focusing conditions and of pulse waveform in determining both the residual damage morphology and the dynamics of damage formation have been demonstrated. Data has been obtained from ten different materials which show that there is no sharp threshold for the occurrence of damage, but rather that there exists some probability for the formation of damage over a wide range of incident intensities. These observations led to the development of a model of electron avalanche breakdown to describe the probabilistic phenomenon. In this model, the principal source of the damage statistics was assumed to be the statistics involved in starting the avalanche. The results and conclusions in this paragraph were described in Scientific Report No. 1 of this program.*

Measurements of the laser-induced surface damage process at both ruby and Nd:YAG laser wavelengths were obtained using experimental procedures which made direct comparison possible. These first directly comparable laser damage measurements showed that, in general, materials are harder to damage at 0.69 μm than at 1.06 μm. In addition, the relationship between damage probability and the optical electric field strength at 0.69 μm, though similar to that at 1.06 μm, suggests that for some materials different damage mechanisms may be operative at different optical frequencies.

The statistical nature of bulk damage was demonstrated in this program under experimental conditions which eliminated any confusion due to self-focusing or inclusion damage. These results are not subject

---

* M. Bass, H.H. Barrett and L.H. Holway, Jr., Scientific Report No. 1 for Contract No. F19628-70-C-0223, (February 1972).

to objections concerning either dust particles settling out of the air to give rise to damage statistics or focusing irregularities. They therefore lend strong support to the concept that the damage process itself has a probabilistic nature.

The probabilistic nature of the damage process at 1.06 and 0.69 μm was explored further by measuring the distribution of breakdown starting times for both bulk and surface damage. Two different experimental techniques were used to obtain this data and each yielded similar distributions. In one, a high-speed, image-converter streak camera was used to monitor both the arrival of light in the sample and the temporal evolution of the bright spark that accompanied the formation of damage. In the other, the breakdown starting time was taken to be the interval between the first measurable light signal transmitted through the sample and the occurrence of a very fast, well-defined attenuation of the transmitted light. Experiments had shown that such an attenuation was always correlated with a residual damage characteristic of damages caused by an intrinsic process.

For a particular laser pulse a threshold-like damage process would result in a very narrow distribution of breakdown starting times and would not include times after the peak of the pulse. In contrast, the measured distributions showed a large spread in starting times with the most likely time for breakdown occurring before the peak of the pulse. The distributions generally included some damages which started after the peak of the pulse.

The qualitative features of the distributions of breakdown starting times are given by the compound probability that breakdown occurs at a particular instant, given that it has not occurred before that time. A simple physical model for the damage probability per unit time based on the experimentally determined relation between damage probability and field was used to compute the distribution of starting

times for two different applied fields in fused quartz. The excellent agreement between this model and the experimental data shows that the two are consistent. This agreement therefore lends support to the avalanche breakdown model with statistics arising from the chance nature of starting an avalanche.

Measurements were made of intrinsic optical bulk breakdown in ten different alkali-halide crystals at 1.06 μm and in nine at 0.69 μm. By comparing the results to previously reported experiments conducted at 10.6 μm and at dc it was possible to identify the damage mechanism as electron avalanche breakdown. At 1.06 μm the process appears still to be in its dc limit but at 0.69 μm some evidence for departure from the dc form is noted.

The measurements of bulk damage reported in this program were the first of their kind — unambiguous measures of the damaging interaction between light and transparent media. This was possible because experimental procedures were used which eliminated any confusion due to self-focusing or absorbing inclusions. Self-focusing was controlled by restricting the probe powers to well below the critical powers for catastrophic self-focusing. Damage from inclusions was identified by its morphology and irregular manner of attenuating the transmitted light.

A comparison of laser-induced damage on the surfaces and in the volume of transparent media was made in which the role of surface finish quality was demonstrated. The data showed that if the electric field E can cause bulk damage with a probability p_B or entrance surface damage with probability p_S then

$p_B = p_S$ for surfaces free of polishing imperfections

and

$p_B < p_S$ for conventionally finished surfaces.

The ratios of the applied fields which cause equal bulk and surface damage probability for three different materials with conventionally finished surfaces were determined. The concept of electric field enhancement at certain types of polishing imperfections was used to explain the measured ratios.

Several points of compatibility between the probabilistic and threshold-like interpretations of laser damage were analyzed during this program. Among the most important is the influence of the size of the irradiated volume on the experimental data and thus on one's interpretation. It was shown that only by irradiating a small volume can one generally avoid irradiating an absorbing inclusion. Damage due to such inclusions would appear as a threshold-like process. In addition, when the volume irradiated is large it was shown that the interval in power density over which the probability is less than unity can be so small that it is not observed experimentally. Other experimental procedures which can erroneously lead to a threshold-like result were explained.

In parallel with these, mainly experimental efforts, an effort to analyze the temporal growth of an electron avalanche was maintained. A Fokker-Plank equation in energy space was used to calculate the value of the rate of avalanche growth as a function of applied field. When this growth rate is such that a damaging avalanche could form within the pulse duration, one could say that a damaging field had been reached. These computations give results for sapphire which are only about a factor of three larger than experimental values. "Average electron" theories give results which differ from experiment by nearly an order of magnitude.

Since the results of this program were of general interest, several papers were prepared and submitted for publication in the open literature. Each of these papers covers one or more areas of

major effort and so are included in this report. The paper "Laser-Induced Damage Probability at 1.06 and 0.69 μm" in Sec. II describes the comparison of surface damage at 1.06 and 0.69 μm and the qualitative properties of the distributions of breakdown starting times. It also includes a discussion of the compatibility between the probabilistic and threshold-like points of view. In Sec. III statistics in bulk damage and the technique for identifying intrinsic damage events are described in the paper entitled, "Surface and Bulk Laser Damage Statistics and the Identification of Intrinsic Breakdown Processes." This paper contains the comparison between computations based on our statistical-electron avalanche breakdown model of the intrinsic damage process and the measured distributions of bulk breakdown starting times. Bulk breakdown measured in the absence of self-focusing is described in Sec. IV in the paper "Confirmation of an Electron Avalanche Causing Laser-Induced Bulk Damage at 1.06 μm." This paper explains the technique for avoiding self-focusing, includes a discussion of the electron avalanche breakdown damage mechanism and in its appendices presents a review of self-focusing theory. Section V is concerned with the avalanche breakdown mechanism at 0.69 μm and the possibility that at this high frequency the process is no longer in its dc limit. Our tests of the effect of surface finish quality on the surface damage field are described in Sec. VI in the paper "A Comparison of Laser Induced Surface and and Bulk Damage." Section VII consists of the theoretical breakdown field computations for sapphire. Some results and analyses which were not included in these papers are given in Sec. VIII and our principal results are summarized in Sec. IX. We have also included in Appendix A a discussion of a simple techniques for longitudinal mode selection developed for the damage experiments.

II. LASER INDUCED DAMAGE PROBABILITY AT 1.06 AND 0.69 μm

A. Introduction

This section consists of a paper entitled "Laser Induced Damage Probability at 1.06 and 0.69 μm." The first direct comparison of damage in transparent media produced by ruby and Nd:YAG lasers is described. These studies show that a material is less likely to damage when subjected to a particular optical field at 0.69 μm than at 1.06 μm. Comparison of the 0.69 μm data with that recorded at 1.06 μm also shows that the relationship between the damage probability, p_1, and the applied optical electric field strength, E, though still generally of the form $p_1 \propto \exp(-K/E)$, has changed to a greater degree than predicted by a very simplified avalanche breakdown model. In fact, for at least two materials studied, K is so large at 0.69 μm that the damage process at this wavelength might properly be characterized by a well-defined threshold field. The inadequacies of the simplified optical-frequency avalanche-breakdown model are discussed and the possibility that more than one damage mechanism may be operative is examined in view of the experimental data.

Experiments are described in which a very fast image-converter streak camera was used to study the distribution of starting times for 1.06 μm laser-induced surface breakdowns. If the breakdown or damage process were completely described by a well defined threshold, then this distribution should be very narrow and no breakdowns should occur after the laser field reached its maximum. The data, however, shows broad distributions, particularly when the applied field is such that $p_1 < 1$. In all cases the most probable time for breakdown is before the time of maximum field, though some breakdowns do occur later. The properties of the measured distributions are described by the compound probability that breakdown occurs at a particular instant, given that it has not occurred before that time and, as such, are added evidence for the probabilistic interpretation of the 1.06 μm damage process.

Several connections between the probabilistic and threshold-like interpretations of laser induced damage are also discussed. It is shown that these two points of view are not totally incompatible. The possibility that fluctuations in the laser pulse which were not detected experimentally caused the statistical nature of the damage data is considered. We show experimentally, however, that such fluctuations were not present.

B. LASER-INDUCED DAMAGE PROBABILITY AT 1.06 AND 0.69 μm*†

Michael Bass and Harrison H. Barrett
Raytheon Research Division
Waltham, Massachusetts 02154

ABSTRACT

The first directly comparable measurements of the laser-induced surface damage process at both ruby and Nd:YAG laser wavelengths are reported. The most striking feature of the data is that all the materials studied are harder to damage at 0.69 μm than at 1.06 μm. The probabilistic nature of the laser-induced damage process at 1.06 μm was explored further by measuring the distribution of breakdown starting times with an image-converter streak camera. The observed distribution is described by the compound probability that breakdown occurs at a particular time, given that it has not occurred before that time. In addition, several connections between the probabilistic and threshold-like interpretations of laser-induced damage are discussed. It is shown that these points of view are not totally incompatible.

---

* This research was supported by the Advanced Research Projects Agency of the Department of Defense and was monitored by the Air Force Cambridge Research Laboratories under Contract No. F19628-70-C-0223.

† This paper was presented at the Fourth Laser Damage Symposium at Boulder, Colorado, June, 1972.

1. INTRODUCTION

The first direct comparison of damage in transparent media produced by ruby and Nd:YAG lasers was performed using experimental techniques described previously.[1] These studies have shown that a material is less likely to damage when subjected to a particular optical field at 0.69 μm than at 1.06 μm. Comparison of the 0.69 μm data with that recorded at 1.06 μm also shows that the relationship between the damage probability, p_1, and the applied optical electric field strength, E, though still generally of the form $p_1 \propto \exp(-K/E)$, has changed to a greater degree than predicted by a very simplified avalanche breakdown model.[1,2] In fact, for at least two materials studied, K is so large at 0.69 μm that the damage process at this wavelength might properly be characterized by a well defined threshold field. The inadequacies of the simplified optical-frequency avalanche-breakdown model[1,2] are discussed and the possibility that more than one damage mechanism may be operative is examined in view of the experimental data.

A very fast image-converter streak camera was used to study the distribution of starting times for 1.06 μm laser-induced surface breakdowns. If the breakdown or damage process were completely described by a well defined threshold, then this distribution should be very narrow and no breakdowns should occur after the laser field reached its maximum. The data, however, shows broad distributions, particularly when the applied field is such that $p_1 < 1$. In all cases the most probable time for breakdown is before the time of maximum field, though some breakdowns do occur later. The properties of the measured distributions are described by the compound probability that breakdown occurs at a particular instant, given that it has not occurred before that time and, as such, are added evidence for the probabilistic interpretation of the 1.06 μm damage process.

Several connections between the probabilistic and threshold-like interpretations of laser induced damage are also discussed. It is shown that these two points of view are not totally incompatible. The possibility that fluctuations in the laser pulse which were not detected experimentally caused the statistical nature of the damage data is considered. We show experimentally, however, that such fluctuations were not present.

2. COMPARISON OF RUBY AND Nd:YAG LASER INDUCED DAMAGE

a. Experiments

An examination of the available literature reveals that due to variations in experimental conditions there are no directly comparable published results for 0.69 and 1.06 μm laser induced damage. In the experiments described below the same sample was studied at both wavelengths. Self focusing was eliminated by studying surface damage only and the critical laser beam parameters were carefully held constant as shown in Table I. Under these conditions and using a slightly modified version of the experimental techniques described previously[1] directly comparable laser damage data was obtained.

The general experimental arrangement of Ref. 1 was modified as shown in Fig. 1. The laser focusing optics was unchanged but an automated pulse monitoring and damage detection system was installed. One pen of the dual-pen chart recorder was driven with a signal proportional to the laser pulse energy and the other pen monitored the intensity of a beam of light transmitted through the region which was exposed to the laser pulses. This arrangement was sensitive to the appearance of surface damage craters ~ 0.003 cm in diameter and ~ 2000Å deep, the smallest damage observed by earlier monitoring techniques.[3] A typical recording, derived from this arrangement, is shown in Fig. 2 where a ruby laser at ≈ 9 GW/cm^2 was used to irradiate an x-cut crystalline quartz sample. Note the ± 10 percent laser pulse energy variation. The first pulse to strike the sample is marked with an arrow and the 99th pulse, marked with a star, is the one which produced damage. This is indicated by the sharp reduction in the transmitted monitor intensity. The laser trigger signal was picked up by the photomultiplier and so resulted in a fiducial marker on the record of the transmitted light intensity.

TABLE I

LASER PARAMETERS

Wavelength	Nd: YAG 1.06 μm	Ruby 0.694 μm
Energy TEM_{00} Mode	1.5 mJ	2.0 mJ
Beam Diameter at Output Mirror TEM_{00} Mode	0.8 mm	0.7 mm
Polarization	Linear	Linear
Pulse Repetition Rate	1 pps	1 pulse/5 sec
Pulse Duration in TEM_{00} Mode	4.7 nsec (FWHP)	14 nsec (FWHP)
Pulse-to-Pulse Energy Reproducibility	$\pm$ 7%	$\pm$ 10%

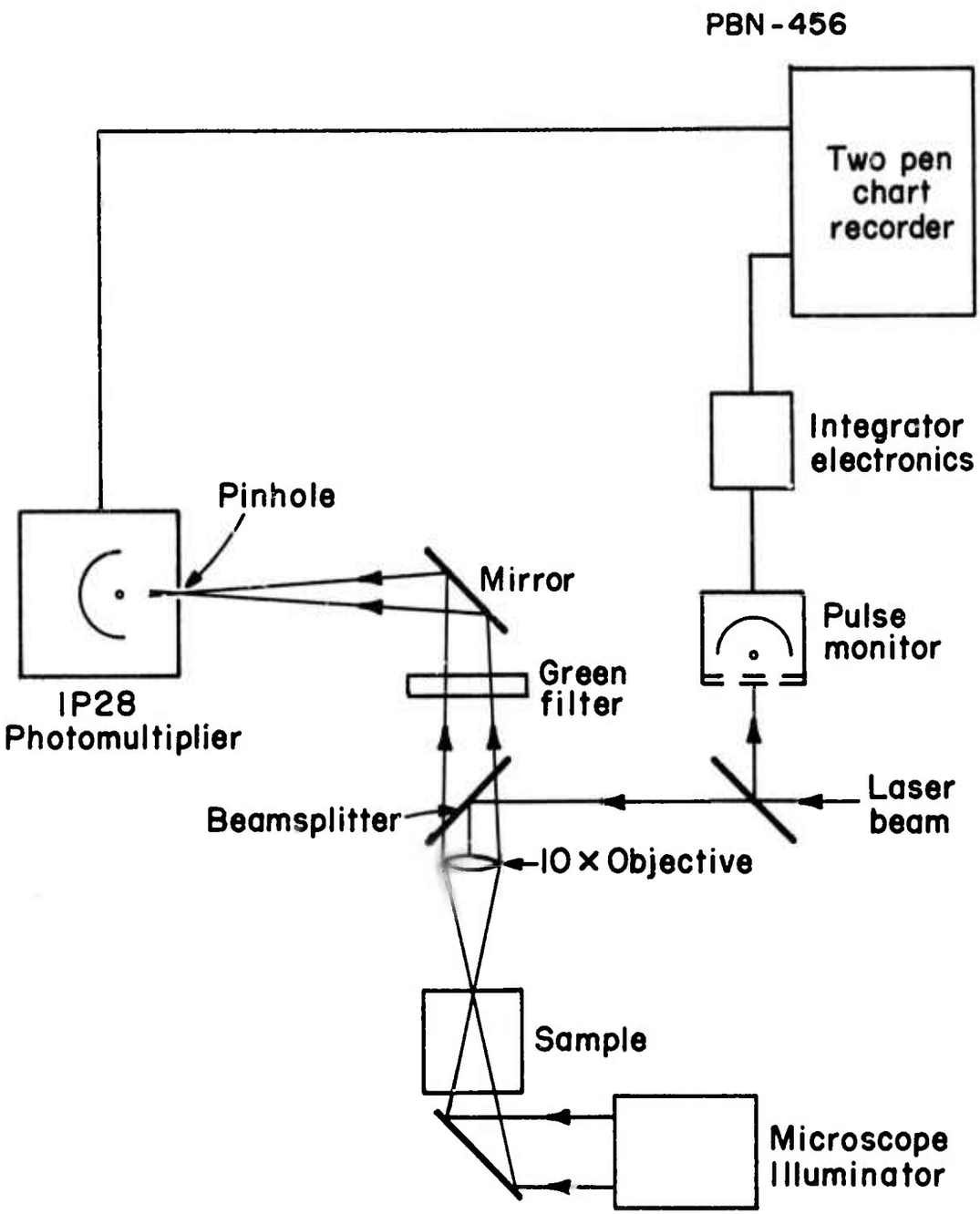

Fig. 1 Schematic Diagram of Automatic Pulse and Damage Monitoring Apparatus.

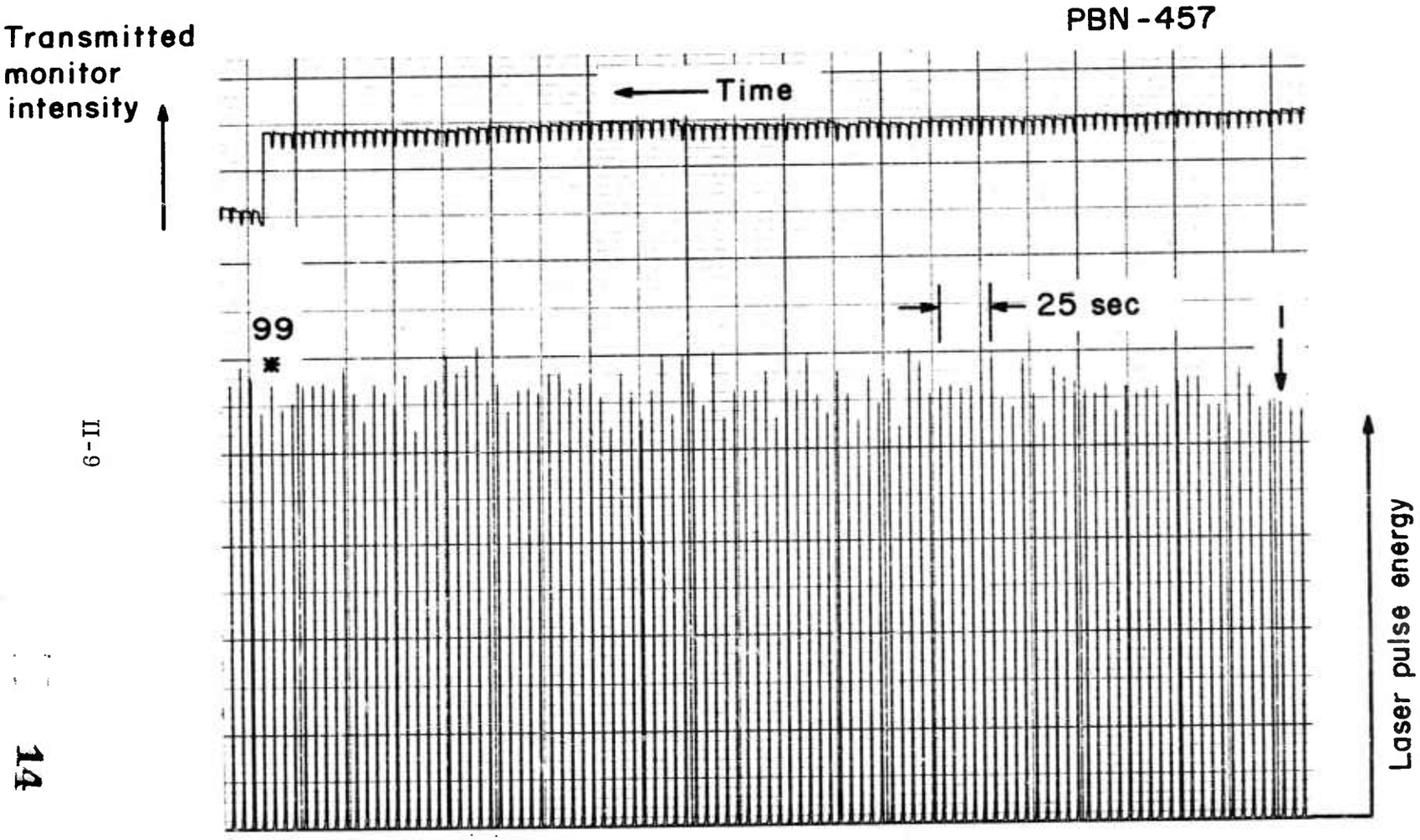

6-II

Fig. 2 Record of Exposures of X-Cut Crystalline Quartz to Pulses of Ruby Laser Light ~ 9 GW/cm^2.

The data in Fig. 2 shows that at this level of irradiation the sample does not have to damage when exposed to any particular pulse. In fact, preceding the damaging pulse (no. 99), there were several more energetic pulses which, according to the "threshold point of view," should have been the ones to cause damage.

The data in Fig. 3, while similar to that in Fig. 2, show the improved pulse-to-pulse energy reproducibility of the ruby laser achieved by more careful tuning of the laser cavity components. Alignment of the flat, parallel rod faces with the cavity mirrors was found to be critical. Proper rod alignment was always accompanied by a dramatic smoothing of the pulse waveform as recorded by a high-speed photodiode and a 519 oscilloscope. Figure 4 shows this effect for the TEM_{00} ruby laser. Similar results were obtained by aligning the Nd:YAG rod in its laser cavity.

The detection of a smooth pulse by a limited bandwidth detector may be the result of either single-frequency output or the simultaneous oscillation of many randomly phased modes. In order to resolve this question the lasers' output spectra have been studied with Fabry-Perot interferometers. The lasing bandwidth narrowed significantly as the rod was aligned to achieve smoother pulses. Unfortunately, our interferometers lacked sufficient finesse to resolve individual laser cavity modes ($\Delta\nu \approx 300$ MHz). The longitudinal mode content of a perfectly smooth laser pulse can be inferred, however, by combining the interferometer and pulse waveform data. The observed interferometer limited bandwidth of a smooth ruby laser pulse was ≈ 1.5 GHz, implying that a maximum of ~ 5 modes could have been oscillating. Since the photodiode-oscilloscope combination could detect frequencies as high as ~ 3 GHz, the presence of five oscillating modes would have been detected through the presence of mode beating as in Fig. 4b. Therefore, our perfectly smooth ruby laser pulses, as shown in Fig. 4c, were caused by single longitudinal mode lasing. In support of this

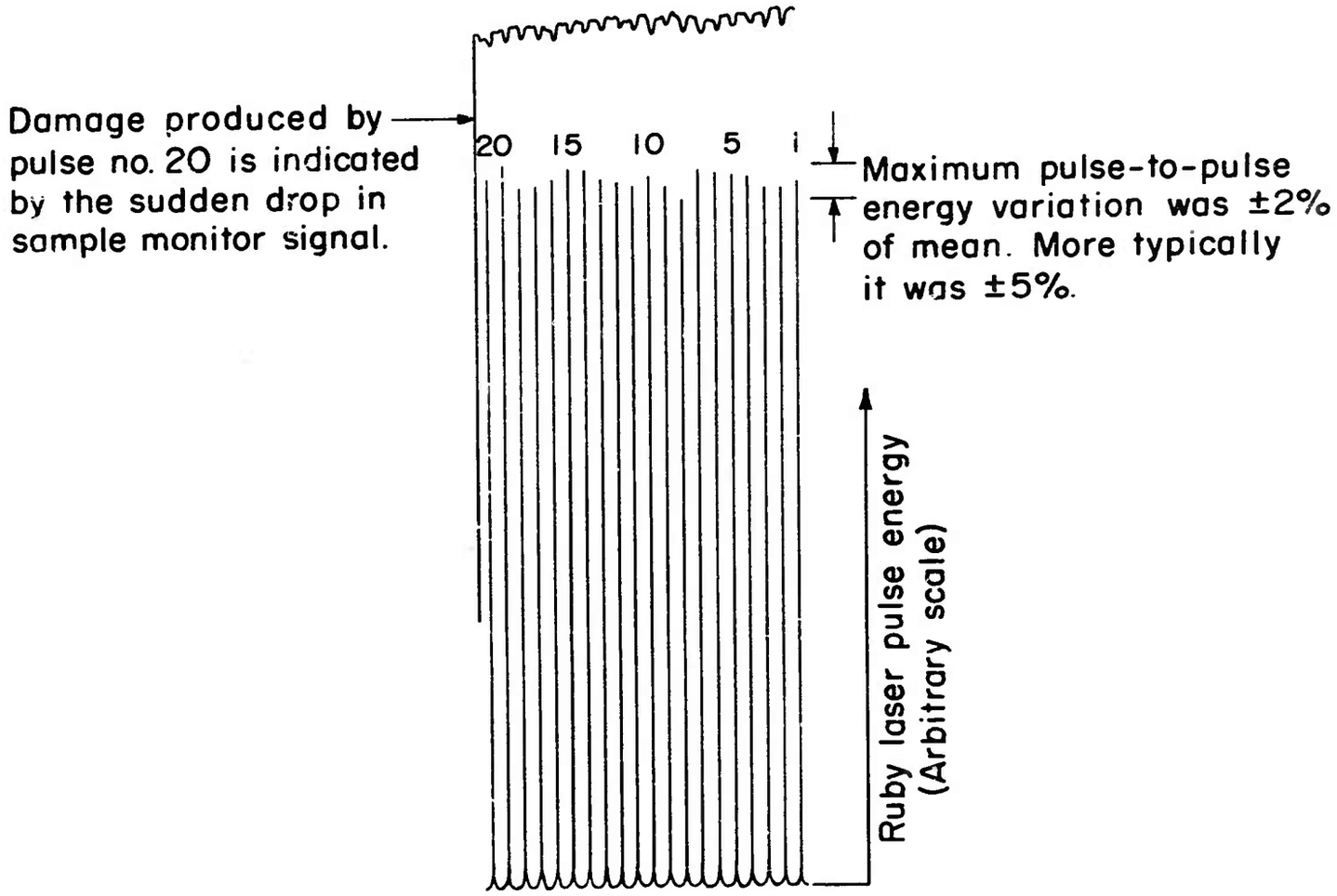

Fig. 3 Ruby Laser Energy Recording Showing Best Pulse-to-Pulse Stability.

(a)

(b)

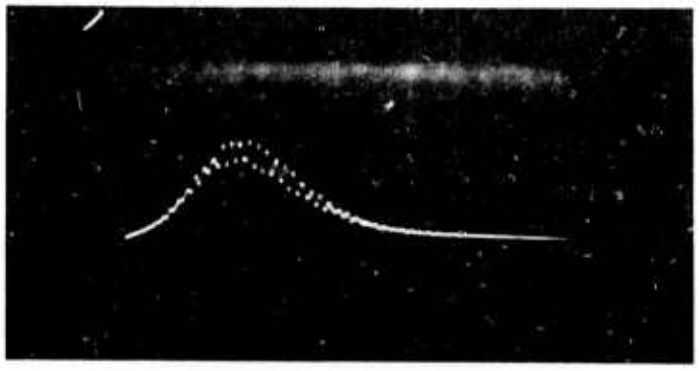

(c)

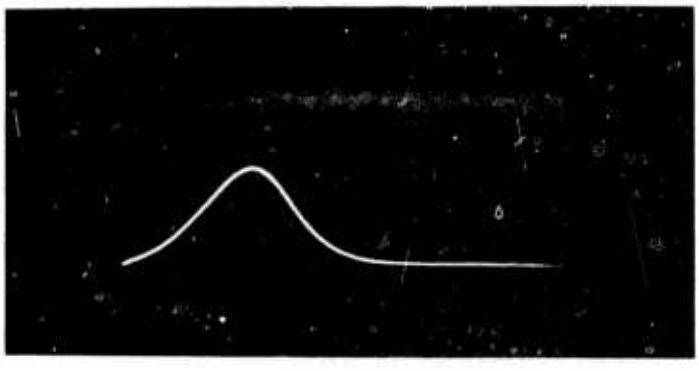

10 ns

Fig. 4 Effects of Rod Alignment on Output Pulses for Q-Switched Ruby.
(a) Rod badly misaligned
(b) Rod coarsely aligned
(c) Cavity finely tuned

conclusion we note that Giuliano et al.[4] reported that perfectly smooth pulses correspond to single mode oscillation while non-smooth waveforms were always associated with two or more oscillating modes.

Single longitudinal mode oscillation is generally obtained by placing and intracavity resonator in the laser with sufficient finesse to limit the number of modes.[4] In the present experiments intracavity resonators were created by aligning the plane parallel faces of the laser rods with the plane parallel cavity mirrors as shown in Fig. 5. The finesse of each of the indicated resonators is very low because the rod faces were antireflection coated for less than 0.25 percent reflectivity at the laser wavelength. However, when lasing occurs, resonators M_1-A, B-A, and A-M_2 contain a medium with gain. Thus the effective reflectivity of the rod face in these resonators is increased and so is the effective finesse. Resonator M_1-A which includes the 100 percent reflecting laser cavity mirror has the highest finesse and is felt to be responsible for limiting the number of oscillating modes. For example, in the ruby laser, we used a 10 cm long rod with a gain coefficient of $\approx 0.25\ cm^{-1}$,[5] resulting in an effective finesse of ~ 6.

The possibility that subnanosecond fluctuations in the laser field during a single pulse which were not detected by the photodiode-oscilloscope combination caused the statistical nature of the damage data had been suggested.[6] However, the study of the frequency content of the smooth laser pulses showed that the experimental data given here and in Refs. 1 and 2 was obtained with a single longitudinal mode laser pulse or, at worst, with one containing only a few oscillating modes. Therefore, such fluctuations could not have been present and could not have been the source of the form of the damage data. In addition, the data for $SrTiO_3$ in Ref. 1 covers a range in power of 36 to 1 and fluctuations of this magnitude in a laser pulse would certainly have been noticed.

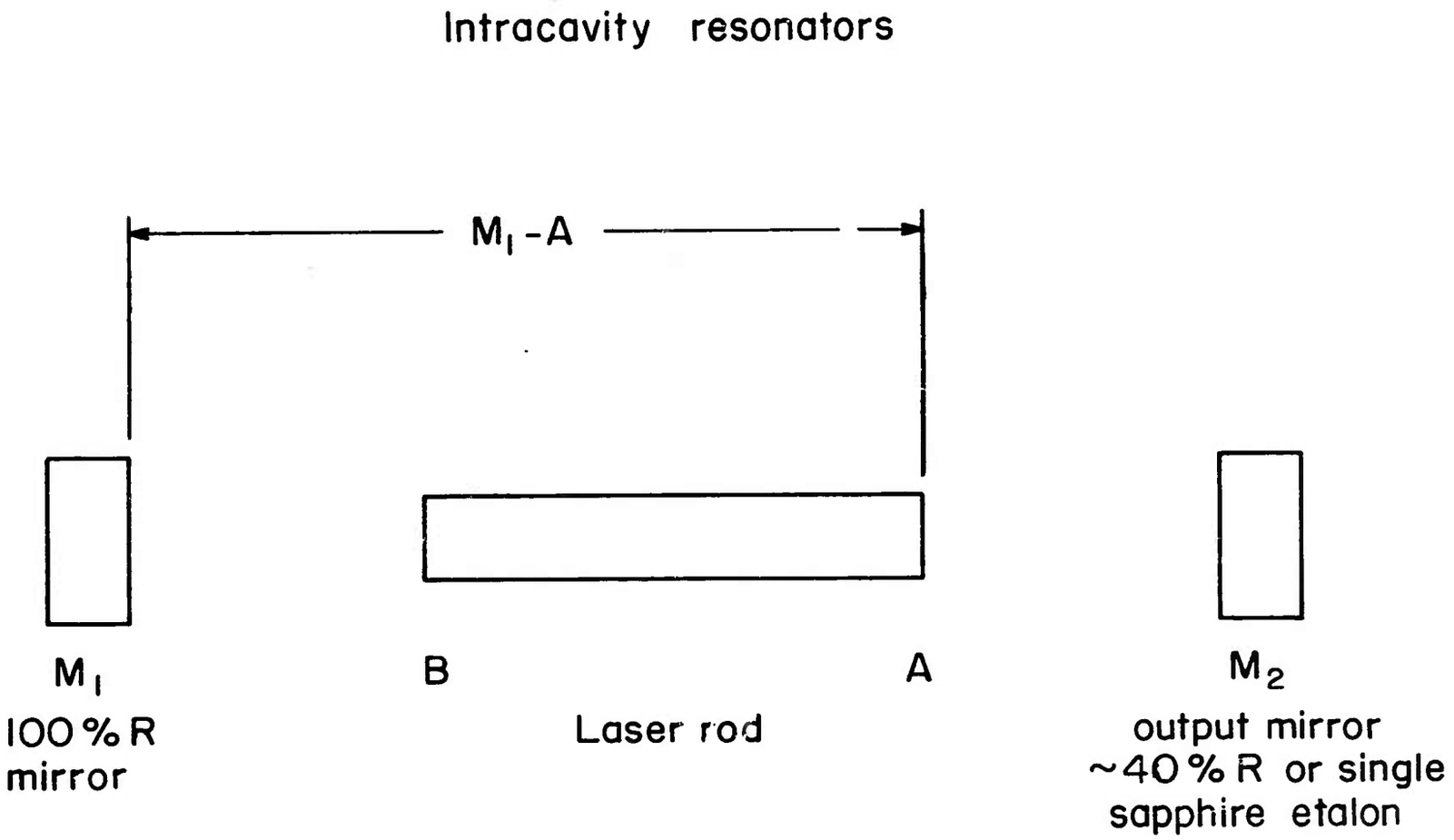

Fig. 5 Schematic Diagram of a Laser Cavity Showing Potential Mode Selecting Intracavity Resonator.

Using the smooth-pulse, reproducible lasers the damage data for 0.69 and 1.06 μm summarized in Table II was obtained. As shown therein the lowest power density required to always produce damage in a single pulse, P_1, is generally higher at 0.69 μm than at 1.06 μm. In addition, the quantity K in the relation

$$p_1 \propto \exp(-K/E) \qquad (1)$$

is larger for ruby irradiation.

b. Discussion

In Refs. 1 and 2 a model for the damage mechanism based on electron avalanche breakdown was proposed for two main reasons: 1) It gave the experimentally observed relation between damage probability and optical electric field; and 2) It did not require material properties inconsistent with transparent, insulating dielectrics. This model was fashioned on the assumptions that the statistics of the avalanche breakdown process were largely determined by the first one or two ionizations and that the fraction of collisions which the accelerating electron could make and remain acceptably in phase with the optical field, f, was independent of electron energy. It was also assumed that the collision rate, τ_{coll}^{-1} was independent of electron energy. In this very simplified model, in contrast to the data, K has a weak dependence on the optical frequency and large changes in P_1 are not predicted. However, because of the successes of the avalanche breakdown mechanism mentioned above a re-examination of its dependence on optical frequency is in order. The very speculative discussion which follows is presented only because it agrees with the most important experimental facts and in order to stimulate interest in further theoretical study of the avalanche breakdown process in optical frequency fields.

TABLE II

COMPARISON OF DAMAGE PROPERTIES AT 1.065 m AND 0.6943 m

	$K(10^8$ V/M)		P_1 (GW/cm^2)	
Laser Wavelength (μm)	1.0645	0.6943	1.0645	0.6943
X-Cut Crystal Quartz	33.0	60.5	5.4	20.2
KDP	28.5	92.8	16.6	27.6
$LiNbO_3$	16.6	> 200	11.1	11.1
$LiIO_3$	7.1	16.3	2.8	3.9
$SrTiO_3$*	8.7	> 500	0.8	15.3

* This $SrTiO_3$ was sample No. 2 and was cut from a different boule than the one used in Refs. 1 and 2.

If, as in our simplified model, the steps in the avalanche are all highly likely after the first one or two, then the statistics of these early steps will dominate and the process will appear probabilistic. This formulation is conceptually identical to that used in the analysis of the statistical variations of the output pulse height from photomultipliers used with scintillator detectors.[7] If, on the other hand, the probability for each step in the avalanche is the same, damaging avalanches will not be possible until a field is applied which is large enough to make the probability for each step near unity. In this case the process will appear threshold-like.

Consider the sequence of events whereby an electron in an optical field is accelerated to ionizing energies. Since the field direction reverses periodically the electron must undergo collisions at the proper times to be able to efficiently extract energy from the field. At low energies inelastic optical phonon collisions dominate the electron-lattice interaction[8] and are, in effect, a frictional force on the electron's motion. This means that there is some "friction barrier" to the electron's energy which is determined by the energy range over which optical phonon interactions dominate. At higher energies elastic collisions with acoustic phonons dominate and it is much easier for the electron to accelerate further to ionizing energies. Therefore electrons with initial energies greater than this "friction barrier" can dominate the avalanche process.

Now assuming an electron reaches the ionization energy, ϵ_I, it cannot undergo an ionizing interaction until it gains some additional energy since the ionization cross section is zero at ϵ_I. The probability for ionization, however, increases rapidly with electron energy.[9] Ionization is most likely to occur, then, when there is a substantial excess energy over ϵ_I, with this extra energy divided between the two ionization products. If the energy of these products exceeds the "friction barrier" then they can be more easily accelerated to produce

the next step in the avalanche and so on for each succeeding step until damage occurs. The ionization products dominate the avalanche. On the other hand, if the excess energy is small, the ionization products may have energies less than the "friction barrier" and be virtually indistinguishable from the rest of the free electrons. Each step in the avalanche then must follow the same course as the first, requiring large fields to produce damage.

In Figs. 6 and 7 the 1.06 and 0.69 μm electric field required to accelerate an electron to a particular energy is plotted. The curves are numbered according to the number of half cycles of the field required to accelerate the electron to that energy assuming an optimally lucky collision occurs each time the field reverses. This number is also the number of collision which must occur if the electron is to continue to accelerate. For example, 12 collisions are required to reach the curve labeled 13. Perfectly lucky collisions are those which exactly reverse the electron momentum. The results show that in a Nd:YAG laser field and electron will gain more energy through fewer collisions than if the same field were due to a ruby laser. Both the collision rate, τ_{coll}^{-1}, and f decrease with increasing electron energy. In fact, above 2-4 eV the cross section for acoustic phonon scattering is strongly peaked in the forward direction which means that "lucky" collisions at high energies are very unlikely.[8] Thus, since fewer collisions are required, the energy of an electron in a 1.06 μm field which causes ionization will, in general, be further in excess of ϵ_I than when ionization is caused by a 0.69 μm field. In the 1.06 μm field then the ionization products have less of a "friction barrier" to clear than in the latter and an avalanche can proceed with high probability. In the 0.69 μm case the ionization products are less distinguishable from other free electrons and an avalanche may not develop. Larger fields should then be necessary to produce ionization at 0.69 μm and the mechanism of producing a damaging avalanche should exhibit higher K value or be more threshold-like than at 1.06 μm.

PBN-72-475

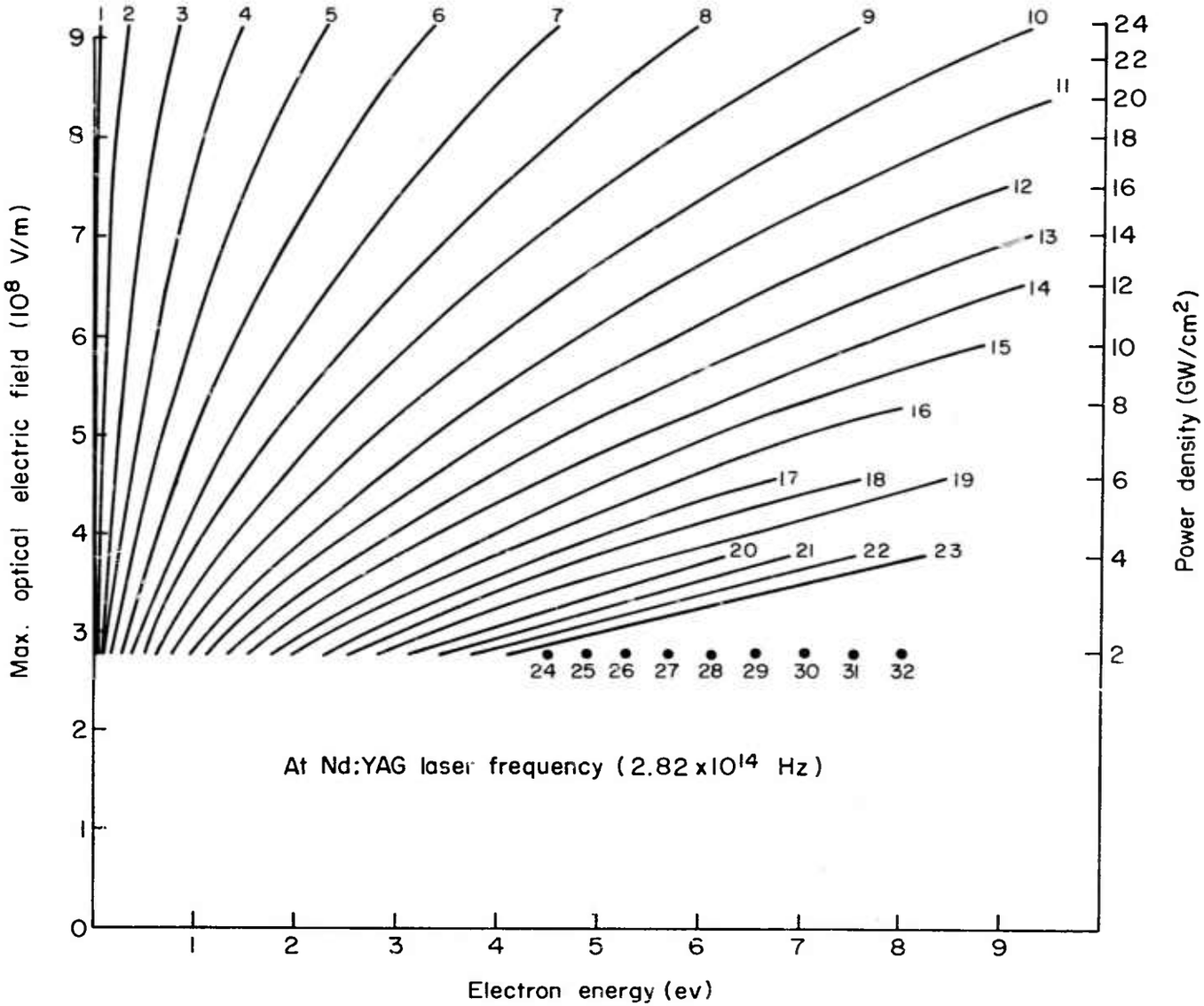

Fig. 6 Electric Field at 1.06 μm Required to Accelerate an Electron to a Particular Energy. Each curve is numbered according to the number of half cycles of the field required to accelerate the electron assuming only perfectly lucky collisions occur. The number then is also the number of the collision which must occur for the electron to continue to gain energy from the field.

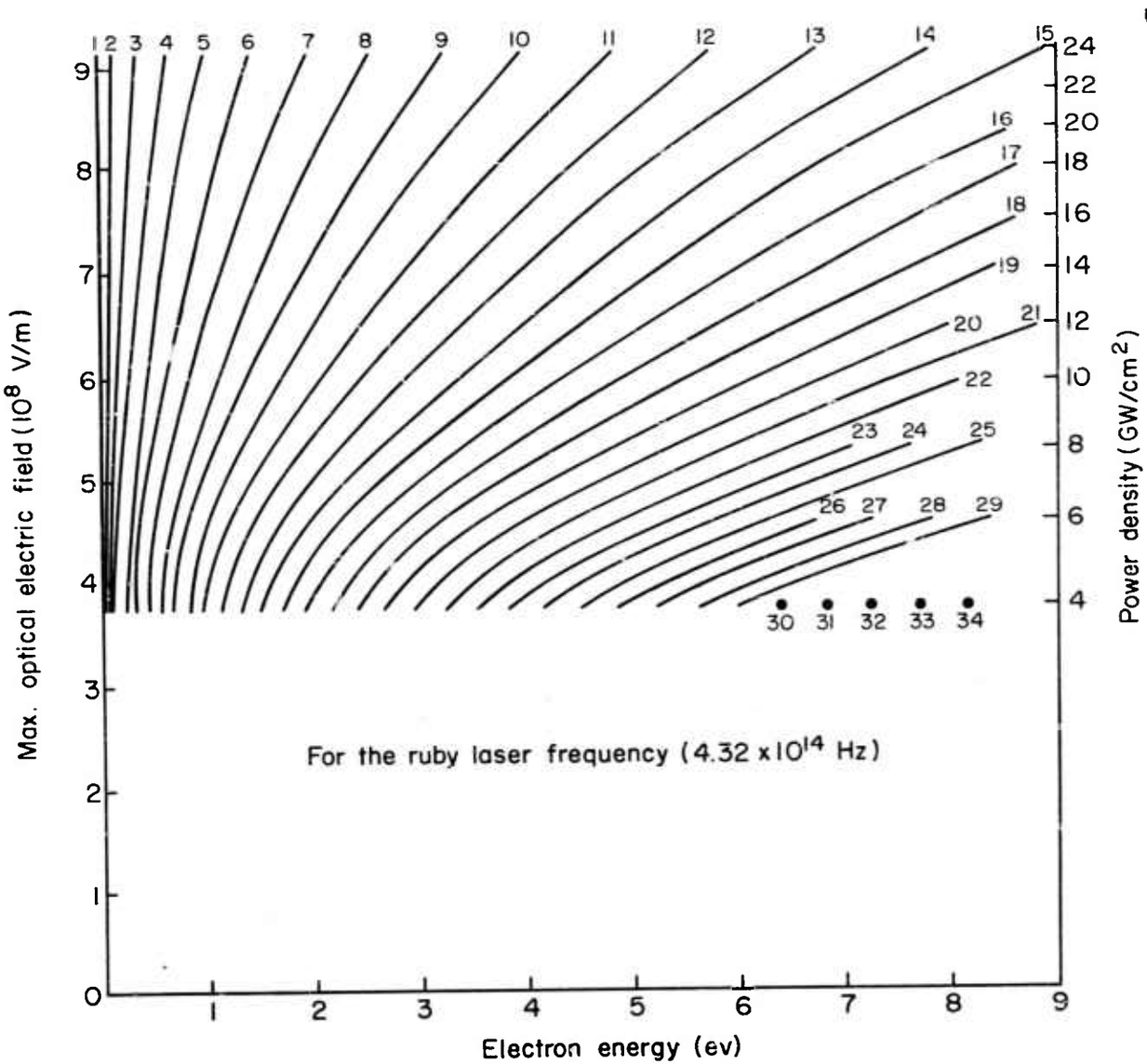

Fig. 7 Electric Field at 0.69 μm Required to Accelerate an Electron to a Particular Energy. Each curve is numbered according to the number of half cycles of the field required to accelerate the electron assuming only perfectly lucky collisions occur. The number then is also the number of the collisions which must occur for the electron to continue to gain energy from the field.

Figure 6 and 7 also show that between 3 and 5 more "lucky" collisions are required to reach a particular energy in a ruby laser field than in a Nd:YAG field. Thus if f is a constant, say 0.1,[1,2] the probability for damage at 0.69 μm is between 10^{-3} and 10^{-5} times less than at 1.06 μm. However, as stated above, f decreases with increasing electron energy and so the probability for ionization in a given field at 0.69 μm is even smaller. We have therefore an additional reason for the fact that damage with the ruby laser always requires higher fields.

It appears reasonable from the preceding discussion that the electron avalanche breakdown process, which gives a qualitatively good picture of 1.06 μm laser induced damage, will be observed only at much higher optical fields at 0.69 μm. However, as the ruby laser field is increased to find avalanche breakdown damage, it is possible that some materials may display damage due to another mechanism. In $LiNbO_3$ and $SrTiO_3$, both of which absorb strongly at 0.35 μm and have well defined experimental damage thresholds for 0.69 μm irradiation, this mechanism may be two-photon absorption.

Both the 1.06 and 0.69 μm data in Table II for $SrTiO_3$ were taken for sample No. 2 so that direct comparison is possible. In Refs. 1 and 2, the value of K for $SrTiO_3$ at 1.06 μm, obtained using a sample cut from a different boule, was about one fourth that in Table I. This is the first instance yet encountered where so large a sample-to-sample variation in K was observed. On checking with the manufacturer,[10] however, we found that sample No. 2 was doped with tungsten while sample No. 1 was not. Tungsten had been added to make the materials visually clearer and satisfy our order for "optical quality $SrTiO_3$." The two samples therefore were not the same material and so differences can be expected. More experimental data will be obtained on other samples as soon as possible.

3. DISTRIBUTION OF BREAKDOWN STARTING TIMES

Since the observation of a visible spark upon laser irradiation is always followed by the detection of damage in the irradiated area, a study of the temporal development of such sparks was initiated. The initial observations of this study were concerned with self-focusing and its relation to the internal damage process.[1] More recent work has been concerned with measuring the distribution of surface breakdown starting times and the interpretation of such data.

Using the high speed image converter streak camera technique described previously[1] and the TEM_{00} mode Nd:YAG laser, the distributions shown in Figs. 8 and 9 were obtained. Twenty-five different measurements of starting times were made to obtain each distribution. Plate glass and $SrTiO_3$ were studied because they have very different K values and because at convenient optical field strengths $p_1 \leq 1$ could be obtained.

The most obvious feature of these distributions is that, except for the highest field applied to plate glass, a high K material, they are not very sharp. Assuming constant pulse shape and material properties, as implied by the excellent fit of the measured distribution of N (the number of pulses required to damage) to the binomial distribution assuming a constant p_1,[1] a process described by a well defined threshold would yield distributions of breakdown starting times which ranged over an interval of time much less than the laser pulse duration. In addition, such a process would not permit any breakdowns to occur after the time of maximum field strength: If breakdown did not occur in the most intense field it would certainly not occur when the field was weaker. Both of these requirements for the distribution of breakdown starting times of a threshold-like process are violated by the data and so an interpretation based on the probabilistic point of view is sought.

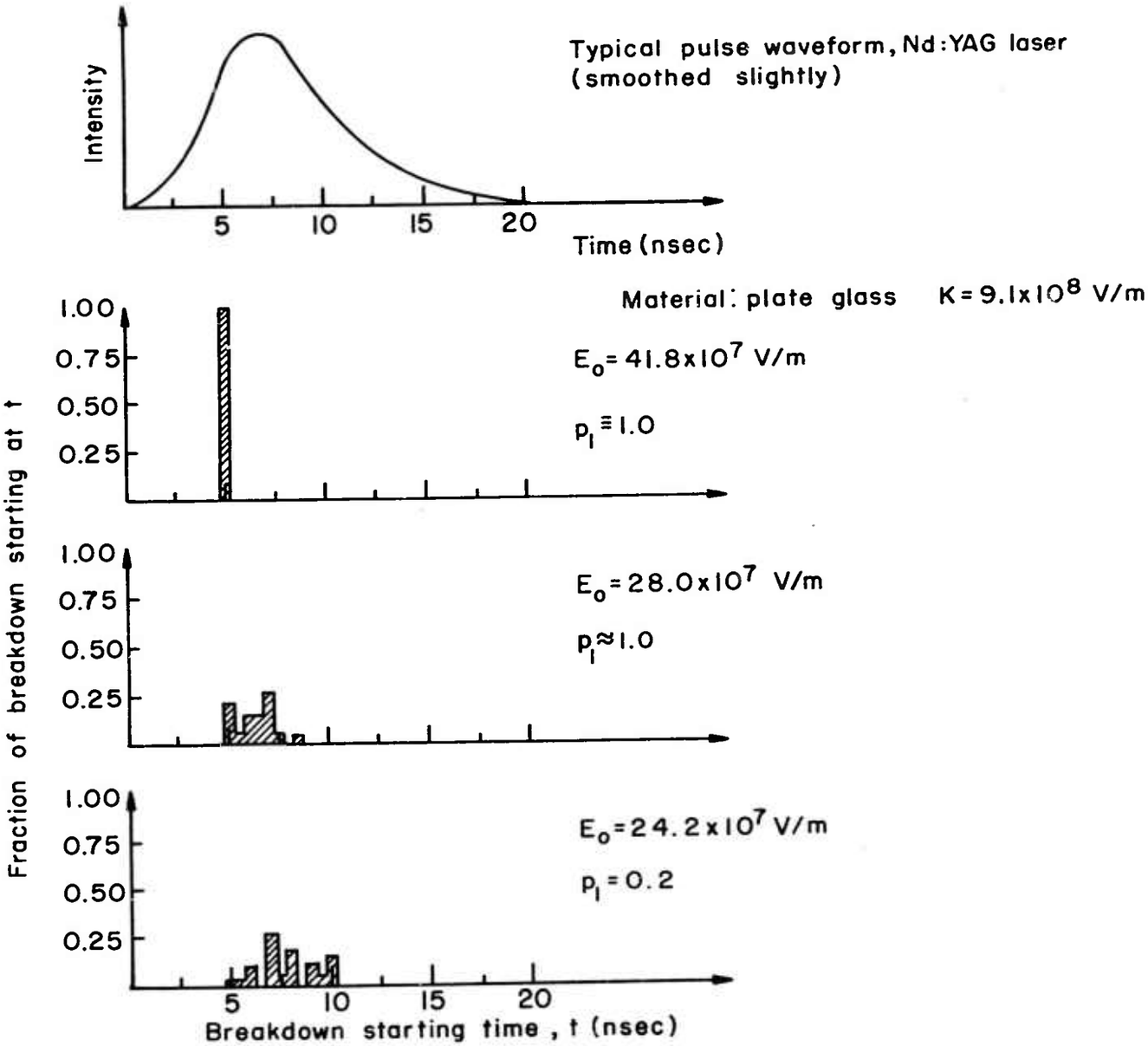

Fig. 8 Distribution of Surface Breakdown Starting Times for Plate Glass for Three Different Damage Probabilities.

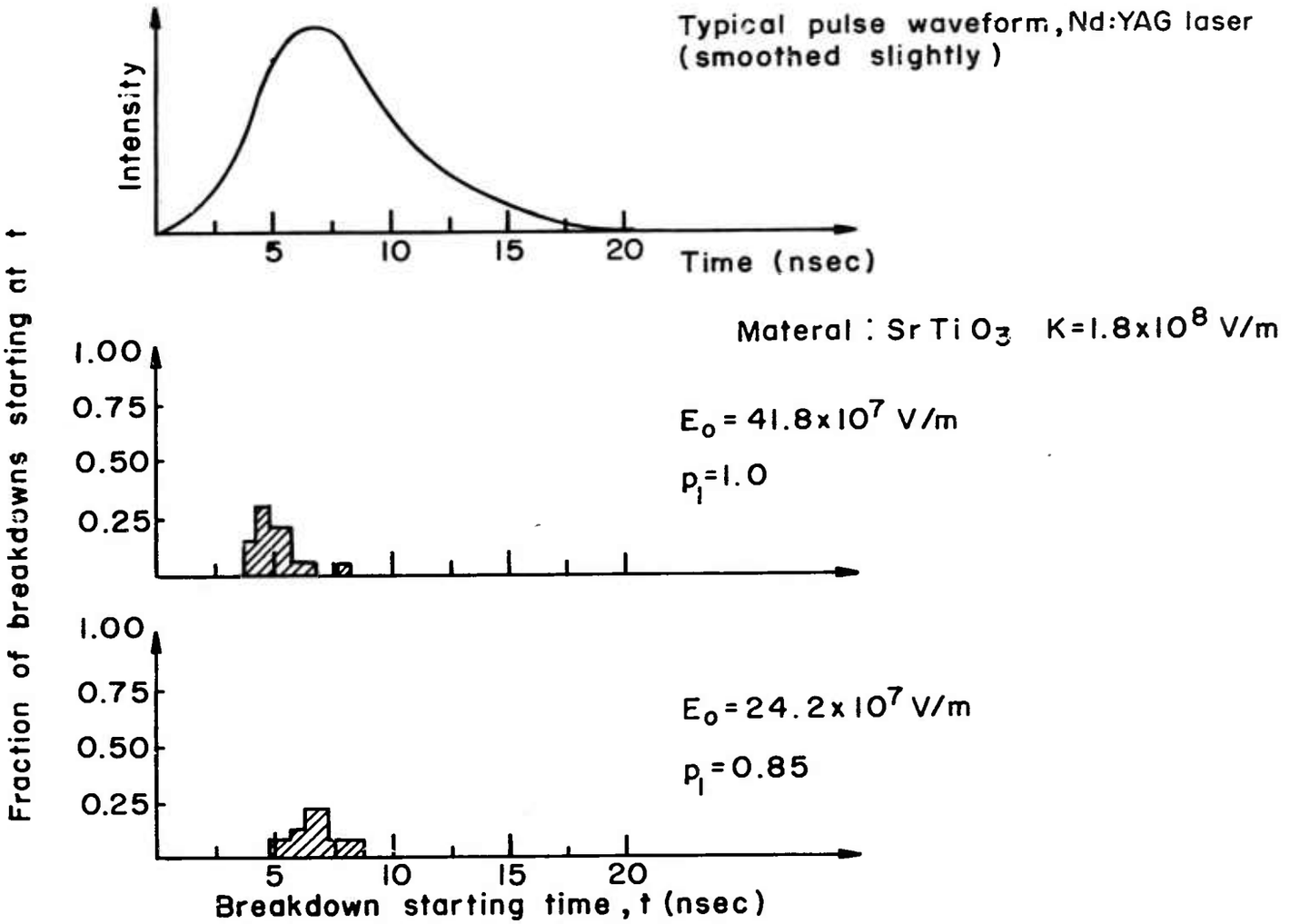

Fig. 9 Distribution of Surface Breakdown Starting Times for $SrTiO_3$ for Two Different Damage Probabilities.

Consider an ensemble of samples, each subjected to the same laser pulse, E(t), such that E(t) = 0 for $t \leq 0$. Let $\nu(t)$ be the fractional number which have not damaged at time t and let g(t) be the fractional rate with which the surviving samples breakdown. Note than that, within a scale factor, g(t) is the distribution of breakdown starting times. The applied laser field results in a probability per unit time that breakdown occurs, h(t), and so

$$g(t) = -\frac{d\nu(t)}{dt} = \nu(t)\ h(t) \ . \tag{2}$$

Solving the second part of this equation gives

$$\nu(t) = \exp\left(-\int_0^t h(t')\,dt'\right) \tag{3}$$

which satisfies the obvious initial condition that $\nu(0) = 1$.

Thus we have for the form of the distribution of breakdown starting times

$$g(t) = h(t)\ \exp\left(-\int_0^t h(t')\,dt'\right) . \tag{4}$$

Initially g(t) grows as h(t) but the influence of the exponential term rapidly becomes dominant and eventually g(t) decreases towards zero. The time interval over which g(t) is not negligibly small (the time width of the distribution) depends on the precise form of h(t) for the particular material and laser pulse duration and can include times after the peak field is reached.

The most probable time for breakdown to begin is the time, t_M, when g(t) is maximum. Thus we consider

$$\frac{d(g(t))}{dt}\bigg|_{t_M} = \left(\frac{d(h(t_M))}{dt} - (h(t_M))^2\right)\exp\left(-\int_0^{t_M} h(t')dt'\right) = 0. \tag{5}$$

Since $\exp\left(-\int_0^{t_M} h(t')\,dt'\right) \neq 0$, Eq. (5) holds when

$$\frac{d(h(t_M))}{dt} = (h(t_M))^2 \quad . \tag{6}$$

The solution for t_M is then found during the interval when

$$\frac{dh(t)}{dt} > 0 \, . \tag{7}$$

Since the applied field, E(t), determines the time dependence of h(t), we have

$$\frac{dh}{dt} = \frac{dh}{dE}\,\frac{dE}{dt} \quad . \tag{8}$$

It is physically reasonable to require that the damage rate increase as E increases and decrease as E decreases so that

$$\frac{dh}{dE} > 0 \text{ for all } t \, . \tag{9}$$

Thus g(t) reaches its maximum at a time when

$$\frac{dE}{dt} > 0 \tag{10}$$

or before the peak field strength is reached. This result agrees with the experimental data in Figs. 8 and 9 where the most probable time for breakdown to occur is always found before the time at which the optical field strength is maximum.

Further evidence for a probabilistic interpretation of the damage process is shown in Fig. 10. In this case a TEM_{00} mode ruby laser pulse was focused inside a NaCl crystal and the transmitted laser

a) Damaged when the peak laser field was reached
$E_{Damage}/E_{Peak} = 1$

b) Damaged before the peak laser field was reached
$E_{Damage}/E_{Peak} = 0.896$

c) Damaged after the peak laser field was reached
$E_{Damage}/E_{Peak} = 0.954$

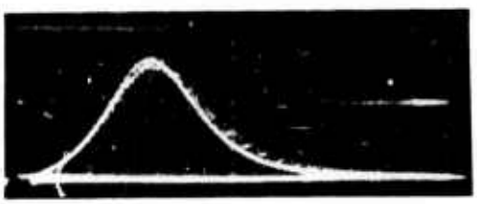

d) 3 successive pulses
no damage
$E_{Peak} \equiv 1$ (Arbitrary units)

A TEM_{00} mode ruby laser with total pulse energy of 0.3 mJ was focused inside the inclusion free sample with a 14mm focal length lens

Fig. 10 The Occurrence of Internal Damage in NaCl Due to Ruby Laser Irradiation. The laser intensity transmitted through the sample is shown in these photos.

intensity monitored with a fast photodiode-519 oscilloscope combination. As discussed elsewhere[11] the laser power was such that no self-focusing was likely. The photos in Fig. 10 are representative samples of the many that were taken and show that damage does not have to occur for every pulse. In addition, they show that when ruby laser induced internal damage does occur, it can begin before, at, or after the peak of the laser pulse.

The use of the breakdown or damage starting time to study the probabilistic nature of laser damage is especially important for materials with large K's. In such cases one may not have sufficiently fine control over the laser pulse parameters to confidently resolve the region of intermediate damage probabilities. Thus data such as that in Fig. 10 can be used to assist in identifying such important characteristics of the damage mechanism as its statistics.

4. COMMENTS ON THE PROBABILISTIC AND THRESHOLD POINTS OF VIEW

The last paragraph of the preceding section indicates just one of the problems involved in distinguishing between probabilistic and threshold-like phenomena. For all practical purposes, materials having large K's can be considered to have a damage process which is governed by a well-defined threshold. It is possible however, as shown above, to perform studies of the damage dynamics which reveal some probabilistic properties.

The experiments described in this paper and in Refs. 1 and 2 employed the techniques of irradiating a particular region of the sample until either damage occurred or 500 pulses spaced by a 1 or 5 second interval had been tried. A new region was then studied in the same manner at the same level of irradiation. Having done this at least 25 different times an estimate of the damage probability was obtained by dividing the number of damages by the total number of laser pulses. We then always examined the set of values obtained for the number of pulses required to damage at each region, N, to see if this set is distributed according to

$$f_N = p_1 (1 - p_1)^{N-1} \quad . \tag{11}$$

If good agreement is found, then it is fair to say that the probability for damage in each region and for each pulse was always p_1 even though damage did not always occur. Data of this sort, obtained from sets of ~ 100 values of N for two different materials, fused quartz and $SrTiO_3$, are shown in Figs. 11 and 12 respectively.

If the fluctuations in N values which led to the probabilistic interpretation of damage represented local variations in the threshold for damage due to dirt, stresses or other material imperfections then the distribution of N values would not be given by Eq. (11). Instead,

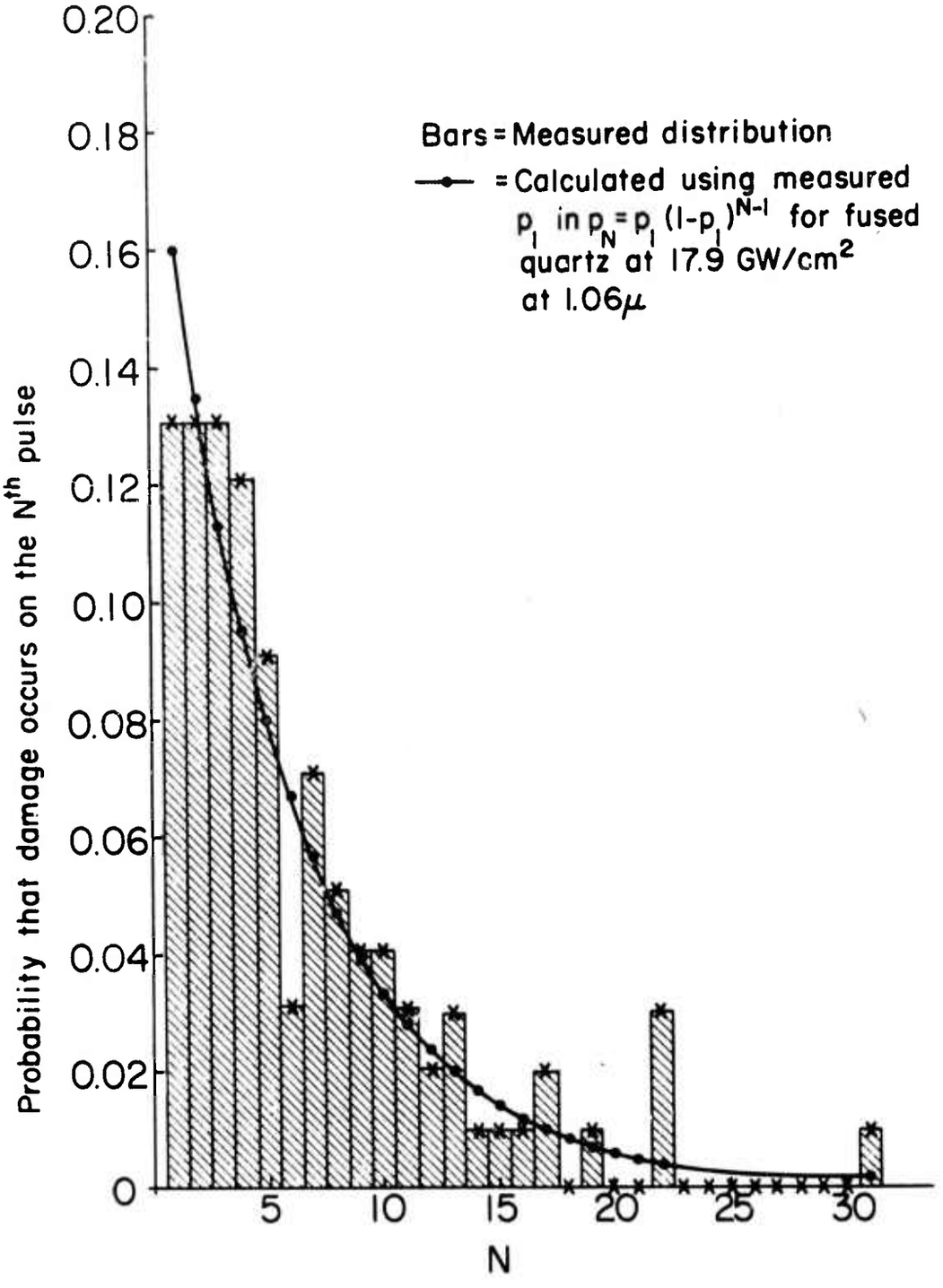

Fig. 11 Probability that Damage Occurs on the Nth Pulse vs N for Fused Quartz. A 17.9 GW/cm^2 TEM_{00} mode 1.064 μm beam was used.

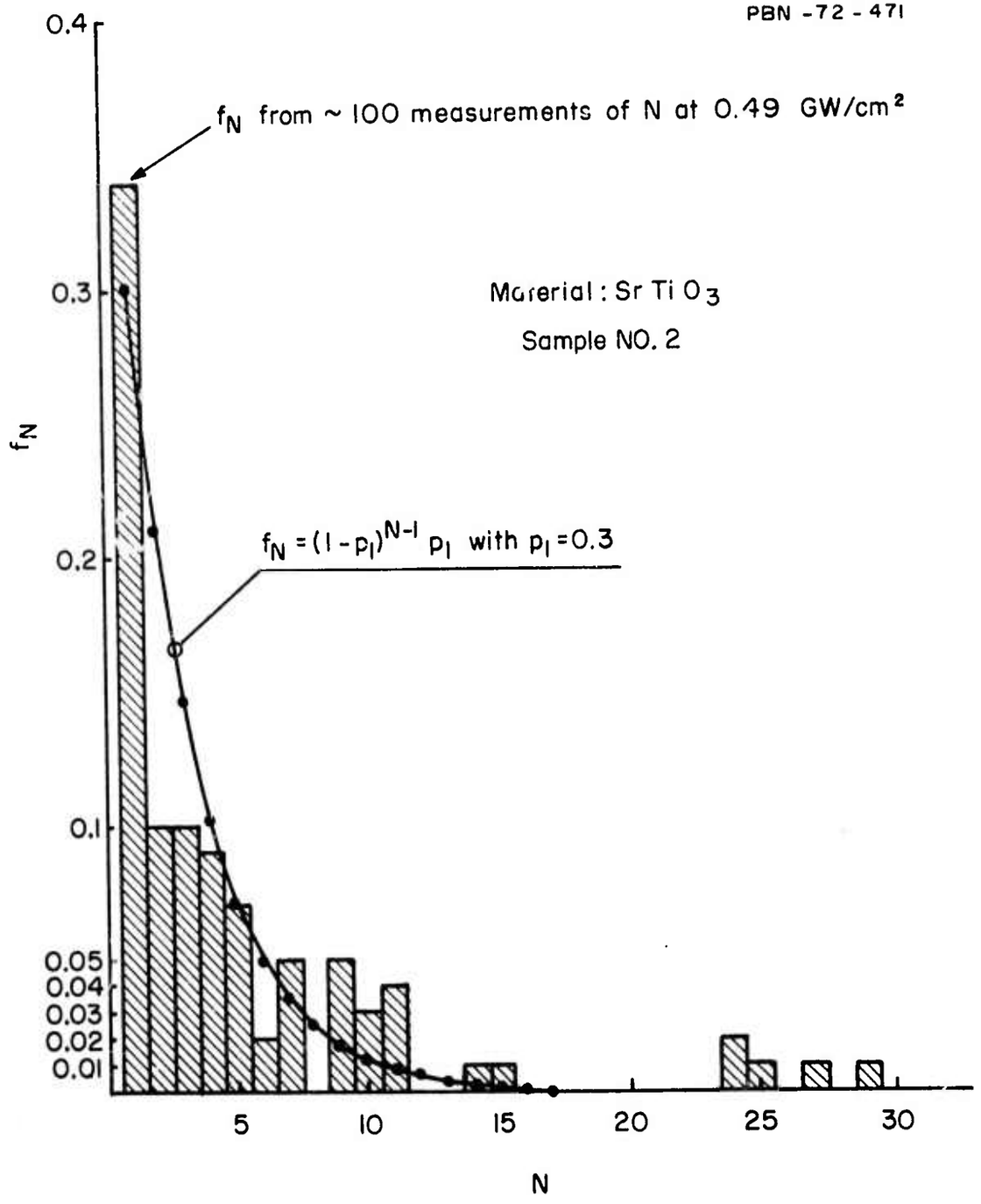

Fig. 12 Probability that Damage Occurs on the Nth Pulse vs N for $SrTiO_3$. A 0.5 GW/cm^2 TEM_{00} mode 1.06 μm beam was used.

f_N would be determined by the density of regions which had damage thresholds less than or equal to the maximum optical field strength. Suppose, for example, that the maximum optical field strength is such that 20 percent of the material could be damaged. Our experimental procedure would then generate approximately 5 places where N = 1 and ~ 20 where N = 500 pulses with no damage were recorded. We would then obtain a damage probability of $p_1 \approx 5 \times 10^{-4}$. Since the probability that 25 samples of numbers distributed according to Eq. (11) with $p_1 = 5 \times 10^{-4}$ contain five 1's and twenty 500's is very small, the set of measured N values and the resulting p_1 would not be accepted. This type of disagreement for the N value distribution would indicate material variations or laser fluctuations. We feel that these are minimal in view of Figs. 11 and 12. However, as in the case of the $LiNbO_3$ sample discussed in Ref. 1, instances where such disagreements occurred would be reported separately from more reliable measurements of p_1.

We now consider the effect of varying the irradiated area on the rate of change of damage probability with applied optical power density. If the optical field is kept constant and the irradiated area is increased, then the number of electrons in the sample subjected to the optical field is increased. In effect then, one can perform many experiments at once under the new conditions and so to the extent that different regions are independent the probability for at least one breakdown must increase with area.

If p = p(E) is the probability for breakdown when one initial electron is present, then

$$p'(E) = Np(E) \qquad (12)$$

is the probability for breakdown when the area isincreased and N initial electrons are now sampled. Here we assume that $N \neq N(E)$. If $Np(E) > 1$ we must obviously set $p'(E) = 1$. From our damage data[1,2]

$$\frac{d(\ell n\, p(E))}{d(1/E)} = -K \qquad (13)$$

and so, from Eq. (12),

$$\frac{d(\ell n\, p'(E))}{d(1/E)} = -K \quad . \qquad (14)$$

Thus the two cases will appear in a log of probability vs 1/E graph as sketched in Fig. 13. From this we find that

$$\Delta\left(\frac{1}{E}\right) = \Delta\left(\frac{1}{E'}\right) \qquad (15)$$

where E and E' are defined in Fig. 13. Now, in arbitrary units,

$$P = E^2 \qquad (16)$$

where P is the power density. By differentiation we find

$$\Delta\left(\frac{1}{E}\right) = -\frac{\Delta P}{P}\ \frac{1}{2E} \qquad (17)$$

and

$$\Delta\left(\frac{1}{E'}\right) = \frac{-\Delta P'}{P'}\ \frac{1}{2E'} \quad . \qquad (18)$$

Therefore, the required fractional changes in power density necessary to achieve a change in damage probability from say p_i to p_j are related by

$$\frac{\Delta P'_{i\to j}}{P'_i} = \frac{E'_i}{E_i}\ \frac{\Delta P_{i\to j}}{P_i} \quad . \qquad (19)$$

But $E'_i/E_i < 1$ and so

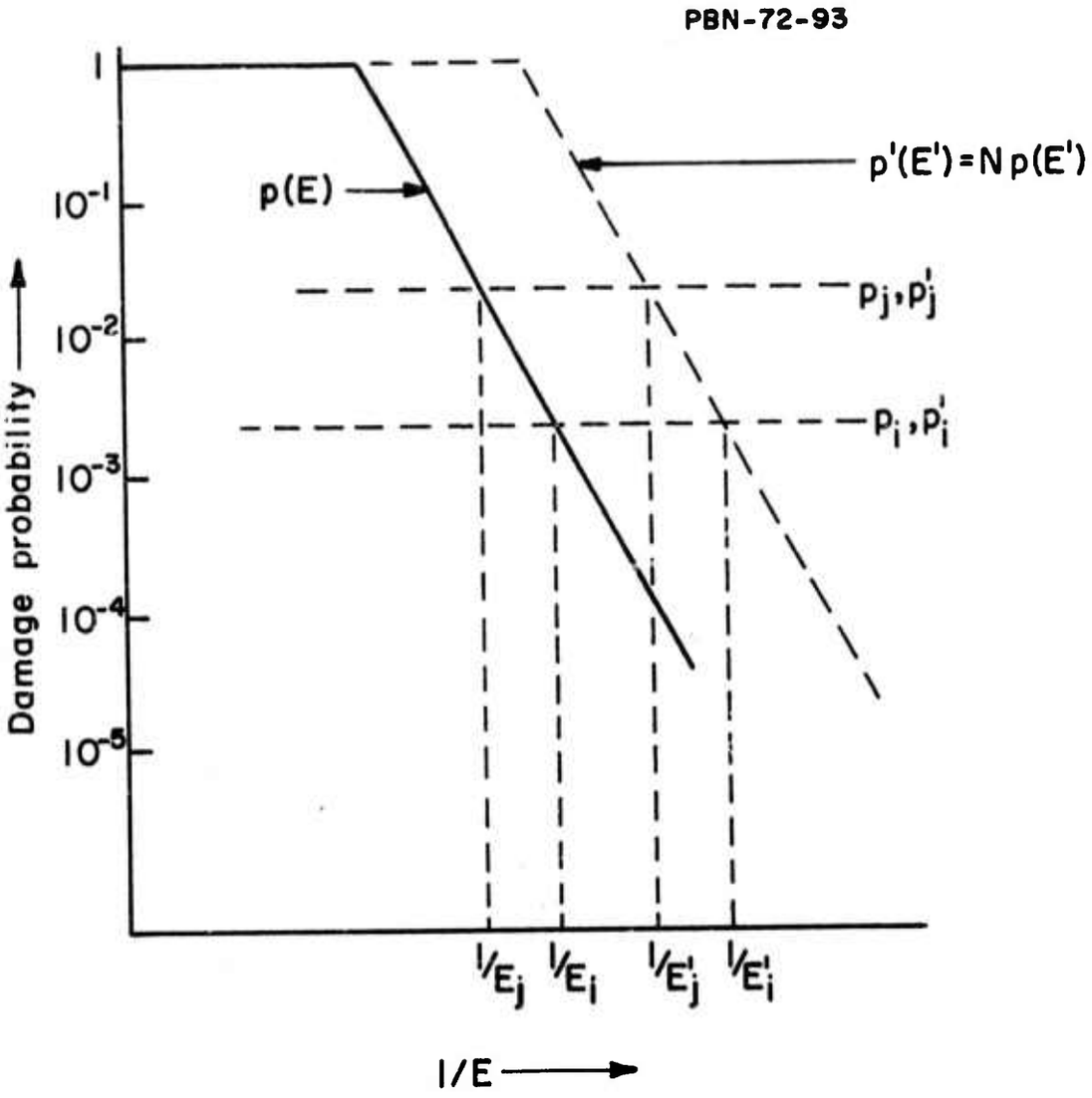

Fig. 13 Sketch of a Plot of the Log of Damage Probability vs The Inverse Optical Electric Field for Two Different Irradiated Areas. p'(E') is the result for an irradiated area larger than used to obtain p(E).

$$\frac{\Delta P'_{i\to j}}{P'_i} < \frac{\Delta P_{i\to j}}{P_i} \qquad (20)$$

or

$$\Delta P'_{i\to j} < \Delta P_{i\to j} \quad . \qquad (21)$$

This means, for example, that if the area is large enough so that the damage probability changes from say 10^{-3} to 1 over a small range in power density then it is possible to perform experiments where the probabilistic nature of the damage process could be overlooked. (See Fig. 14)

The preceding consideration of the case of increasing the area irradiated while maintaining the electric field strength shows that the probability of at least one breakdown occurring also increases. However, the probability for damage per unit area is independent of the irradiated area and would be a useful quantity for describing a material's damage properties.

If the area of the beam is increased while the total pulse power is kept constant, the electric field, E, decreases and the damage probability decreases.

We see from this treatment that is is essential to maintain constant irradiated area or volume when comparing laser damage properties with different lasers or when comparing different materials. It is also critical to take this into account when comparing the work of different researchers.

In the probabilistic view a report of a damage threshold could correspond to 1) a very high value of K in Eq. (1), 2) a study of a much larger volume of material than that which is small enough to reveal

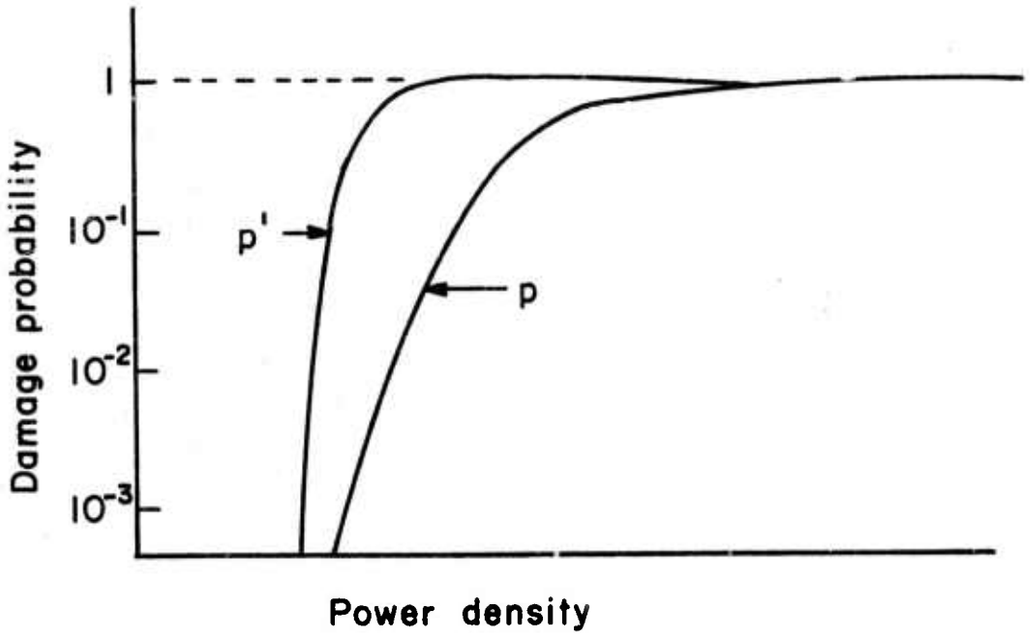

Fig. 14 Sketch of a Plot of the Log of Damage Probability vs Power Density for the Same Two Cases as in Fig. 13.

the probabilistic properties of damage, 3) an experiment in which the intermediate range of power densities (power densities where $0 < p_1 < 1$) was missed due to experimental procedure or 4) an experiment in which self-focusing always produced an intensity so high that the intermediate range was never studied. It is also possible that there is more than one damage mechanism and that some mechanisms, such as avalanche breakdown, are probabilistic while others are threshold-like.

5. SUMMARY

The first direct comparison of damage in transparent media produced by ruby and Nd:YAG lasers revealed that: 1) A material is less likely to damage when subjected to a particular optical field at 0.69 μm than at 1.06 μm; and 2) The relationship between damage probability, p_1, and applied optical electric field strength, E, though still generally of the form $p_1 \alpha \exp(-K/E)$, has a value of K at 0.69 μm which is substantially greater than at 1.06 μm. A tentative interpretation of these changes based on a modified optical frequency avalanche breakdown model was proposed. In addition the possibility that in some materials more than one damage mechanism may be operative was discussed.

The distribution of damage starting times was studied experimentally for two different materials. In contrast to the very small spread expected for a threshold process, broad distributions were found. Each distribution showed, in addition, that the most likely starting time for damage is before the time of maximum field. The properties of the measured distributions were described by the compound probability that breakdown occurs at a particular time, given that it has not occurred before that time and, as such, provided added evidence for the probabilistic interpretation of the 1.06 μm damage process.

Several possible connections between the probabilistic and threshold-like interpretations of laser-induced damage were considered and the two points of view were shown not to be totally incompatible. Unnoticed, subnanosecond fluctuations in the laser pulse as the source of the statistics in the experiments were ruled out by evidence showing that only one or at most a very few longitudinal modes could oscillate in our lasers. This meant that shortest possible duration of any fluctuation was still long enough to have been detected by our fast photodiode-519 oscilloscope monitor system.

ACKNOWLEDGEMENTS

The authors wish to acknowledge the invaluable experimental assistance of D. Bua. The work of D. Bua in automating the data recording and along with D. Fradin in establishing and interpreting the procedure which results in smooth laser pulses is especially gratefully acknowledged. Valuable discussions were held with E. Bliss, D. Milam, D. Fradin and F. Horrigan.

6. REFERENCES

1. M. Bass and H.H. Barrett, NBS Special Publication 356 (1971) p. 76 and IEEE J. Quant. Elect. QE-8, 338 (1972).

2. M. Bass, H.H. Barrett and L.H. Holway, Jr., Scientific Report No. 1 for Contract No. F19628-70-C-0223 (February 1972).

3. M. Bass, IEEE J. Quant. Elect. QE-7, 350 (1971).

4. C.R. Guiliano, R.W. Hellwarth, L.D. Hess and G.R. Rickel, Semiannual Report No. 2 for Contract No. F19628-69-C-0277 (July 1970).

5. V. Evtuhov and J.K. Neeland, "Pulsed Ruby Lasers," Lasers, Vol. I, ed. A.K. Levine (M. Dekker, Inc., New York, N.Y.) (1966).

6. E. Yablonovitch, Ph.D. Thesis, Harvard University (June 1972).

7. J.B. Birks, "The Theory and Practice of Scintillation Counting," (Pergamon Press, London) (1967).

8. F. Seitz, Phys. Rev. 76, 1376 (1949).

9. E.O. Kane, Phys. Rev. 159, 624 (1967).

10. Private communication, L. Merker and J. Cobb, N.L. Industries.

11. D.W. Fradin, E. Yablonovitch and M. Bass, "Comparison of Laser Induced Bulk Damage in Alkali-Halides," 4th ASTM-NBS Symposium on Damage in Laser Materials (1972).

III. SURFACE AND BULK LASER DAMAGE STATISTICS AND THE IDENTIFICATION OF INTRINSIC BREAKDOWN PROCESSES

A. Introduction

The studies of damage statistics through measurements of the distribution of breakdown starting times were extended as described in this section. Data showing a statistical damage process in both surface and bulk breakdown at 1.06 and 0.69 μm is described. It is shown that the measured statistical time lags are similar to those observed in dc breakdown and are fully compatible with the probabilistic point of view. In addition, data is presented which shows that the statistics of surface and bulk damage are the same. As part of this effort, a new, dynamic procedure was developed for distinguishing between intrinsic damage events and those caused by absorbing inclusions.

A brief review of the probabilistic interpretation of laser damage is given. The contrast between the measured distributions of breakdown starting times and the form required by a threshold-like damage mechanism is described. The techniques for determining the cause of laser damage and for experimentally avoiding self-focusing are explained in the body of the paper and the appendix, respectively. New data which demonstrate the statistical nature of both bulk and surface laser damage to transparent media are presented and these data are analyzed in terms of the statistical-electron avalanche breakdown model for the laser damage process. The data and model are shown to be consistent.

Surface and Bulk Laser Damage Statistics and the Identification of Intrinsic Breakdown Processes

Michael Bass*
Raytheon Research Division
Waltham, Mass. 02154

and

David W. Fradin†
Harvard University
Cambridge, Mass. 02138

Abstract

The experimental evidence presented confirms the existence of a statistical nature to the laser-induced intrinsic damage process both in the bulk and on the surfaces of transparent materials. A damage process determined by an electron avalanche breakdown with statistical starting properties was found to be consistent with the data.

The importance of irradiating only a small volume of the material in order to avoid studying inclusion induced laser damage is discussed. In addition, a new procedure was developed to permit rapid identification of the occurrence of damage due to an intrinsic process.

---

* Supported by the Advanced Research Projects Agency of the Department of Defense and was monitored by the Air Force Cambridge Research Laboratories under Contract No. F19628-70-0223.

† Supported by the Joint Services Electronics Program at Harvard University under Contract No. N00014-67-A-0298-0006.

I. INTRODUCTION

Recently, the concept of a statistical nature to the laser irradiation induced damage process in transparent media was introduced by Bass and Barrett.[1] It was shown that this point of view permits one to understand the very wide range of reported damage thresholds and the generally unpredictable nature of optical damage. The probabilistic approach, in addition, gave evidence for avalanche breakdown as the intrinsic damage mechanism when the surfaces of transparent media are exposed to 1.06μm laser beams. Evidence showing that avalanche breakdown was also responsible for bulk damage was obtained by Yablonovitch[2] at 10.6μm and Fradin et al.[3] at 1.06 and 0.69μm in alkali halide crystals. In the latter work it was found that the avalanche process is in its d.c. limit at frequencies as high as 3×10^{14} hertz.

A statistical nature to d.c. avalanche breakdown in both gases[4] and solids[5] has been described and measured for a number of years. Studies on such systems show that there are two time lags observed between the application of the field and the observation of breakdown. These time lags, statistical and formative, have been examined in order to obtain information on the dynamics of the electron avalanche processes.[6] Initial measurements of the dynamics of optical surface breakdown in solids revealed a statistical time lag which was compatible with the probabilistic interpretation of laser induced damage.[7]

In the present paper additional data for statistical time lags in both surface and bulk breakdown studies at 1.06 and 0.69μm is described. It is shown that the measured statistical time lags are fully compatible with the statistics observed in Ref. 1. In addition, data is presented which shows that the statistics of surface and bulk damage are the same. As part of this effort, a new, dynamic procedure was developed for distinguishing between intrinsic damage events and those caused by absorbing inclusions.

A brief review of the probabilistic interpretation of laser damage and the experimental results of Bass and Barrett is given in Section B-2.

In that section the contrast between the measured distributions of breakdown starting times and the form required by a threshold-like damage mechanism is described. The techniques for determining the cause of laser damage and for experimentally avoiding self-focusing are explained in Sec. B-3 and B-8, respectively. New data which demonstrate the statistical nature of both bulk and surface laser damage to transparent media are presented in Sec. B-4. Then, in Sec. B-5 these data are analyzed in terms of the statistical electron avalanche breakdown model for the laser damage process and the data and model are shown to be consistent. The conclusions drawn from this work are summarized in Sec. B-6.

II. PROBABILITY AND AVALANCHE BREAKDOWN IN LASER DAMAGE

Bass and Barrett[1] observed that a precisely defined threshold for laser induced damage does not exist. It was found that at a particular level of irradiation, laser-induced surface damage to 10 different materials could be produced with some probability per pulse, p_1. The measured value of p_1 was obtained by measuring the number of pulses required to produce damage, N, at a minimum of 25 different points on the surface and setting

$$p_1 = \frac{\text{total number of damages}}{\text{total number of pulses}} .$$

The set of values of N was then examined in order to be certain that at a constant power level, p_1 was the same for each laser pulse. The fractional number of times N pulses were required to produce damage, f_N, is given by the product of the probability that no damage occurs during the first N-1 pulses, and the probability that it then occurs during the subsequent pulse. If p_1 is constant, f_N is given by

$$f_N = (1 - p_1)^{N-1} \; p_1 . \qquad (1)$$

Since the only way this distribution of N values could be obtained was if

p_1 were constant, the excellent agreement between the measured values of f_N and those computed from Eq. 1 was taken as confirmation of the use of stable laser pulses and uniform surface conditions in the experiments.[1] Thus, measurement of p_1 and f_N and comparison of the measured f_N with Eq. 1 is an important test of the probabilistic nature of the damage event.

The relationship between the damage probability and the optical electric field strength, E, was found experimentally to be

$$p_1 \propto \exp(-K/E) \tag{2}$$

where K is an experimentally measured constant determined by the material studied. This functional dependence of p_1 on E suggests that the damage mechanism is an avalanche breakdown because the d.c. ionization coefficient which governs avalanche breakdown in gases[8] and semiconductors[9] depends on field in the same manner. The model of optical avalanche breakdown proposed in Ref. 1 was formulated in analogy to Shockley's "lucky electron" model of d.c. breakdown.[10] The optical breakdown model, based on the assumption that the damage statistics were determined by those of the first one or two ionizations, gave the experimentally observed relation between damage probability and optical electric field and did not require material properties inconsistent with transparent insulating dielectrics.

Additional evidence for the probabilistic nature of laser damage was obtained in experiments in which an image converter streak camera was used to measure the distribution of breakdown starting times for surface damage to two different materials.[7] If the breakdown or damage process were completely described by a well-defined threshold, then this distribution should be very narrow and no breakdowns should occur after the laser field reached its maximum. The data, however, showed broad distributions, particularly when the applied field was such that $p_1 < 1$. In all cases the most probable time for breakdown occurred before the time of maximum field, though some breakdowns did occur later.

The distribution of breakdown starting times of a probabilistic breakdown process is just the compound probability per unit time that breakdown occurs at a particular instant given that it has not occurred before that time. It was shown in Ref. 7 that this compound probability, g(t), is given by

$$g(t) = h(t) \exp\left(-\int_0^t h(t')dt'\right) \tag{3}$$

where h(t) is the probability per unit time that the applied laser field, E(t), causes breakdown. This form for the distribution of breakdown starting times was shown to explain the main qualitative features of the measured distributions.

III. THE DISTINCTION BETWEEN INTRINSIC AND INCLUSION INDUCED DAMAGE

Transparent materials often contain absorbing inclusions which are too small to be easily detected by optical inspection. Calculations[11] of the thermodynamics of laser irradiation heating of such objects have shown that when their diameters are greater than about 0.1 μm, they can produce local melting of the surrounding material. Experiments have, in fact, been performed in which inclusions were identified as the major source of optical damage.[11, 12]

In experiments where intrinsic breakdown mechanisms have been investigated, damaging inclusions have been largely avoided by strongly focusing the laser light into small volumes which in general do not contain inclusions. Two techniques have been used in these studies to determine the relative frequency of occurrence of inclusion damage. In the first, one examines the morphology of the residual damage for characteristics related to its cause. This procedure is useful only for bulk studies.[2, 3] The second technique which utilizes the damage statistics can be applied to both surface and bulk studies but requires a large number of light probes by a highly stabilized laser. A third technique, which is reported here for the first time,

allows an immediate determination of the general source of optical damage at individual sites both in the bulk and on the surface. This technique does not require an amplitude stabilized laser and thus simplifies the problem of identifying intrinsic surface and bulk damage.

Yablonovitch first observed the distinctive morphology normally produced by intrinsic bulk breakdown and used it to distinguish between intrinsic and inclusion damage at 10.6 μm.[2] This same technique was used in bulk studies at 1.06 μm[3] and at 0.69 μm.[13] It was found that when intrinsic breakdown occurs, a narrow melted region begins at the geometrical focus and increases in cross-section as it grows back a very short distance towards the laser to give a tear-drop appearance. Inclusion damage, on the other hand, generally forms as spherical regions randomly distributed about the focal point. For both mechanisms thermally-induced cracks can develop after the laser pulse has passed.[14] Because of these observations, inclusion and intrinsic damage can be reliably distinguished in the bulk by examining the damage morphology.

The damage statistics can be used to estimate the frequency of occurrence of inclusion induced damages by studying the deviations of the measured values of f_N from those calculated with Eq. 1. As pointed out in the preceding section, good agreement between the predictions of Eq. 1 and the measured f_N's indicates that material inhomogeneities did not measurably affect the damage data. However, when large disagreements are detected or when a sharp threshold is observed it is likely that inclusions are the major cause of damage.

A third method for distinguishing between inclusions and intrinsic damage was developed and used in the present work. It consists of observing the light transmitted through the sample by using a fast photodiode-oscilloscope combination. When damage occurs, the transmitted laser pulse is attenuated in a manner which is found to be characteristic of the source of damage.

Pulses which are attenuated very rapidly form damage regions in the bulk which are characteristic of the intrinsic mechanism. In addition, for the materials with large values of K studied in the present work, the intensity at the instant of attenuation for such pulses varies by no more than about 25 percent about some average value. An example of this type of attenuated pulse-shape is given in Fig. 1b.

A number of damaging pulses are attenuated in a very different manner and produce damage regions that appear to result from inclusion absorption. For this class of damage events, the attenuation is not as rapid and as complete as with intrinsic damage nor are the transmitted pulse-shape and intensity at the first instant of attenuation as repeatible. Examples of this type of attenuation are given in Figs. 1c and d.

There is, in addition, a small percentage of damage events which cannot be unambiguously identified by this scheme or by microscopic investigation of the damage site. In the present work, data obtained from such pulses were not used.

Another distinction between inclusion and intrinsic breakdown involves the intensities of the sparks created by damaging laser pulses. In general, intrinsic events produced bright sparks while damage from inclusions occasionally resulted in sparks which were barely visible.

Except for extremely high laser intensities, intrinsic breakdown occurs near the peak of the laser pulse so that the energy which is available to take part in the damage process is consistently about half the total pulse energy. This was observed experimentally (see Figs. 5-6) and can be explained by theoretical considerations of avalanche breakdown (see Sec. V). It is thus to be expected that the energy deposited in the focal region is reasonably constant for intrinsic breakdown and that the intensity of the sparks which apparently always accompany such damage is, therefore, also reasonably constant.

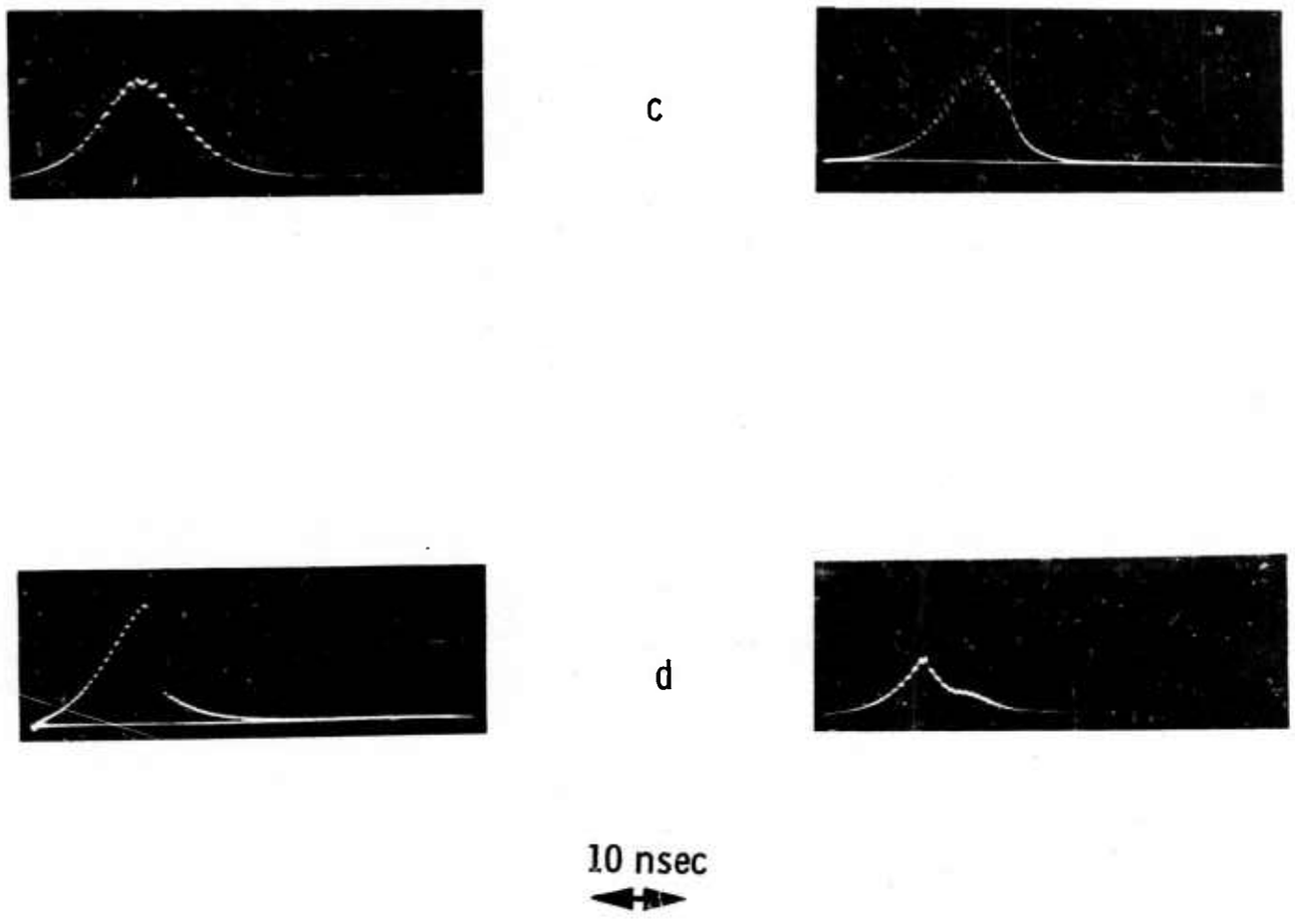

Fig. 1 Ruby Laser Pulses Transmitted Through NaF.

a. No damage occurred
b. Transmitted pulse which produced intrinsic bulk damage
c. Transmitted pulse which produced bulk damage from inclusion absorption
d. Transmitted pulse which produced bulk damage from inclusion absorption

Figs. 1c and d suggest that these same conclusions do not hold for inclusion damage, and, indeed, there is no reason why they should. Damage from inclusion absorption is energy-dependent for different inclusion geometries,[11] and actual material damage may not develop until very late in the laser pulse (ie: after most of the optical energy has passed through the sample). The focal region may thus be melted but not heated sufficiently to produce a bright spark. A number of experimenters have, in fact, reported material damage without sparks.[15] The arguments advanced here indicate that some type of extrinsic absorptive mechanism such as inclusion absorption very likely caused the damage in their work.

IV. EXPERIMENTAL RESULTS

Since the lasers and experimental procedures used in these experiments are described in detail elsewhere[1, 3, 7] they will not be discussed here. It is important to note, however, that only TEM_{00} mode laser beams were used. Furthermore unambiguous bulk damage data was obtained by using beams with total power less than about one tenth the critical power for self-focusing in combination with focusing optics to obtain optical fields intense enough to cause breakdown.[3] Tests for self-focusing in fused quartz are described in Appendix A.

In Refs. 1 and 7 the appropriate match between the measured values of f_N and those obtained from Eq. 1 using the measured damage probability was shown for surface damage studies. The elimination of the confusing effects of self-focusing made possible meaningful measurements of bulk damage probability. Data in the present work show that bulk damage is caused by the same probabilistic process as surface damage. The results for bulk damage in fused quartz are shown in Fig. 2. The curve plotted in this figure was calculated using the measured damage probability as defined in Section B-2, $p_1 = 0.38$, in Eq. 1. Another determination of p_1 can be obtained by computing that value of p_1 which gives the best fit to the measured distribution of N values. This was done by finding the value of p_1 which minimizes the quantity

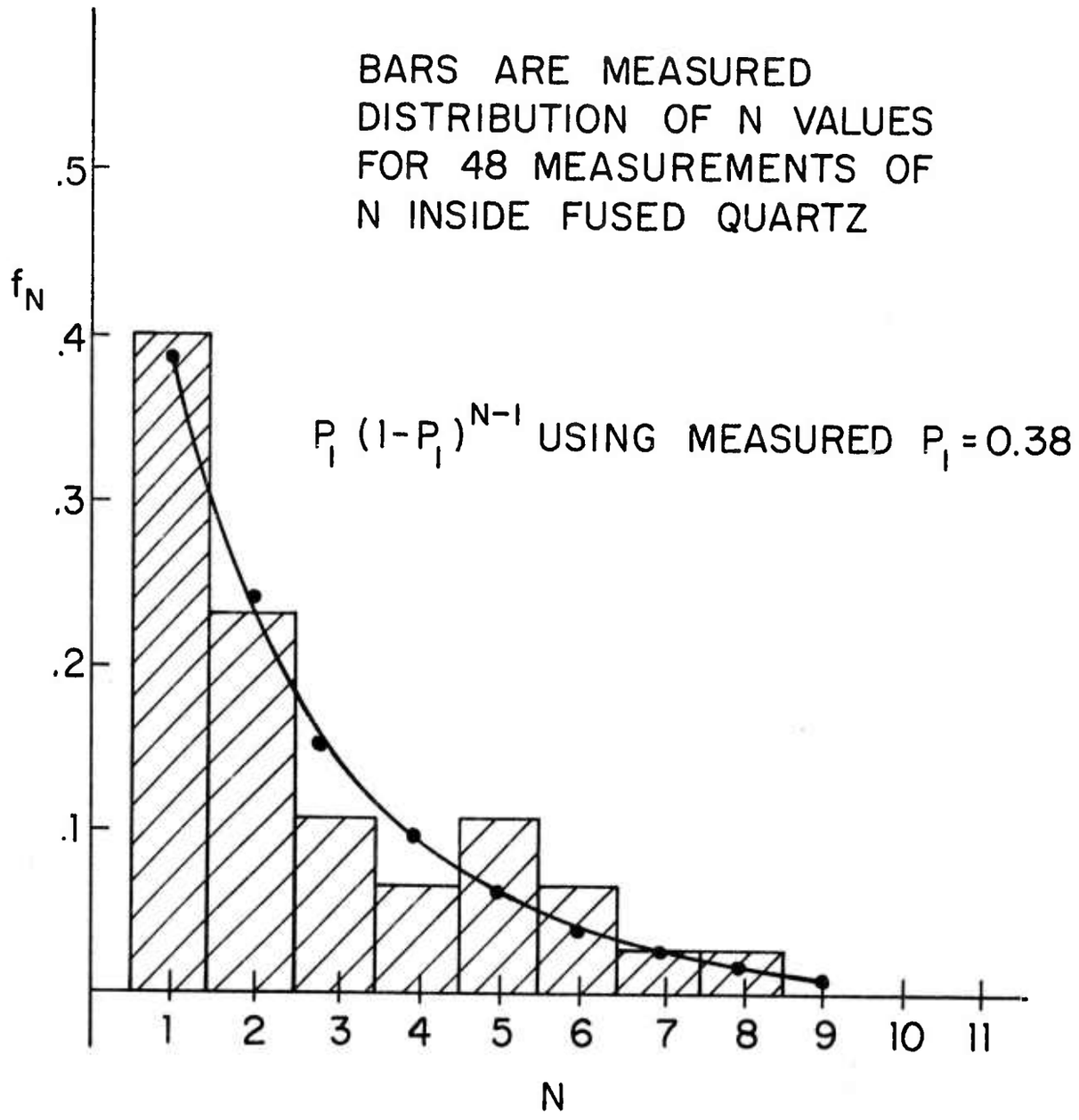

Fig. 2 Comparison of Measured f_N with $p_1(1-p_1)^{N-1}$ for Intrinsic Bulk Damage in Fused Quartz.

f_N is the fractional number of times N pulses where required to produce damage

p_1 is the measured damage probability

$$\Delta = \sum_{N=1}^{N_{max}} (f_N - p_1(1 - p_1)^{N-1})^2 \qquad (4)$$

In the case of Fig. 2, $p_1 = 0.380$ gives $\Delta = 5.67 \times 10^{-3}$ and the minimum value of Δ, 5.64×10^{-3} is obtained for $p_1 = 0.374$. The difference in these two values of p_1 is only 1.6 percent and the difference in the total squared error is only $\sim 1/2$ percent. At a given power level, then, p_1 has the same value for each laser pulse, and a sufficient number of positions have been probed in the sample to accurately measure p_1. Similar excellent agreement between these two choices of p_1 is also obtained for bulk damage in other materials.

Data such as shown in Fig. 2 which are taken from bulk measurements, are not subject to objections concerning either dust particles settling out of the air to give rise to damage statistics or focusing irregularities. These results, with the support of the statistics of breakdown dynamics discussed below, demonstrate that the statistics are not caused by spatial inhomogeneities in the sample's surface or fluctuations in the laser output. They must result from the intrinsic probabilistic nature of the bulk damage process itself.

Using the procedure described in Section B-3, data for intrinsic breakdown starting times such as shown in Fig. 3 was obtained. A single longitudinal TEM_{00} mode, Q switched ruby laser[16] produced these results inside a sample of NaCl under conditions which precluded catastrophic self-focusing.[3] The breakdown starting time can be measured from such photos to an accuracy of $\pm$ 0.05 times the oscilloscope sweep speed in nsec/cm. These data show that inside NaCl breakdown can occur at, before, or after the peak of the laser pulse. Fig. (3c), where damage occurs after the peak of the pulse, demonstrates unequivocally that the intrinsic breakdown process on this time scale does not have a unique intensity threshold. A case where the first pulse incident at a particular place in NaCl did not produce damage but a second, identical pulse, incident at the same position five seconds later did cause damage is shown in Fig. 4. Figs. 3 and 4 are striking examples of the non-threshold-like behavior

a) 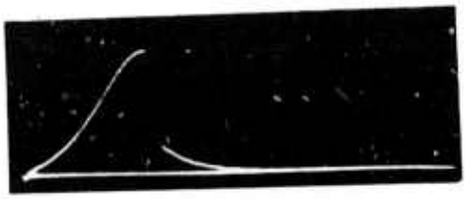

Damaged when the peak laser field was reached
$E_{Damage}/E_{Peak} = 1$

b) 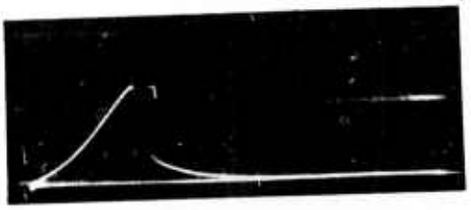

Damaged before the peak laser field was reached
$E_{Damage}/E_{Peak} = 0.896$

c) 

Damaged after the peak laser field was reached
$E_{Damage}/E_{Peak} = 0.954$

d) 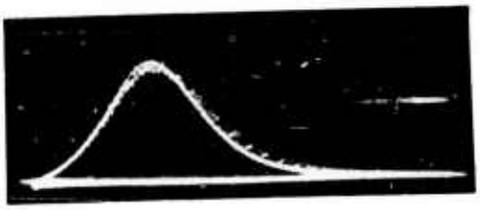

3 successive pulses
no damage
$E_{Peak} \equiv 1$ (Arbitrary units)

10 nsec

A TEM_{00} mode ruby laser with total pulse energy of 0.3 mJ was focused inside the inclusion free sample with a 14mm focal length lens

Fig. 3 The Occurrence of Internal Damage in NaCl Due to Ruby Laser Irradiation. The laser intensity transmitted through the sample is shown in these photos.

PBN-72-543

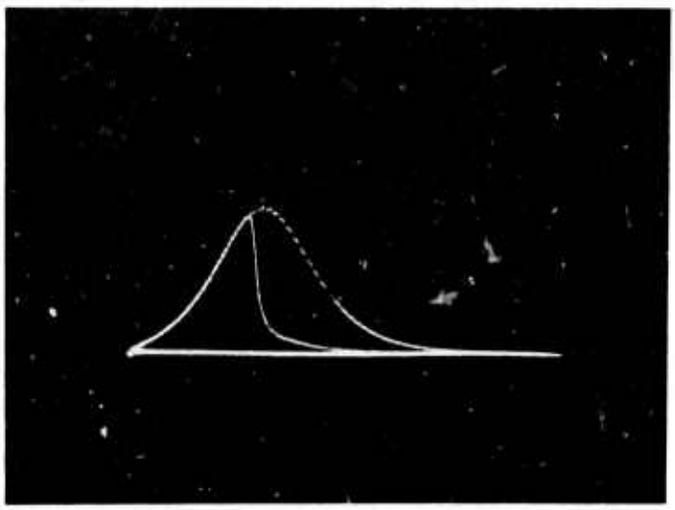

10 nsec

Fig. 4 Intrinsic Bulk Damage Occurring in NaCl on the Second of Two Ruby Laser Pulses. Five seconds passed between pulses.

59

of the breakdown starting time for bulk damage. Note that Fig. 4 also shows that the statistical nature of internal damage is not caused by point-to-point material inhomogeneities but by some probabilistic property of the breakdown process itself.

The distributions of breakdown starting times for both surface and bulk 1.06 μm damage to fused quartz are shown in Fig. 5. These distributions have the same characteristics as those reported by Bass and Barrett for entrance surface damage.[7] The breakdown can begin at any time over a relatively long interval which includes times after the peak intensity in contrast to the very sharply defined breakdown starting time expected for a threshold-like process. The most probable time for damage is in all cases before or at the instant of maximum intensity or optical field, and as the applied field is reduced (p_1 is lowered), the time of maximum damage probability shifts to the peak of the pulse (compare Figs. 5b and c.) These qualitative properties were shown in Ref. 7 to be explained by the probabilistic point of view from which Eq. 3 for g(t) was derived.

In Ref. 3 the intrinsic bulk damage mechanism for NaF and several other alkali-halide crystals was shown to be electron avalanche breakdown at 1.06 μm as well as at 10.6 μm and d.c. Similar experiments[13] indicate that this is also true at ruby frequency even though the avalanche may no longer be in its d.c. limit. The damage process in NaF at 0.69 μm, as shown in Fig. 6 has a statistical distribution of starting times. This is additional reason to examine in the next section damage starting time fluctuations for an avalanche breakdown mechanism.

V. DISCUSSION

A. The Importance of Irradiating a Small Volume

The statistical properties of laser induced damage were observed in these and other measurements because self-focusing had been eliminated and the laser beam was tightly focused by an aberration-free lens into a very small volume of the medium. If the strongly irradiated volume is taken to be approximately the focal depth ($\sim$ 200 μm) times the focal spot area

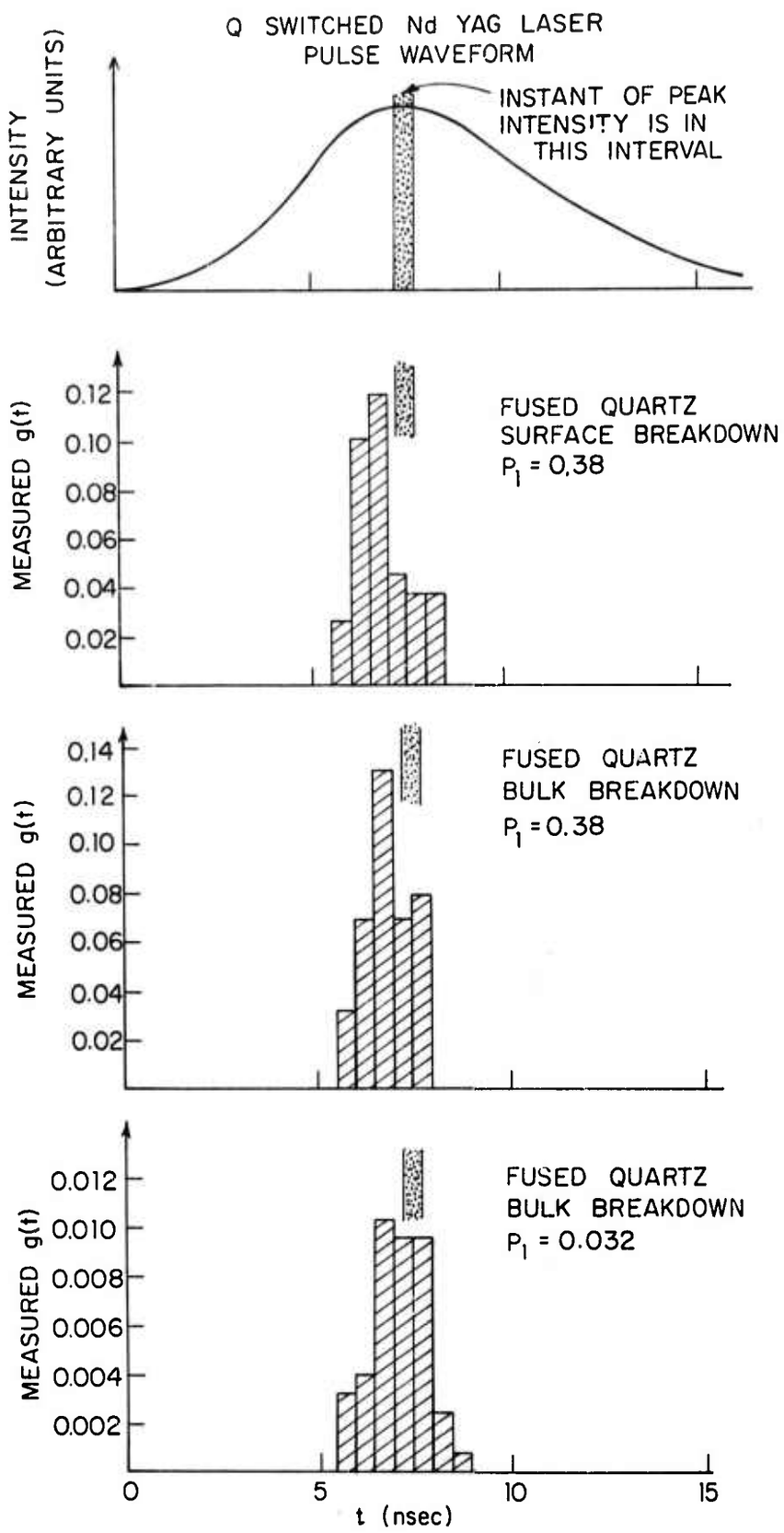

Fig. 5 Measured Distributions of Breakdown Starting Times for Fused Quartz Using Nd:YAG Laser Irradiation.

61

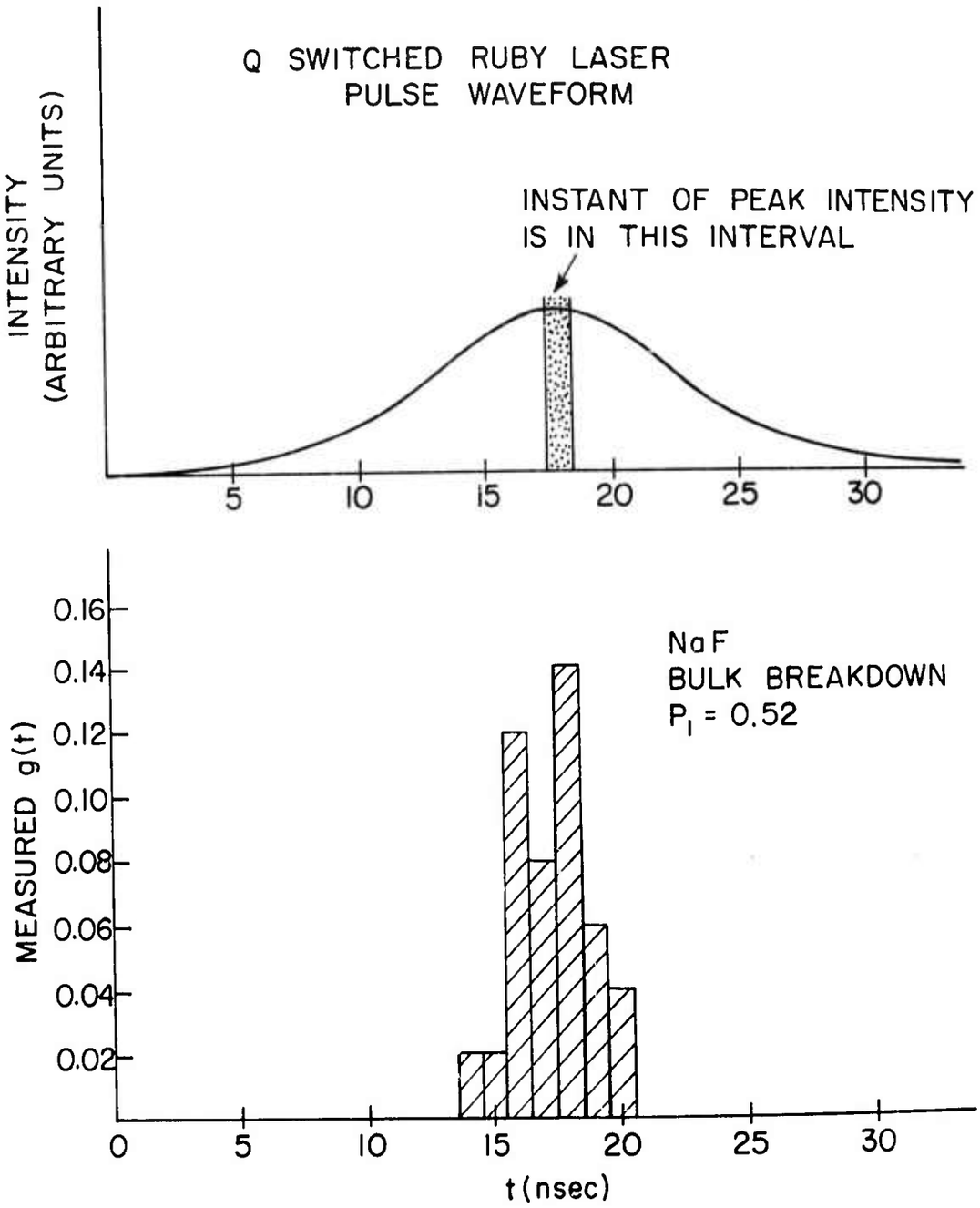

Fig. 6 Measured Distribution of Breakdown Starting Times for NaF Using Ruby Laser Irradiation.

($\sim$ 20 μm dia), then the maximum volume sampled by any one laser pulse in a bulk damage test was $\sim 5 \times 10^{-8}$ cm^3. This small volume generally does not contain large absorbing inclusions,[17] and so whatever damage occurs should be caused by an intrinsic process. In any case, the technique described in Sec. B-3 for distinguishing between intrinsic and non-intrinsic damage events was always employed to prevent us from including the latter in our data. These experimental precautions made possible this study of an intrinsic damage process and detection of its statistical nature.

In contrast to our experiments, those which employ large diameter laser beams ($\gtrsim$ 0.1 mm) may generally irradiate at least one absorbing inclusion and therefore actually measure inclusion induced damage.[11, 12] This type of damage process would not show the statistical properties we have observed and would lead one to report a damage threshold. For such measurements there would actually be a sharp damage threshold but it would not be that of an intrinsic process.

Bass and Barrett[1, 7] pointed out that directly comparable surface damage probability measurements could only be obtained from experiments in which the irradiated area (volume) were the same. This was necessary in order to ensure that the numbers of potential starting electrons irradiated were equal. If this number increased, then the probability for at least one damaging avalanche to begin and develop increased. It was shown that the interval in power density over which the damage probability changed from say 10^{-3} to 1 decreased with increased irradiated area (volume).[7] For sufficiently large irradiated volumes then, this interval in power density would be so small that one would simply miss the statistics and erroneously conclude that a sharp threshold for damage existed.

B. An Analysis of the Distribution of Breakdown Starting Times

In Eq. (3) the distribution of breakdown starting times is given as

$$g(t) = h(t) \exp\left(-\int_0^t h(t')dt'\right)$$

where h(t) is the probability per unit time that the laser field causes breakdown. If h(t) can be expressed quantitatively, then g(t) can be computed and compared with data such as that in Figs. 5 and 6. The measurements by Bass and Barrett[1] of the relationship between damage probability and optical field strength suggest that in a field, E(t), the damage rate should be of the form

$$h(t) = A_0 \exp(-K/E(t)). \tag{5}$$

A_0 is a normalization constant and K is the experimentally determined quantity in Eq. 2. E(t) is determined from the peak laser field, E_0, and the electric field waveform.

Eq. 5 would be the appropriate expression for h(t) if a damaging avalanche could form for all values of E(t). However, for values of E(t) less than some minimum field, E_{min}, the time required for a damaging avalanche to form will exceed the pulse duration. At such fields the damage rate must be zero. On the other hand, damage can occur when $E(t) \geq E_{min}$. For a pulsed field which reaches E_{min} at t_{min} and falls below E_{min} at t_{max}, Eq. 5 should be replaced by

$$h(t) = \begin{cases} 0 & 0 < t < t_{min} \\ A_0 \exp(-K/E(t)) & t_{min} \leq t \leq t_{max} \\ 0 & t_{max} < t \end{cases} \tag{6}$$

This expression assumes that between t_{min} and t_{max} the avalanche formation time is negligibly small (i.e. $\leq$ 0.1 nsec). When Eq. 6 is used to compute g(t), the statistics are implicitly assumed to arise from the chance manner in which avalanches are started. t_{min} and t_{max} can be chosen from the experimentally measured form of g(t). Alternatively E_{min} can be approximated by the smallest field which was observed to produce damage in a given material

and t_{min} and t_{max} obtained from the electric field waveform. This second manner of estimating t_{min} and t_{max} is independent of g(t) and is the one used in our computations of the starting time distributions. As another alternative, one can attempt to compute the applied field necessary to reduce the avalanche formation time to a small fraction of a nanosecond and select t_{min} and t_{max} accordingly.[18, 19]

In order to compute g(t) it is now necessary to find the value of A_0 for the material in question. To do this we consider v(t), the fractional number of tests where no damage has occurred by the time t. When the laser pulse is completed, v(t) must equal $1 - p_1$, the probability that no damage was produced.

In Ref. 5 v(t) is given as

$$v(t) = \exp\left(-\int_0^t h(t')dt'\right). \tag{7}$$

Combining Eqs. 6 and 7 and the final condition on v(t), we find that

$$A_0 = \left(-\ell n\,(1 - p_1)\right) \Big/ \left(\int_{t_{min}}^{t_{max}} \exp\left(-K/E(t)\right)\, dt\right). \tag{8}$$

If the damage mechanism and the source of damage statistics assumed in writing Eq. 6 is consistent with the experimental data, then A_0 should be a constant for a particular material.

Figs. 7a and b show the computed and experimentally measured distributions of breakdown starting times when two different applied fields produce bulk damage in fused quartz. The parameters appropriate to these cases are summarized in Table I. For these computations the value of E_{min} was taken to be the lowest field at which any damage occurred. Thus, the values of t_{min} and t_{max} used to compute g(t) were experimentally determined and independent of g(t).

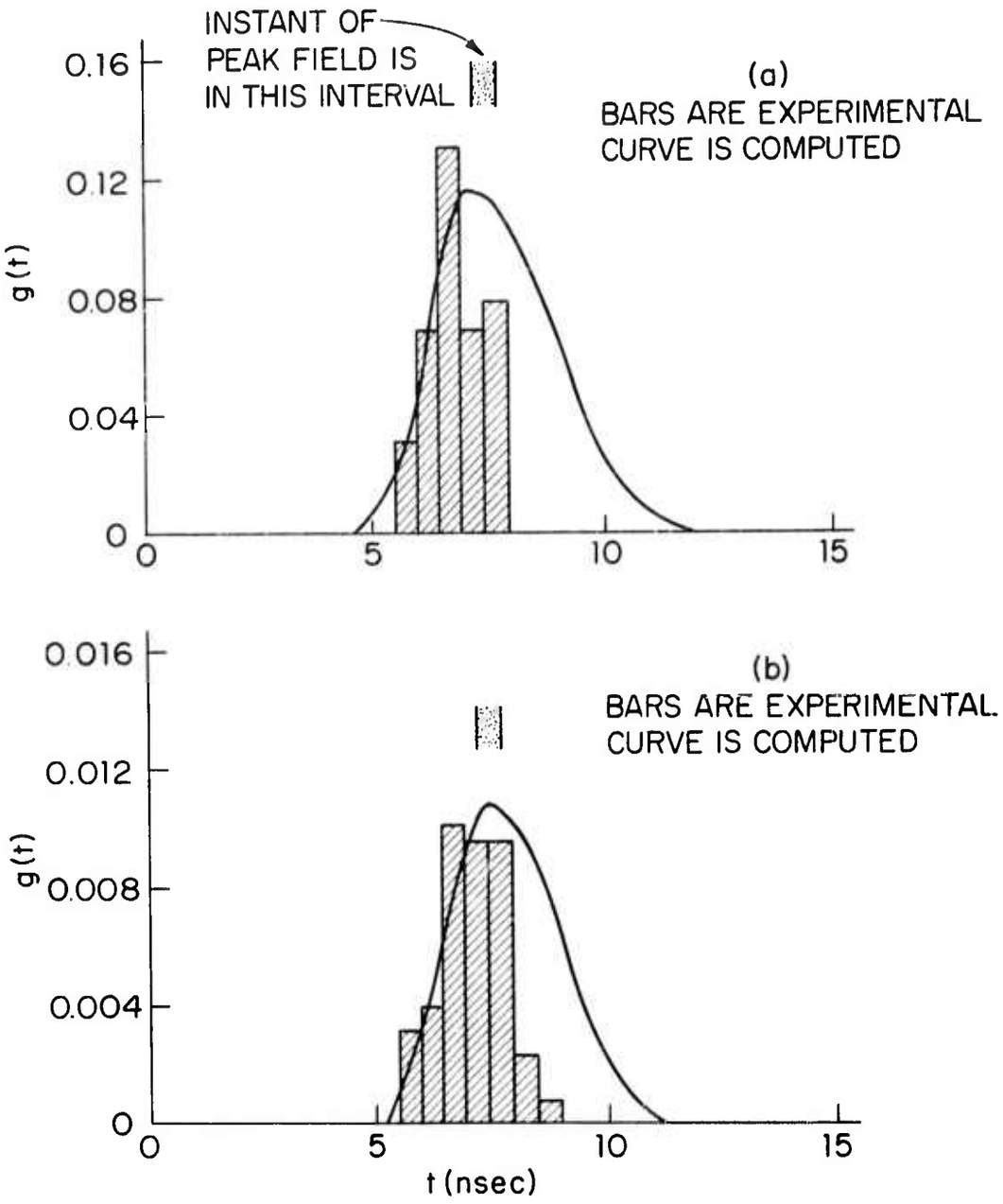

Fig. 7 Measured and Calculated Distributions of Breakdown Starting Times for Bulk Damage in Fused Quartz using a Nd:YAG Laser. The parameters relevant to these figures are listed in Table I.

TABLE I

Parameters Used to Calculate g(t) in Fig. 7

Materials Studied: Fused Quartz

	Experimentally Determined				Calculated
	p_1	E_o (a)	K	A_o	$\int_{t_{min}}^{t_{max}} g(t)dt$
Fig. 7a	0.380	7.3×10^8 V/m	71×10^8 V/m	2599.8	0.373
Fig. 7b	0.032	5.7×10^8 V/m	71×10^8 V/m	2776.4	0.031

(a) E_o is the peak value of the applied optical field within the medium. The electric field waveform is the square root of the waveform in Fig. 5a.

Fig. 7 shows good qualitative agreement between our model and the experimental data. There is, however, some deviation between the two for times after the peak of the laser pulse; that is, for times when E(t) decreases to E_{min}. As mentioned above, the form we used for h(t) when $t_{min} \leq t \leq t_{max}$ assumed that the avalanche formation time was negligibly small. However, as E(t) decreases the formation time must increase at an increasing rate. This means that at such times h(t) will be decreased over the value in Eq. 6 at a rate which increases as $t \rightarrow t_{max}$. The computed values of g(t) will be reduced accordingly. The effect of allowing for finite formation time, then, would make the computed curves in Fig. 7 decrease more rapidly for times past the peak of the pulse. The qualitative agreement in that figure would therefore improve.

The agreement between model and experiment which has already been achieved is strengthened by the results in Table I. There we find that both cases were computed with nearly the same value of A_0. The $\pm$20 percent experimental error in K and E_0 can easily account for the 10 percent difference between the A_0's. As a further check on the consistency of our model, we also computed the time integral of g(t) since, by definition, it should equal the experimentally determined value of p_1. In Table I we find that this condition is also satisfied. We note that these computations do not involve any "fitted parameters" and as such are a useful test of the consistency of our model with the experimental data.

VI. CONCLUSIONS

Experimental evidence has been presented for the statistical nature of the laser-induced intrinsic bulk damage process in transparent solids. This point of view was supported by the statistical nature of the measured distributions of laser induced breakdown starting times. A simple model for the damage process in which an electron avalanche breakdown having statistical starting properties was the assumed damage mechanism was found to be consistent with the experimental data.

An important new technique for identifying damage events caused by intrinsic processes was developed to facilitate the studies of damage dynamics. It was based on the observation that there is a very high correlation between a very rapid and well-defined transmitted pulse attenuation and the occurrence of damage due to an intrinsic process. In addition, the necessity of irradiating only a small volume of the medium in order to avoid measuring inclusion induced laser damage was described.

The present work confirms the existence of a statistical nature to the laser induced intrinsic damage process and supports the notion that the damage mechanism both on the surface and in the bulk is an electron avalanche breakdown with statistical starting properties.

ACKNOWLEDGMENTS

The authors wish to thank D.P. Bua for designing the excellent stable lasers used to obtain the data. Valuable discussions of damage mechanisms were held with L.H. Holway, F.A. Horrigan and H.H. Barrett.

VII. REFERENCES

1. M. Bass and H. H. Barrett, "Avalanche Breakdown and the Probabilistic Nature of Laser-Induced Damage," IEEE J. of Quantum Elec., QE-8, 338 (March 1972).

2. E. Yablonovitch, "Optical Dielectric Strength of Alkali-Halide Crystals Obtained by Laser Induced Breakdown" Appl. Phys. Letters 19, 495 (Dec. 1971).

3. D. W. Fradin, E. Yablonovitch and M. Bass, "Confirmation of an Electron Avalanche Causing Laser-Induced Bulk Damage at 1.06 Microns" to be published, Applied Optics (April 1973) and in the Proceedings of the 1972 ASTM-NBS Symposium on Laser Damage, Boulder, Colo. (June 1972).

4. R. A. Wijsman, "Breakdown Probability of a Low Pressure Gas Discharge," Phys. Rev. 75, 833 (March 1949).

5. H. Kawamura, H. Ohkura and T. Kikuchi, "The Statistical Time Lag of the Dielectric Breakdown of Mica, Glass and KCl," J. Phys. Soc. of Japan 9, 541 (July 1954).

6. J. J. O' Dwyer, "The Theory of the Dielectric Breakdown of Solids" (Oxford University Press, London, 1964), and references therein.

7. M. Bass and H. H. Barrett, "Laser-Induced Damage Probability at 1.06 and 0.69 μm" to be published, Applied Optics (April 1973) and in the Proceedings of the 1972 ASTM-NBS Symposium on Laser Damage, NBS Special Publication 372 (1972).

8. A. Von Hippel, "Molecular Science and Molecular Engineering" (Technology Press of MIT, Cambridge, Mass. and John Wiley and Sons, New York, N. Y. 1959) Ch. 5.

9. A. G. Chynoweth, "Ionization Rates for Electrons and Holes in Silicon" Phys. Rev. 109, 1537 (March 1958) and "Uniform Silicon p-n Junctions. II. Ionization Rates for Electrons" J. Appl. Phys. 31, 1161 (July 1960).

10. W. Shockley, "Problems Related to p-n Junctions in Silicon," Czech. J. Phys. B11, 81 (1961) and Solid-State Electron. 2 35 (Jan. 1961).

11. R. W. Hopper and D. R. Uhlman, "Mechanisms of Inclusions Damage in Laser Glass," J. Appl. Phys. 41, 4023 (Sept. 1970).

12. Yu. K. Danileiko, A. A. Manenkov, A. M. Prokhorov, and V. Ya. Khaimov-Mal'kov, "Surface Damage of Ruby Crystals by Laser Radiation," Zh. Eksp. Theor. Fiz. 58, 31 (Jan. 1970)[Sov. Phys. JETP 31, 18 (July 1970)] .

13. D. W. Fradin and M. Bass, "Electron Avalanche Breakdown Induced by Ruby Laser Light," to be published, Appl. Phys. Lett. (March 1973).

14. F. A. Horrigan, private communication. (September 1970).

15. I. A. Fersman, L. D. Khazov and G. P. Tikhomierov, "Stages of Laser-Radiation Damage to the Surface of a Transparent Dielectric," Sov. J. of Quantum Elect. 1, 248 (Nov. 1971).

16. D. Bua, D. W. Fradin and M. Bass, "A Simple Technique for Longitudinal Mode Selection," IEEE J. of Quant. Elect., QE-8, 916 (Dec. 1972).

17. O. J. Guentert, private communication. An electron microprobe survey of the surface of one of the pieces of fused quartz used in the damage probability measurements revealed no more than $\sim$ 100 impurities per cm^2. The microprobe could sense impurities with diameters $\geq$ 1 μm and to a depth of 5 μm. Since the sample had been conventionally polished and cleaned some of these impurities were not intrinsic to the material. Thus the inferred impurity density, $2 \times 10^5/cm^3$, is an overestimate of the density of this size impurities to be found in the bulk material.

18. E. Yablonovitch and N. Bloembergen, "Avalanche Ionization and the Limiting Diameter of Filaments Induced by Light Pulses in Transparent Media," Phys. Rev. Letters 29, 907 (Oct. 1972).

19. L. Holway, private communication (October 1972).

20. C. R. Guiliano and J. H. Marburger, "Observation of Moving Self Foci in Sapphire," Phys. Rev. Letters 27, 905 (Oct. 1971).

21. N. Bloembergen, "The Stimulated Raman Effect," Am. J. Phys. 35, 989 (Nov. 1967).

22. C. C. Wang and E. L. Baardsen, "Study of Optical Third-Harmonic Generation in Reflection," Phys. Rev. 185, 1079 (Sept. 1969).

23. B. E. Newnam and L. G. DeShazer, "Direct Nondestructive Measurement of Self-Focusing in Laser Glass," p. 113 NBS Special Publication 356 Damage in Laser Materials: 1971 (Nov. 1971).

J. M. McMahon, "Damage Studies with Subnanosecond Pulses" N.B.S. Special Publication 372, p. 100, Damage in Laser Materials: 1972 (December 1972).

24. Y. R. Shen, "Electrostriction, Optical Kerr Effect, and Self-Focusing of Laser Beams," Phys. Lett. 20, 378 (March 1966).

25. The response time of electrostriction is the time required for an acoustical wave to travel across the radius of the laser beam. It is less than the duration of the input pulses for the present work. If this were not the case, n_{2s} would be decreased and P_c correspondingly increased. In the extreme transient case, the critical power for electrostrictive self-focusing is proportional to d^2 and it is more accurate to speak of a critical intensity for self-focusing.

26. Special Optics Corp., Cedar Grove, N. J. 07009.

APPENDIX A TESTS FOR THE ABSENCE OF SELF-FOCUSING

In early experiments on laser-induced bulk damage, significant beam intensification from self-focusing was normally present.[20] Because of this intensification, reported measurements of damage were actually measurements of self-focusing thresholds. It has been recently shown,[3] however, that catastrophic self-focusing can be eliminated and the effects of beam distortion from the index nonlinearity made negligible by confining laser input powers to well below the threshold power, P_c, for catastrophic self-focusing. The high intensities necessary to induce damage are reached by strong external focusing using optics with negligible aberrations.

The technique for verifying the absence of self-focusing is described in detail in Ref. 3. To illustrate how this technique was used in the present work, we consider the calculations and measurements made for fused silica.

For solids there are two contributions to the self-focusing index nonlinearity. The first is electronic and as determined by measurements of third-harmonic generation[21,22] is normally quite small in transparent crystals. For amorphous materials the electronic contribution can be quite large because the band structure is severely distorted, and, in fact, measurements in various glasses including fused silica yield values of n_{2e} as high as 2×10^{-13} esu.[13] The second contribution is from electrostriction, and for cubic materials (except perovskites), liquids, and amorphous materials, its steady-state value can be found quite accurately from the Clausius-Mosotti equation.[24] For fused silica $n_{2s} \approx 2 \times 10^{-13}$ esu, and the process is in the steady-state for the conditions of the measurement.[25]

Summing the two nonlinear indices gives a total n_2 of about 4×10^{-13} esu and a calculated critical power of about 2×10^6 watts at 1.06 μm. During the actual measurements reported in the text, the probe power was confined to values less than 0.2×10^6 watts, so that catastrophic self-focusing should not have occurred and beam intensification should have been small.

The experimental check for the absence of self-focusing consisted of measuring optical breakdown strength of fused silica using two different lenses. One with a focal length of about 13 mm and the other about 5.2 mm. Both lenses were designed for minimum spherical aberrations, but only for the first were the aberrations truly negligible.[26] A total power of 0.2×10^6 watts was necessary to produce damage with a probability 0.5 using the first lense and 0.08×10^6 watts using the second. These powers were compared to the corresponding powers for NaCl. Previous work[3] had established that with the focusing conditions described above, there was no catastrophic self-focusing in NaCl and that, in fact, any beam distortions from the index nonlinearity were immeasurably small.

Because there was no self-focusing present, the input powers for NaCl scaled as the focal lengths when a small correction had been made for aberrations in the 5.2 mm focal length lens. In the absence of any self-focusing, the corresponding powers for fused silica would have to scale in precisely the same manner since the laser transverse structure and all properties of the focusing system (including aberrations) were the same as for NaCl. As expected, the scaling was identical. If the input powers for fused silica had exceeded the actual value of P_c, then the same input power which produced damage with the second lense would have produced damage with the first. Measurable beam distortion, which can occur for powers less than P_c, would also have changed the scaling.[3]

Experiment thus confirmed the theoretical calculations: at the input powers used in the present work, catastrophic self-focusing was absent from fused silica, and beam distortion from the index nonlinearity was negligible.

IV. CONFIRMATION OF AN ELECTRON AVALANCHE CAUSING LASER-INDUCED BULK DAMAGE AT 1.06 MICROMETERS

A. Introduction

In this section the first unambiguous measurement of laser-induced bulk damage in nonabsorbing media are described in the paper "Confirmation of an Electron Avalanche Causing Laser-Induced Bulk Damage at 1.06 Micrometers." The laser induced breakdown phenomenon may be described by the following sequence of steps: First, absorption occurs at microscopic absorbing inclusions or by means of an intrinsic nonlinear absorption process such as multiphoton absorption or electron avalanche breakdown. Second, the energy absorbed from the beam heats the medium, and, finally, a thermally induced fracture or a phase change occurs which in solids results in permanent material damage.

Experimental studies of intrinsic laser breakdown processes can be seriously misinterpreted if catastrophic self-focusing occurs in the medium or if absorbing inclusions are present in the irradiated volume. Since self-focusing results in a greatly enhanced beam intensity, experiments in which it occurs cannot accurately measure the level of irradiation for intrinsic laser breakdown. The apparent bulk damage thresholds deduced from such experiments are a measure of threshold for self-focusing and not for laser breakdown. The presence of absorbing inclusions having diameters $>0.1\,\mu m$ in the irradiated volume can dominate the damage process. Such inclusions are probably the most common cause of laser damage especially when large volumes are irradiated. The experimental data in this section therefore was recorded in a manner which permitted accurate identification of inclusion breakdown as distinguished from intrinsic breakdown in order to study the latter unambiguously.

For a laser beam power well below the critical power for self-focusing, catastrophic beam collapse cannot occur and corrections due to the index nonlinearity are quite small. The high intensities necessary for laser breakdown can then be achieved at low powers by strong external focusing which,

as an additional advantage, often allows the probe beam to avoid inclusions. Microscopic inspection of the damaged volume can then be used to distinguish inclusion from intrinsic breakdown. It should be noted that the procedure of using strongly focused beams is very similar to that used in our surface damage studies and so facilitates the bulk and surface damage comparisons described in Sec. VI.

Crystals in the alkali halide family were chosen for these laser breakdown studies because they are useful infrared optical materials and are transparent from about 15 μm to about 0.2 μm so that linear absorption does not present a problem. In addition they have been studied extensively to determine their response to applied fields at dc and at 10.6 μm, so that comparative studies can be made.

In this section the data we present was obtained under experimental conditions which preclude both self-focusing and absorbing inclusions as the causes of damage. It shows striking similarities between 1.06 μm, 10.6 μm and dc breakdown measurements indicating that an avalanche breakdown process, essentially in its dc limit, is responsible for intrinsic damage at 1.06 μm.

Since self-focusing may reach threshold before breakdown at optical frequencies, it is important to understand both the conditions under which catastrophic self-focusing occurs and the corrections from the index nonlinearity when a catastrophic focus is prevented. For this reason an analysis of self-focusing is outlined in the appendices of the paper, and the general results relevant to our measurements are discussed. Confirming theoretical predictions that catastrophic self-focusing is absent, two important experimental checks are also reported.

B. CONFIRMATION OF AN ELECTRON AVALANCHE CAUSING LASER-INDUCED BULK DAMAGE AT 1.06 MICRONS †

D. W. Fradin* and Eli Yablonovitch*
Gordon McKay Laboratory, Harvard University
Cambridge, Mass. 02138

and

Michael Bass Δ
Raytheon Research Division
Waltham, Mass. 02154

ABSTRACT

Measurements have been made of intrinsic optical bulk breakdown in ten alkali halides at 1.06 μm, and in one at 0.69 μm. By comparing the results to previously reported experiments conducted at 10.6 μm and at direct current, it has been possible to identify the damage mechanism as electron avalanche breakdown. Self-focusing has been controlled by restricting the probe powers to well below the critical powers for catastrophic self-focusing, and damage from inclusions has been distinguished from intrinsic damage. Implications of this work for surface damage studies are explored.

---

† A report of this work under the title "Comparison of Laser-Induced Bulk Damage in Alkali-Halides at 10.6, 1.06, and 0.69 Microns" was presented at the 1972 ASTM-NBS Symposium on Laser Damage in Boulder, Colorado.

* Supported by the Joint Services Electronics Program at Harvard University under Contract No. N00014-67-A-0298-0006.

Δ Supported by the Advanced Research Projects Agency of the Department of Defense and was monitored by the Air Force Cambridge Research Laboratories under Contract No. F19628-70-0223.

1. Introduction

When the intensity of light propagating in an initially transparent medium is sufficiently high, the medium will be disrupted. This phenomenon, called laser-induced breakdown,[1] may be described by the following sequence of steps: First, absorption occurs at microscopic absorbing inclusions[2] or by means of an intrinsic nonlinear absorption process such as multiphoton absorption or electron avalanche breakdown. Second, the energy absorbed from the beam heats the medium, and, finally, a thermally induced fracture or a phase change occurs which in solids results in permanent material damage.

Experimental studies of intrinsic laser breakdown processes can be seriously misinterpreted if catastrophic self-focusing occurs in the medium[3] or if absorbing inclusions are present in the irradiated volume. Since self-focusing results in a greatly enhanced beam intensity, experiments in which it occurs cannot accurately measure the level of irradiation for intrinsic laser breakdown. The apparent bulk damage thresholds deduced from such experiments are a measure of threshold for self-focusing and not for laser breakdown. The presence of absorbing inclusions having diameters $> 0.1\mu m$ in the irradiated volume can dominate the damage process.[2,4] Such inclusions are probably the most common cause of laser damage especially when large volumes are irradiated. Experimental data must therefore be recorded in a manner which permits accurate identification of inclusion breakdown as distinguished from intrinsic breakdown in order to study the latter unambiguously.

Recent work at $10.6\ \mu m$ indicates that intrinsic damage can be isolated.[5] For laser beam power well below the critical power for self-focusing, catastrophic beam collapse cannot occur and corrections due to the index nonlinearity are quite small.[6,7] The high intensities necessary for laser breakdown can be achieved at low powers by strong external focusing which, as an additional advantage, often allows the probe beam to avoid inclusions. Microscopic inspection of the damaged volume can then be used to distinguish inclusion from intrinsic breakdown.

The alkali halide family is a natural choice for laser breakdown studies. Besides being useful infrared optical materials, these compounds are transparent from about 15 μm to about 0.2 μm so that linear absorption does not present a problem. In addition, because they have been studied extensively to determine their response to applied fields at d.c.[8] and at 10.6 μm,[5] comparative studies can be made.

In this paper we present measurements of intrinsic bulk laser breakdown in ten different alkali-halide crystals at 1.06 μm, which were obtained under experimental conditions which preclude both self-focusing and absorbing inclusions as the causes of damage. The data show striking similarities among 1.06 μm, 10.6 μm and d.c. breakdown measurements indicating that an avalanche breakdown process,[9] essentially in its d.c. limit, is responsible for intrinsic damage at 1.06 μm.

Since self-focusing may reach threshold before breakdown at optical frequencies,[3] it is important to understand both the conditions under which catastrophic self-focusing occurs and the corrections from the index nonlinearity when a catastrophic focus is prevented. For this reason an analysis of self-focusing is outlined in the Secs. 7, 8, 9, and the general results relevant to our measurements are discussed in Sec. B-2a. Confirming theoretical predictions that catastrophic self-focusing is absent, two important experimental checks are then reported. We present in Sec. B-3 the results of a series of carefully controlled experiments in which intrinsic bulk damage in alkali halides was measured. A well-characterized TEM_{00} mode laser beam with total power more than one order-of-magnitude below calculated critical powers for self-focusing was tightly focused within the samples in order to obtain the high intensities needed for damage. Then, in Sec. B-4 we show how the experimental results can be fully explained in terms of avalanche breakdown.

2. Experiments

a. The Lasers and Beam-Handling Optics

Figure 1 shows schematically the principal features of the laser damage source. The experiments were performed using a pulse pumped, electro-optically Q switched, Nd:YAG laser. Some important properties of this device

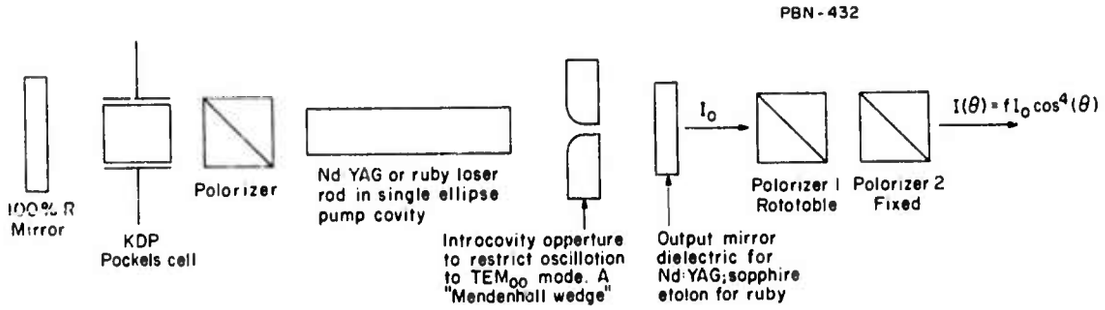

Fig. 1 Laser and Variable Attenuator Configuration for Damage Studies.

are summarized in Table I. Figure 2 shows that the Nd:YAG laser output was in the lowest order Gaussian or TEM_{00} mode.

The time structure of the pulses from the laser appears reasonably smooth when viewed with a fast photodiode oscilloscope combination having a measured risetime of 0.5 nsec. We have conducted Fabry-Perot studies and have found that normally fewer than four adjacent modes are oscillating simultaneously, so that the time structure is effectively fully resolved. Longitudinal mode selection is accomplished by aligning the faces of plane parallel laser rod parallel to the 100% R resonator mirror. Despite the low reflectivity of the anti-reflection coated rod surfaces, the high gain of the rod and the high reflectivity of the mirror create an effective intracavity reflector.

To verify that the transverse mode structure on axis is constant with time, the center of the beam was sampled with a 25-micron pinhole and found to have the same time structure as the entire beam. The stability on axis was found to be superior to that of the spatially integrated power.

The breakdown data was taken by focusing through a 1/2-inch focal length lense to approximately 2 mm inside the samples. Care was taken to insure that spherical aberrations from both the lense and the plane entrance surface of the sample being tested were unimportant. A fast photodiode was used to monitor the transmitted light, and an energy monitor recorded the energy in each laser pulse.

The combination of one rotatable and one fixed polarizer resulted in a variable light attenuator which was highly sensitive, quite reproducible, and which did not affect the laser pulse's polarization, spatial distribution, or duration. If the fixed polarizer is oriented to transmit the laser polarization and if $\theta = 0^{o}$ is the angle of the rotating polarizer which gives maximum transmission through this attenuator, then the transmitted intensity at any other angle of rotation about the beam axis is

$$I(\theta) = bI_{o} \cos^{4}\theta \quad .$$

TABLE I

LASER PARAMETERS

Wavelength	Nd:YAG 1.06μm	Ruby 0.694μm
Energy TEM_{00} Mode	1.5 mj	2.0 mj
Beam Diameter at Output Mirror TEM_{00} Mode	0.8 mm	0.7 mm
Polarization	Linear	Linear
Pulse Repetition Rate	1 pps	1 pulse/5 sec
Pulse Duration in TEM_{00} Mode	4.7 nsec (FWHP)	14 nsec (FWHP)
Pulse to Pulse Energy Reproducibility	$\pm$ 7%	$\pm$ 10%

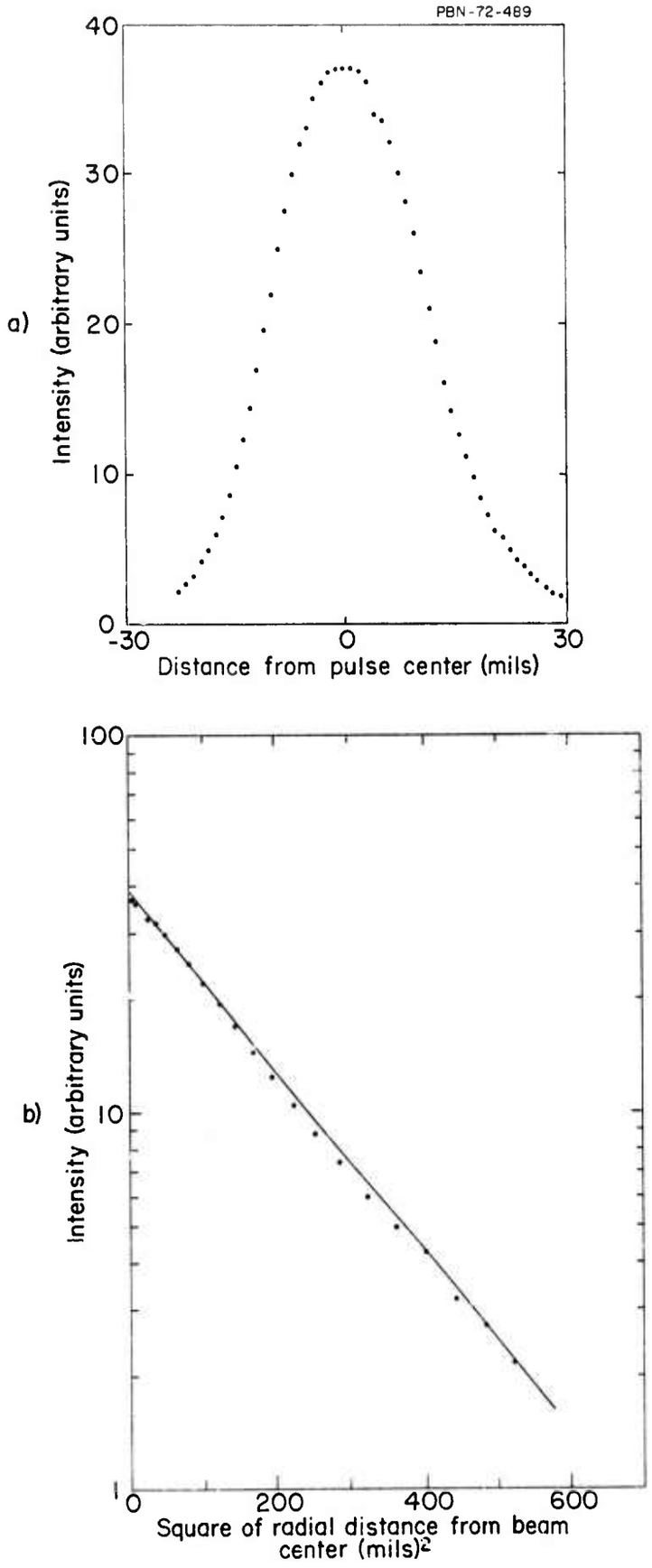

Fig. 2 Intensity Distribution of the YAG Laser as a Function of Radial Distance from the Beam Center at the Position of the Focusing Lens

I_o is the incident light intensity and b is the fraction transmitted when $\theta = 0^o$. Calibrated neutral density filters were often used in conjunction with the variable Glan attenuator.

b. Self-focusing

A laser beam propagating in a transparent medium induces an increase in the index of refraction by an amount proportional to the laser intensity. At powers in excess of some critical power this nonlinearity causes the intensity distribution to become unstable, and a catastrophic beam collapse results.

Self-focusing may occur as the result of a number of nonlinearities. In solids, for Q-switched laser pulses, the process which normally leads to the smallest value of critical power and hence dominates self-focusing is electrostriction.[6] This is the case for the alkali halides where thermal and electronic contributions to self-focusing are much smaller than the electrostrictive effect and can be neglected.[10,11]

An intense light wave whose power lies below a critical power, P_c, will not experience a catastrophic collapse in a nonlinear medium, because although focusing by self-action will always be present, diffraction acts in the opposite sense to cause divergence and dominates at such powers.[7] At powers sufficiently far below P_c, therefore, the intensity distortion due to the index nonlinearity can be treated as a constant perturbation on diffraction effects and usually neglected. These observations allow us to effectively eliminate self-focusing by restricting probe powers to well below calculated critical powers while focusing strongly by external optics to reach the field intensities necessary to cause optical damage.

Theoretical self-focusing parameters are defined and derived in the appendices where quantitative corrections from the index nonlinearity at powers below P_c are discussed. Table II summarizes the numerical results. The probe power is the experimental peak power and is more than one order of magnitude below P_c. From a purely theoretical viewpoint, therefore catastrophic self-focusing is impossible, and it can be shown that beam distortion from the

TABLE II

CALCULATED STEADY-STATE, SELF-FOCUSING PARAMETERS AND EXPERIMENTAL VALUES OF PULSE-WIDTHS AND PEAK POWER

	Wavelength (microns)	τ (10^{-9} sec)	t_p (10^{-9} sec)	$n_2 \times 10^{22}$ (mks)	P_{cr} (10^3 watts)	P_c (10^3 watts)	P_{input} (10^3 watts)
	10.6	5.5	200		48,000	175,000	120
NaCl	1.06	2.7	4.7	2.3	480	1,750	50
	0.69	2.0	14		204	746	26
	10.6	11.2	200		13,200	50,000	20
RbI	1.06	5.4	4.7	8.1	132	500	8.1
	0.69	4.0	14		56	203	—

For $P_{input} < P_c$ catastrophic self-focusing will not occur.

The 10.6μm data is taken from reference 6.

See appendices for definitions of τ, n_2, and P_{cr}. To convert n_2 to esu units, multiply by 0.91×10^9.

index nonlinearity introduces at most a few percent correction in the measured electric field strengths. If catastrophic self-focusing does occur, then the breakdown damage data is a measure of the critical powers rather than intrinsic breakdown field. The measured threshold intensity will then scale with the square of the calculated focal diameter if the process is steady-state and will depend on the pulse-width if the process is transient. (The diameter dependence in the steady-state results from the existence of a constant critical power P_c which does not vary with beam diameter.)

To test our belief that self-focusing was absent we conducted two experiments. In the first the relative field strength threshold for damage in NaCl was measured with three different focusing lenses, corrected for spherical aberrations, and having focal lengths of 1.4, 2.5 and 3.8 cm. The experiment was conducted at 1.06 μm. If steady-state self-focusing were present, the observed damage threshold would have scaled with the inverse of the focal length. It did not, and, in fact, to within 5 percent the field strength was independent of focal length. This effectively eliminated the possibility of steady-state self-focusing. Since $t_p/\tau \geq 1$ from Table II, self-focusing should not be transient. Eq. (A15) however, predicts the results observed when transient self-focusing is present. For this reason a measurement was made of the damage threshold as a function of pulse duration with the beam diameter held essentially constant.

By changing the pumping level for the YAG laser, we were able to extend the pulse width by a factor of 2.3 to 10.8 nsec. In addition, the breakdown strength at 0.69 μm was measured with ruby laser pulses of 14-nanosecond duration and a focused diameter 25 percent smaller than that obtained with the YAG laser. The same 1.3 cm focal length lense was used in all three measurements, and to compute the ruby value, we assumed the same transverse intensity variation as that present at 1.06 μm. To within 15 percent no change was noted in the threshold field despite the pulse-width dependence in Eq. (A15). The agreement for the ruby pulses was especially reassuring, because the critical power varies with wavelength squared. If transient self-focusing were present, we would have seen a change by a factor of 18 in the measured intensity -- an effect which would have been quite dramatic. A factor of nine comes from the pulse-width dependence of the transient critical power and a factor of 2 from the wavelength dependence.

Perhaps the best experimental check for self-focusing is the actual measurement of breakdown strengths. Self-focusing theory appears to be totally unable to account for the experimental results given below in which both relative and absolute values of breakdown strengths show striking similarities to 10.6 μm values. We thus conclude that prior to the onset of material damage, self-focusing has been effectively eliminated as a competing nonlinearity.

The possibility may exist that self-focusing occurs after a sufficient number of electrons have been generated to cause intense local heating of the sample. We note, however, that in our measurements any late developing nonlinearity is unimportant.

3. Experimental Measurements of Breakdown

a. Damage measurements at 1.06 μm

To measure the breakdown strengths of the alkali halides, we focused the laser beam approximately 2 mm into each sample and recorded the number of laser pulses necessary to produce internal damage at various power levels. In every case where damage occurred, a white spark was produced, and the damage was later carefully inspected with a microscope. Because of the small volume damaged by our highly focused 1.06 μm pulses (less than 2×10^{-5} mm^3), a large number of data points could be taken with each sample (40 to 100).

Defining threshold as that value of incident power necessary to produce intrinsic damage in a single shot for 50 percent of the positions probed[5], we calculated the rms, on-axis electric field at the measured threshold in NaCl. Corrections were made for reflections from various surfaces and the changes in the beam diameter due to the effect of the index nonlinearity. This was the

basic calibration, and all other values of threshold were measured relative to E_{NaCl}. In order to avoid errors from daily power fluctuations and possible alignment changes, a single sample of NaCl was tested with each alkali halide. It was readily determined that a slight misalignment of the focusing lens (14 mm focal length) had no measurable effect on the relative breakdown strengths.

Visual inspection and the breakdown statistics suggested that spatial inhomogeneities from inclusions were not affecting the results except in the single case of RbCl. Damage which we regarded as intrinsic consisted at each damage position of a single pointed region which began at the geometrical focus and extended a very short distance back toward the laser, increasing in cross-section to give a tear-drop appearance. A typical example is indicated in Fig. 3. In RbCl, on the other hand, regions with low breakdown thresholds consisted typically of one or more spherical voids randomly distributed about the focus (Fig. 4). A number of points, however, did appear visually to have intrinsic damage and were consistently more difficult to breakdown. These data points were used for the RbCl results.

Finally, a fast photodiode detector system with a 0.5 nsec risetime monitored the transmitted light as shown in Fig. 5 and was used to confirm threshold levels in NaCl and KCl as well as to establish the approximate time structure and stability of the laser output.

Values for the breakdown field obtained at 1.06 μm are summarized in Fig. 6 and in Table III along with both the 10.6 μm data collected by Yablonovitch[5] and accepted d.c. results.[8] These results are normalized to the respective values of field necessary to damage NaCl listed in Table IV. This allows the striking similarity in trends of breakdown field to be easily observed and the possible systematic deviations at 1.06 μm to be recognized. The quoted errors at 10.6 μm are ± 10 percent, and our random experimental errors in relative fields are estimated to be no more than ± 10 percent with possible errors due to microscopic strains adding another ± 5 percent. Two different samples of both NaCl and KBr from two different manufacturers gave nearly identical results.

PBN-72-401

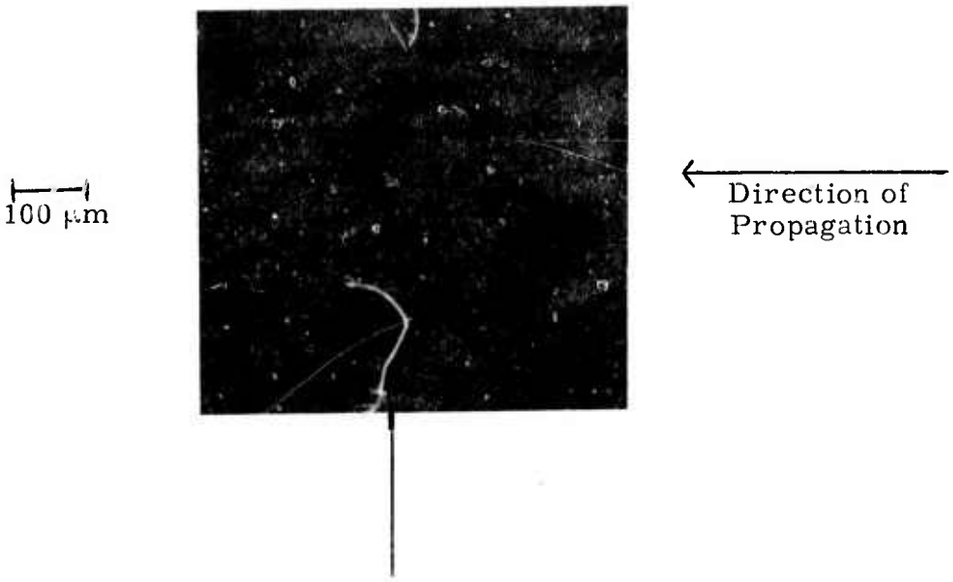

Fig. 3 Intrinsic Damage in RbCl.

PBN-72-400

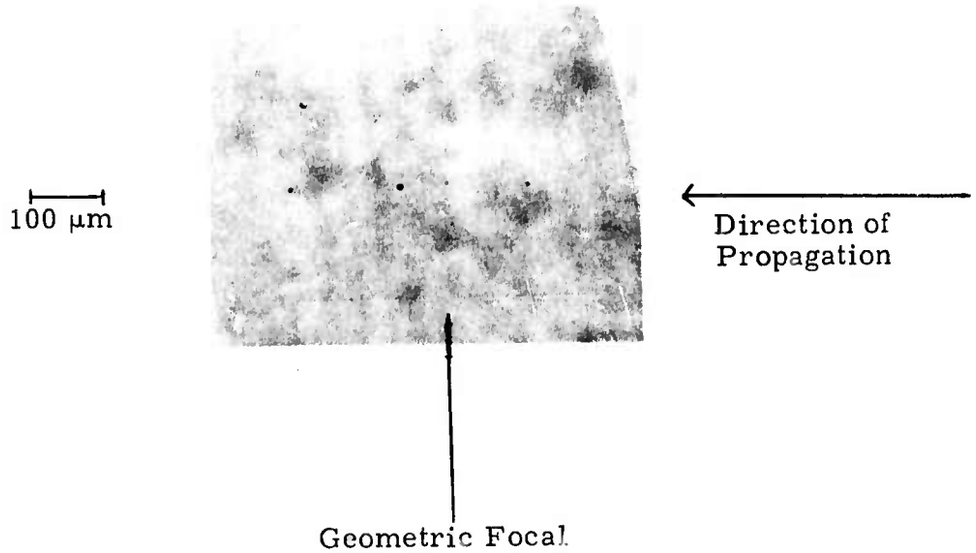

Fig. 4 Inclusion Damage in RbCl.

PBN-72-397

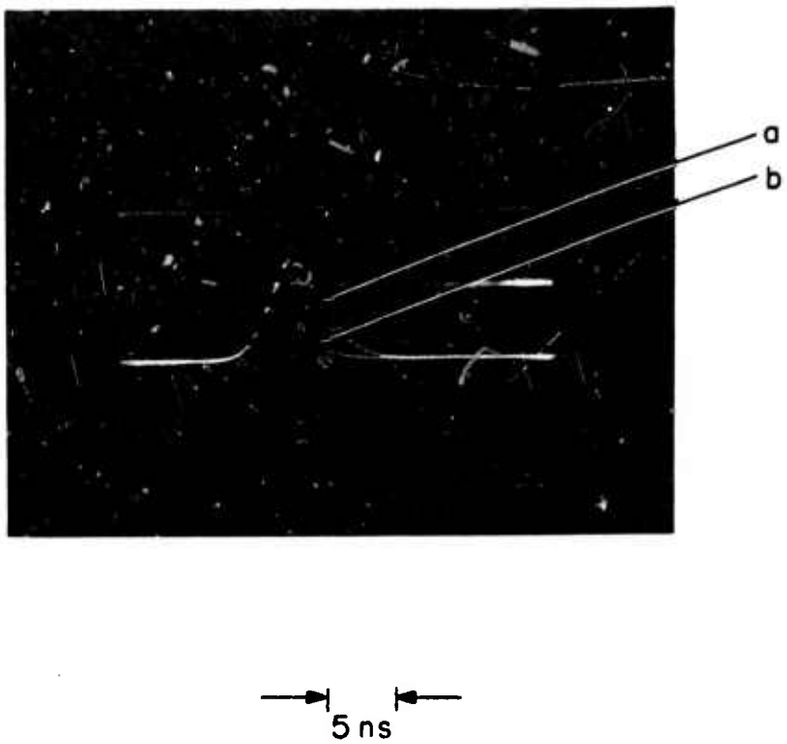

Fig. 5 Nd:YAG Laser Pulse Transmitted Through the Sample.

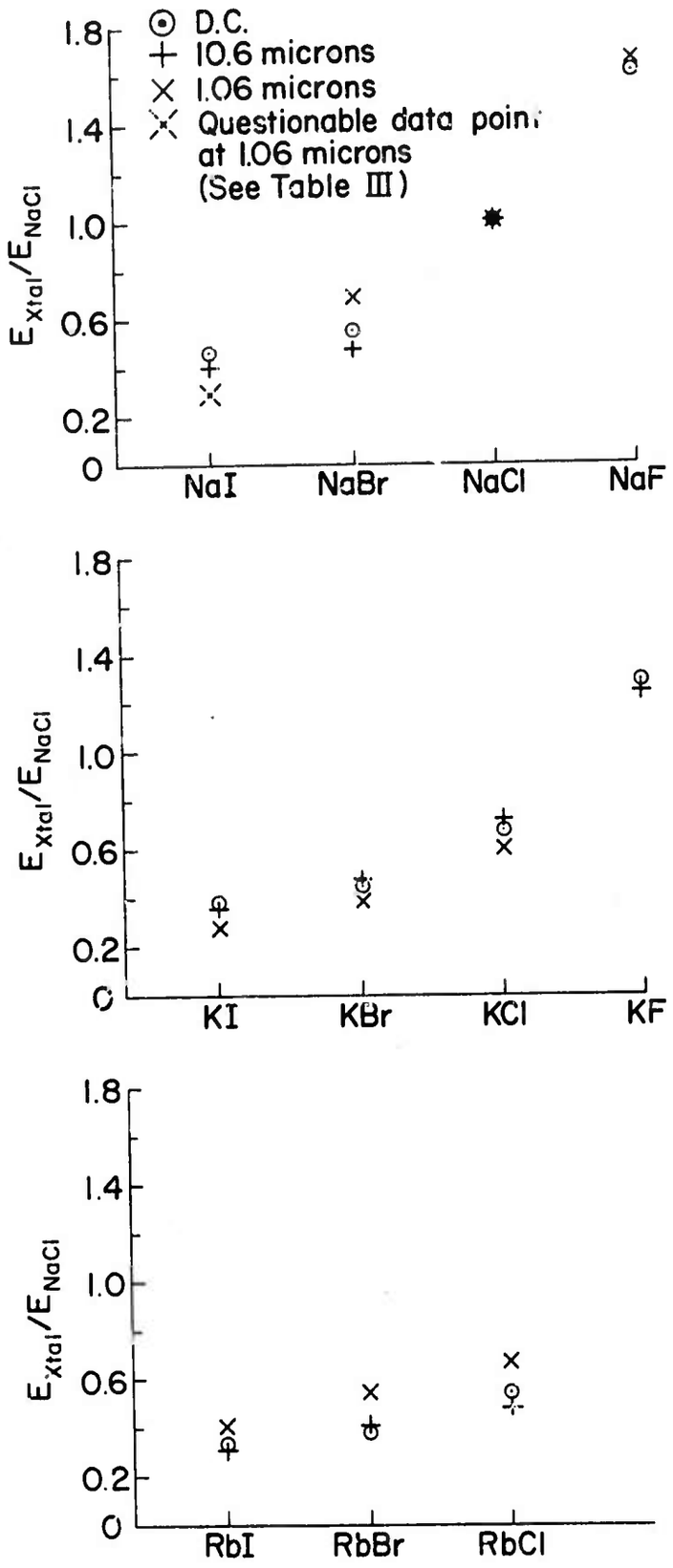

Fig. 6 Comparison of Breakdown Strengths for Various Alkali Halides Studied at dc, 10.6 μm and 1.06 μm.

TABLE III

RELATIVE BREAKDOWN FIELDS - NORMALIZED TO $E_{NaCl} \approx 2 \times 10^6$ V/cm

	NaI	NaBr	NaCl	NaF
DC	0.460	0.553	1	1.60
10.6μm	0.405	0.476	1	
1.06μm	(0.29)*	0.67	1	1.64
	KI	**KBr**	**KCl**	**KF**
DC	0.380	0.460	0.667	1.27
10.6μm	0.369	0.482	0.713	1.23
1.06μm	0.27	0.38	0.57	
	RbI	**RbBr**	**RbCl**	
DC	0.327	0.387	0.553	
10.6μm	0.323	0.400	0.472	
1.06μm	0.40	0.55	0.67	

*Crystal was extremely hydroscopic and no final check was made with the microscope to determine if inclusions were responsible for the damage observed.

TABLE IV

ABSOLUTE BREAKDOWN STRENGTH OF NaCl

E_{peak}(dc)	1.50×10^6 V/cm	
E_{rms} (10.6 microns)	1.95×10^6 V/cm	± 10 Percent
E_{rms} (1.06 microns)	2.3×10^6 V/cm	± 20 Percent
E_{rms} (1.06 microns)*	2.2×10^6 V/cm	± 20 Percent

*Gaussian profile assumed.

An rms field of 2×10^6V /cm inside NaCl at 1 μm corresponds to a peak incident intensity of about 16×10^9 watts/cm^2.

Careful statistics for variations in the breakdown strength were collected on NaCl because of the high quality of the two samples we obtained. It was found that, within experimental error the damage process in NaCl appears thresholdlike. Though larger fluctuations were noticed for other material the uncertainties are considered to result from surface imperfections, internal strains, and laser fluctuations. No measurement of any probabilistic nature of breakdown was made.

Some evidence for intrinsic fluctuations, however, was found by monitoring the light transmitted through the samples. On several occasions a laser pulse produced damage in the same position where a more intense pulse one second before had been focused without damaging the sample. While these observations may have resulted from unresolved time-structure in the second laser pulses, the same observations were made at ruby wavelength where Fabry-Perot studies indicated that the pulses were normally free of such fluctuations.

b. Damage measurement of 0.69 μm

The breakdown strength of NaCl was also measured with a ruby laser to confirm the absence of self-focusing as noted in Section 3. Table IV records the average of about 50 damage measurements. Although the laser was normally operating in a single longitudinal mode as indicated by Fabry-Perot and photodiode studies, each laser shot during the measurement was monitored with a fast photodiode and recorded.

In Fig. 7 time-resolved photographs of transmitted light indicate the sudden attenuation normally seen for laser pulses which caused damage. Because of the smooth time-structure of most of the pulses, we were able to record a few cases in which the instant of first attenuation, considered to be the onset of material damage, occurred after the peak of the laser pulse had passed. An example is given in Fig. (7c). The same effect was observed at 1.06 μm. This may be explained both by invoking a statistical model for breakdown[9] or by the considerations of a time-dependent avalanche discussed in the next section.

a) Damaged when the peak laser field was reached $E_{Damage}/E_{Peak} = 1$

b) Damaged before the peak laser field was reached $E_{Damage}/E_{Peak} = 0.896$

c) Damaged after the peak laser field was reached $E_{Damage}/E_{Peak} = 0.954$

d) 3 successive pulses no damage $E_{Peak} \equiv 1$ (Arbitrary units)

10 nsec

A TEM_{00} mode ruby laser with total pulse energy of 0.3 mJ was focused inside the inclusion free sample with a 14mm focal length lens

Fig. 7 Ruby Laser Pulses Transmitted Through NaCl Sample.

4. Discussion

a. Bulk damage

The experiments reported here were performed under carefully controlled conditions using stable, well-characterized lasers and optical systems for which aberrations were unimportant. Because we were able to probe each sample in many different positions, random fluctuations in breakdown strength were averaged out. It was possible to distinguish between inclusion and intrinsic damage by inspection of the residual damage and to correct for the effects of inclusions in the one material for which they were important. In addition, experimental tests showed that catastrophic self-focusing was absent and, consistent with theory, that the index nonlinearity did not affect the results to within experimental error. It is therefore concluded that the results of the 1.06 and 0.69 μm study as summarized in Fig. 6 and Table IV represent accurate measurements of intrinsic bulk damage.

Because the techniques of this study are virtually identical to those of reference 5, direct comparison can be made to breakdown strengths at 10.6 μm. It has already been observed that the damage thresholds for the alkali-halides at 1.06 μm follow a trend nearly identical to that observed with the CO_2 laser and, in fact, to the d.c. measurements of reference 8. It thus appears that the intrinsic process of laser-induced damage for the alkali-halides has the same fundamental character as both a.c. damage in the infrared and d.c. avalanche breakdown. Moreover, the consistency of the optical breakdown strengths at 0.69 μm suggests that this same process may dominate up to frequencies approaching 4×10^{14} herz.

Data from Fig. 6 and Table IV have established the relationship $(E_{1.06})_{rms}$ is about $1.5 \times 10\ E_{d.c.}$ for ten different compounds. The precise value of the factor 1.5 is not important since d.c. measurements are known to be somewhat sensitive to experimental techniques.[12,13] It is important, onthe other hand, that consistent measuring techniques have measured roughly the same factor of 1.5 for all ten alkali halides.

Additional support for an avalanche mechanism comes from three experimental observations concerning the time-structure of the laser probe pulses. The first is that increasing the pulse-width of the YAG laser output by a factor of 2.3 resulted in a 14-percent average drop in threshold intensity for NaCl. Averages were taken at about 20 shots at each pulse-width. This change, though small, is probably real, because the test was made on a single sample of high-quality NaCl and thereby avoided a major source of experimental uncertainties arising from material variations. The second observation, noted at both 1.06 and 0.69 μm, is that high-frequency time-structure on the pulse has little measurable effect on the breakdown strength. And finally, after adjusting the power level so that damage occurred regularly near the top of the laser pulses, the probe intensities were increased by a factor of about three by changing the beam attenuation. When this was done, the intensity at which the transmitted light dropped (see Fig. 7) was higher by 25 percent or more than it had been with the lower intensity pulses. This was interpreted to mean that increasing the effective risetime of the optical field raises the measured breakdown strength. To understand both this set of observations and the results from Table IV, some discussion of existing electron avalanche theories[1,12] is given.

An electron avalanche in solids is a rapid multiplication of conduction-band electrons in which an initially low density N_o of free carriers interacts with an intense electric field in the presence of phonons. The number of electrons increases with time as

$$N(t) = N_o \exp \left[\int_o^t \alpha(E)dt \right] . \qquad (1)$$

The gain coefficient $\alpha(E)$ is a strongly-varying function whose value can be inferred from d.c. measurements of breakdown strength as a function of sample thickness for extremely thin specimens. For Eq. (1) to be valid the rate at which electrons are lost by trapping and diffusion out of the focal volume must be small compared to the rate at which they are generated. For Q-switched laser pulses, the electron losses are, in fact, negligible.[14]

Two important conclusions develop from such an analysis. The first is that the entire process of avalanche and damage involves energy exchange between the field and the electrons which is approximately described by the well-known formula for a.c. conductivity[15]

$$\frac{dW}{dt} = \frac{Ne^2\tau}{m(1+\omega^2\tau^2)} E^2 \qquad (2)$$

where N is the time-dependent electron density, ω the angular frequency, and τ the characteristic relaxation-time determined principally from phonon collisions. While this precise form of the conductivity may not be correct for polar materials such as the alkali-halides, we will use it to qualitatively describe breakdown for high frequencies.

Eq. (2) shows that the energy input to the electrons scales with frequency and field as $E^2/(1+\omega^2\tau^2)$, and because the details of energy input determine the electron distribution function and hence N(t), the threshold for damage will scale in the same manner. This justifies the use of root-mean-square fields in Table IV. It also indicates that the a.c. breakdown strength will increase for frequencies near $1/\tau$. Calculation of τ for NaCl[14] indicates that frequency dispersion should begin to occur somewhere near that of the ruby laser.

In d.c. experiments it has been observed that when the time available for the buildup of the avalanche is reduced below about 10 nanoseconds, larger fields are needed to induce damage.[14,16] This may explain some of the differences between the dc and laser measurements summarized in Table IV.

The field dependence of α (E) in NaCl is qualitatively correct to explain our three time-related observations[14] -- the pulsewidth dependence to breakdown, the insensitivity of threshold to fast time-structure, and the increase in breakdown strength for rapidly rising pulses.

Finally, it is quite striking that the threshold field for laser breakdown is virtually identical to that for d.c. breakdown even though the damaged regions appear very different. To understand these two observations, it is convenient to consider the laser breakdown phenomenon in solids in two steps, energy deposition and material disruption. In our experiments the first step is by electron avalanche wherein energy is deposited at a rate given by Eq. (2). In the second step this energy deposition, which may be partially offset by thermal diffusion losses, causes the lattice temperature to rise and finally a phase change or thermally-induced fracture occurs. Without the phase change of fractures there is by definition no breakdown since no irreversible damage develops and, of course, no spark appears. This second step is geometry-dependent and determines the morphology of the damage.

In principle the threshold for damage is dependent on both steps. When inclusions cause damage for example, the details of the thermal diffusion process which enter the problem in the second step determine the pulse-width dependence of the damage threshold.[2,4] On the other hand, if avalanche breakdown is the mechanism of the first step, then the processes of the second step have negligible effect on the threshold field. This is a result of the highly nonlinear dependence of N(t) on the electric field. If the focusing conditions or the electrode design of one experiment make breakdown less likely by altering the processes leading to material disruption and thereby requiring a higher rate of energy deposition, this higher rate of energy input can be achieved by an immeasurably small change in the electric field strength. The apparent threshold for avalanche breakdown, therefore, will depend only on the parameters described qualitatively by Eqs. (1) and (2) and will have no measurable connection with the morphology of the damage.

b. Implications for Surface Damage Studies

Surface damage is often a practical problem in the operation of high-power lasers. For this reason a number of investigations of surface breakdown[17] have been made with the aim of eludicating the conditions and mechanisms of surface damage. The techniques of the studies reported here may provide a valuable tool for understanding surface damage by allowing direct comparison to bulk damage thresholds. This comparison can be made by focusing a low-power laser beam first on a surface and then about 2 mm into the bulk. Because focusing problems are much less severe in the bulk and damage from inclusions can apparently be distinguished by visual observation, a stable and repeatable reference exists for surface studies. Careful investigation should help eludicate, in particular, the mechanisms responsible for surface damage under various conditions of surface preparation.

5. Conclusions

Careful measurements of laser-induced bulk damage have been made in ten alkali-halides without the confusing effects of self-focusing. Comparison of the results to studies at d.c. and at 10.6 μm indicated that the process of a.c. avalanche breakdown, similar in fundamental character to d.c. avalanche breakdown, is responsible for the damage observed. Analysis of time-related observations confirm this conclusion.

Acknowledgments

The skillful assistance and advice of D. Bua and S. Maurici are gratefully acknowledged. We are also indebted to Prof. N. Bloembergen for valuable discussions of breakdown theory and to Dr. P. Miles for stimulating discussions of laser damage.

6. References

1. G. M. Zverev, T. N. Mikhailova, V. A. Pashkov, and N. M. Solov'na, Zh. Eksp. Theor. Fiz. 53, 1849 (1967). [Sov. Phys. JETP 26, 1053 (1968).]

2. R. W. Hopper and D. R. Uhlman, J. Appl. Phys. 41, 4023 (1970).

3. C. R. Guiliano and J. H. Marburger, Phys. Rev. Lett. 27, 905 (1971).

4. Yu. K. Danilciko, A. A. Manenkov, A. M. Prokhorov and V. Ya. Khaimov-Mal'kov, Zh. Eksp. Theor. Fiz. 58, 31 (1970) [Sov. Phys. JETP 31, 18 (1970).

5. E. Yablonovitch, Appl. Phys. Lett. 19, 495 (1971).

6. S. A. Akhmanov et al, Usp Fiz Nauk. 93, 19 (1967) [Sov. Phys. Uspekhi 10, 609 (1968)].

7. R. M. Zverev and V. A. Pashkov, Zh. Eksp. Theor. Fiz 57, 1128 (1969) [Sov. Phys. JETP 30,616 (1970)].

8. A. Von Hippel, J. Appl. Phys. 8, 815 (1937).

9. M. Bass and H. H. Barrett, IEEE J. of Quantum Elec. QE-8, 338(1972).

10. N. Bloembergen, private communication.

11. C. C. Wang and E. L. Baardsen, Phys. Rev. 185, 1079 (1969); Phys. Rev. B1, 2827 (1970).

12. For a review, see J. J. O'Dwyer, The Theory of the Dielectric Breakdown of Solids (Oxford University Press, London, 1964).

13. J. H. Calderwood, R. Cooper, and A. A. Wallace, Proc. IEEE 100 Pt. IIA No. 3, 1051 (1953).

14. E. Yablonovitch, Thesis, Harvard University (1972). Also E. Yablonovitch and N. Bloembergen, Phys. Rev. Letters, 29, 907 (1972).

15. C. Kittel, Introduction to Solid State Physics, Third Edition,(John Wiley and Sons, New York, 1966).

16. D. W. Watson, W. Heyes, K. C. Kao, and J. H. Calderwood, IEEE Trans. Elec. Ins. EI-1, 30 (1965). Also, G. A. Vorob'ev, N. I. Lebedeva, and G. S. Naderova, Fizika Tverdogo Tela, 13, 890 (1971), [Sov. Phys. Solid State, 13, 736 (1971)].

17. C. R. Guiliano, 4th ASTM-NBS Symposium on Damage in Laser Materials NBS Special Publication 372 (1972).

18. Chen-Show Wang, Phys. Rev. 173, 908 (1968).

19. M. Born and E. Wolf, Principles of Optics, (Pergamon Press, Inc., New York, 1959).

20. V. I. Talanov, Zh. Eksperim, i. Theor. Fiz. Pis'ma Redaktsiyu 2, 218 (1965) [Sov. Phys. JETP Letters 2, 138 (1965)].

21. E. L. Dawes and J. H. Marburger, Phys. Rev. 179,862 (1969).

22. E. K. Kerr, IEEE J. Quantum Elec. QE-6, 616 (1970).

7. Appendix A - Self-focusing theory - Catastrophic

To demonstrate the claim that the relative balance between diffraction and self-focusing effects is set at the entrance plane for a general steady state nonlinearity, we calculate the curvature of the ray path from a modified, eikonal equation formalism that incorporates both diffraction effects and the steady-state nonlinearity[18]. Its applicability is restricted to beams with diameters 2a much greater than a wavelength--a condition fulfilled in our experiments.

Writing the electric field vector $\vec{E}(\vec{r})$ as $\vec{A}(\vec{r})\exp i\,[k\phi(r) - wt]$ where $k_o = w/c$ and the index nonlinearity is n_2A^2 and ignoring terms of order n_2A^2/n_o, we can write Maxwell's equations in the simplified form

$$[(n_o + n_2A^2)^2 - (\text{grad}\,\phi)^2]\,\vec{A} + \frac{1}{k_o^2}\,\nabla^2 A = 0.$$

If the scalar product of this equation is taken with $\vec{A}$, a term containing the factor $1/k_o^4$ dropped and a cross term with n_2A^2 neglected, this leads directly to an effective eikonal equation

$$n_1^2 - (\text{grad}\,\phi)^2 = 0 \qquad \text{(A1)}$$

where

$$n_1 = n_o + n_2A^2 + \frac{1}{2k_o^2 n_o}\,\frac{\nabla^2 A}{A}\,. \qquad \text{(A2)}$$

In the limits of zero nonlinearity, and infinitesimal wavelength, this is just the basic equation of geometrical optics. Results derived from the usual eikonal equation[19] can now be used with the index of refraction replaced by Eq. (A2). In particular, the curvature $d^2\vec{r}/d\rho^2$ for a pencil of rays with position vector $\vec{r}$ and with ρ the coordinate along the ray path is given by

$$\frac{d^2\vec{r}}{d\rho^2} = \frac{1}{n_1}\left[\text{grad}\,n_1 - \frac{dn_1}{d\rho}\,\frac{d\vec{r}}{d\rho}\right]. \qquad \text{(A3)}$$

Equation (A3) can be simplified by restricting the treatment to cylindrically symmetric beams and by assuming that the maximum ray slope is small compared to unity. (In our experiments the maximum slope inside the sample and before the focus is less than 0.05.) Both the second term on the right in Eq. (A3) and the longitudinal component of the Laplacian in Eq. (A2) are negligible. The curvature is now expressed in a form first derived by Talanov[20]

$$\frac{d^2\vec{r}}{d\rho^2} \approx \frac{d^2\vec{r}}{dz^2} = \frac{1}{n_1} \operatorname{grad}_\perp n_1. \tag{A4}$$

This result is important to the study of self-focusing effects because the sign of $d^2\vec{r}/dz^2$ indicates whether or not the beam is converging and its magnitude is a quantitative measure of that convergence or divergence. A positive curvature results in an increase in the slope of the ray path with respect to the propagation direction and thus represents a divergence from the axis. Diffraction alone will produce a positive curvature in an isotropic medium. A negative curvature, on the other hand, will cause convergence of the beam towards the axis and indicates the dominance of the self-focusing nonlinearity.

$A^2(r)$ is proportional to the light intensity, and where the beam propagates with little or no change in shape, the intensity is equal to the power in the beam divided by the beam area $\pi a^2(z)$. Let p be an effective power which absorbs these proportionality constants including the factor π in the beam area. (This effective power has, in fact, a functional form -- it may be Gaussian ($\exp[-2r^2/a^2]$) for example -- and it is this functional form which describes the beam shape.) We can therefore consider p to be a function of a radial variable which is independent of the beam size. Defining the coordinate x as $x = r/a(z)$, we can write

$$A^2(r) = \frac{p(x)}{a^2(z)} = \frac{\text{power}}{\text{beam area}} \tag{A5}$$

Eq. (A5) is normally assumed in numerical calculations and has been referred to as the "constant shape approximation"[21]. Along with Eq. (A4) it provides the basic relationships to calculate the critical power, the self-focusing length, and the quantitative influence of the index nonlinearity when diffraction dominates.

By expanding $\nabla_\perp^2$ in cylindrical coordinates r and z it is easily seen that $\nabla_\perp^2 A/A$ is also proportional to a^2. We can then write Eq. (A2) as

$$n_1 = n_0 + \frac{1}{a^2(z)} f(x)$$

where f(x) is the sum of contributions from both diffraction and the index nonlinearity. Since $\text{grad}_\perp$ is just $a(z)^{-1}[\partial/\partial x]$, and since n_1 in the denominator of Eq. (A4) can be replaced by n_0, the derivative of f(x), which contains no dependence on z, determines the relative importance of diffraction and self-focusing. Once this relative importance is determined for one value of z, such as z = 0 at the entrance plane, it is determined for all z.

For completeness we write Eq. (A4) in the final form

$$\frac{d^2r}{dz^2} = \frac{1}{n_o} \frac{1}{a^3(z)} \frac{d}{dx}[f(x)] \qquad \text{(A7)}$$

where, using (A5),

$$f(x) = n_2(aA)^2 + \frac{1}{(2k_0^2 n_0 aA}\left[\frac{d^2(aA)}{dx^2} + \frac{1}{x}\frac{d(aA)}{dx}\right]. \qquad \text{(A8)}$$

The importance of neglected terms can be determined for a particular beam shape and has been shown to be negligible[18] except near a catastrophic self-focus or under experimental condition where extreme external focusing is used.

The critical power P_c is in principle calculated from the requirement that the derivative f(x) vanish for all x, leading to a detailed balance of self-focusing and diffraction. Since f(x) contains no dependence on beam diameter, the critical power will not be dependent on beam diameter for a steady-state nonlinearity.

8. Appendix B - Self-focusing theory - Intensity Distortion

The index nonlinearity leads to intensity distortions even below the critical power for catastrophic self-focusing. Using the results of Appendix A quantitative corrections from the nonlinearity can be derived.

In Eq. (A7) r is replaced by x a(z) and a new function g(x) defined. This gives

$$\frac{d^2a}{dz^2} = \frac{1}{a^3(z)}\, g(x) \tag{A9}$$

where

$$g(x) = \frac{1}{n_o x}\ \frac{d}{dx} f(x). \tag{A10}$$

If Eq. (A9) is multiplied by $z(da/dZ)$ and integrated, we find

$$\left(\frac{da}{dz}\right)^2 = -\frac{g(x)}{a^2} + c. \tag{A11}$$

Considerable simplifications results from expanding A^2 and therefore g(x) about small x and retaining terms to order x^2. In reference 7 this expansion is carried out for a Gaussian beam. We can investigate the geometrical focus at low powers by setting the derivative in Eq. (A11) equal to zero.[7] After some manipulation the focal diameter d is evaluated in terms of d_o, the diameter in absence of a nonlinearity. In particular,

$$d = d_o(1 - P/P_{cr})^{1/2} \tag{A12}$$

Where P is the full power in the beam and P_{cr} is given in cgs units by

$$P_{cr} = \frac{c\lambda^2}{32\,\pi\, n^2} \quad . \tag{A13}$$

The result (A12) is useful for P/P_{cr} less than about 0.5. The calculated on-axis intensity at breakdown must be multiplied by a factor $(d_o/d)^2$ to approximately correct for the effects of the nonlinearity.

More extensive analysis shows that P_{cr} is the critical power for self-focusing near the center of a Gaussian beam[21]. For input powers greater than P_{cr} but less than P_c, diffraction dominates everywhere except near the beam center. A collimated beam will initially intensify at such powers until the diffraction of the wings causes the on-axis intensity to drop. P_{cr} differs

from P_c because the latter is a quantity averaged over the entire beam while P_{cr} is determined by the behavior near the center. In fact, P_c is not a precisely defined quantity because it is not possible to exactly balance diffraction and self-focusing over the entire beam cross-section. At an input power of P_c, therefore, a propagating beam will not change its size measurably and so not experience a catastrophic self-focus, but its intensity distribution will be distorted. P_c has the same functional form as P_{cr} and differs by just a numerical factor as $P_{cr} = 0.273\ P_c$ for Gaussian beams.

9. Appendix C - Self-focusing theory - Transient effects

The analysis of Appendix A and the results derived from it are correct only in the steady state. In solids the dominant nonlinearity is normally electrostriction, and if the process is transient, it is no longer true that the relative balance between diffraction and self-focusing is independent of propagation distance and that the critical powers are independent of beam diameter. The changes occur because electrostriction becomes non-local in both a temporal and a spatial sense. Although a susceptibility approach such as we have used is no longer strictly correct, it is nonetheless useful for establishing functional dependences for self-focusing parameters and approximate quantitative values.

For our experiments two results from a transient analysis are important.[22] The first is that transient effects decrease the effective nonlinear index n_2 and thus make self-focusing more difficult. If we wish to avoid self-focusing by restricting our powers to well below the critical power, the steady-state analysis gives us a lower bound on P_c. Being in a transient regime can, therefore, only increase our margin of safety and improve the accuracy of our experiment by making the corrections indicated by Eq. (A12) less important.

The second important result involves the dependence of the critical power on laser pulse-width and on beam diameters. In the steady state nonlinear index n_2 is given by[6]

$$n_2 = \frac{n_o\left(\rho \frac{\partial n_o}{\partial \rho}\right)^2}{4\pi\rho v^2}$$

where n is the index of refraction in the absence of the nonlinearity, ρ is the material density, and v is the acoustical sound velocity. The quantity $(\rho\ \partial n_o/\partial\rho)$ for cubic materials such as the alkali-halides may be found approximately by differentiating the Clausius-Mosotti equation. The remaining constants are tabulated in handbooks.

When the laser pulse width t_p is shorter than the electrostrictive response time $\tau = a/v$, n_2 is decreased in value, thereby increasing the critical power. For a triangular pulse, Kerr[22] has shown that

$$(n_2)_{\text{transient}} = (n_2)_{\text{steady-state}}\left[1 - \frac{a}{v\rho} D\left(\frac{v\rho}{a}\right)\right] \qquad \text{(A14)}$$

where $D(\frac{v\rho}{a})$ is Dawson's integral with

$$D(\xi) = \exp(-\xi) \int_o^{\xi} \exp \eta^2 d\eta .$$

When $t_p \leq \tau/2$,

$$(n_2)_{\text{transient}} \approx k(n_2)_{\text{steady state}} \frac{v^2 t_p^2}{a^2} .$$

This result is valid for more general and realistic pulse-shapes with the numerical constant k being of order unity and having a value dependent on the precise time-structure of the pulse. When this result is inserted into Eq. (A13), the critical power becomes

$$P_{c\ t_p/\tau \leq 1/2} = (P_c)_{\text{steady state}} \frac{a^2}{kv^2 t_p^2} . \qquad \text{(A15)}$$

For short laser pulses, therefore, when the process is transient, there exists more properly a critical intensity rather than a critical power, and fairly small changes in pulse-width will have a significant effect on the critical power.

As already noted, the index nonlinearity intensifies the peak on-axis intensity even at powers below the catastrophic self-focusing threshold. Using Eq. (A12), we have corrected for this effect in the calculated field strengths listed in Table IV. In addition, because of Eq. (A15) and the results of Appendix A, we can predict the diameter and pulsewidth dependence to breakdown when catastrophic self-focusing is present. This information was used to evaluate the results of the self-focusing tests described in Sec. B-2b.

V. ELECTRON AVALANCHE BREAKDOWN INDUCED BY RUBY LASER LIGHT

A. Introduction

Ruby laser induced intrinsic bulk damage in nine alkali halide crystals is reported in this section. We found that for all of these crystals the damage field was, within experimental error, greater than or equal to that measured at 1.06 μm and at dc. The trend in breakdown fields among these crystals at 0.69 μm differs from that at longer wavelengths and suggests that even though electron avalanche breakdown is the likely damage mechanism, the first signs of a frequency dependence to this process appear by 4.3×10^{14} Hz.

B. ELECTRON AVALANCHE BREAKDOWN INDUCED BY RUBY LASER LIGHT

by

David W. Fradin*
Gordon McKay Laboratory, Harvard University
Cambridge, Mass. 02138

and

Michael Bass†
Raytheon Research Division
Waltham, Massachusetts 02154

Ruby laser induced intrinsic bulk damage in nine alkali-halide crystals is reported. Within experimental error and for all of these crystals the damage field is greater than or equal to that measured at 1.06 μ m and dc. The trend in breakdown fields among these crystals at 0.69 μ m differs from that at longer wavelengths and suggests that, even though electron avalanche breakdown is the likely damage mechanism, the first signs of a frequency dependence to this process appear by 4.3×10^{14} Hz.

---

* Supported by the Joint Services Electronics Program at Harvard University under Contract No. N00014-67-A-0298-0006.

† Supported by the Advanced Research Projects Agency of the Department of Defense and monitored by the Air Force Cambridge Research Laboratories under Contract No. F19628-70-0223.

1. Experiments and discussion

It has been observed for many years that transparent materials can be damaged by sufficiently intense light fields.[1] Such damage can result from contaminants in the material or from processes which are intrinsic in character. Early investigations of intrinsic processes had been confused by a number of problems: uncertainties in the laser mode structure,[2] the presence of inclusions,[3] self-focusing in the bulk,[4] and, perhaps most important, the lack of any theoretical framework for designing and interpreting damage studies.

It is just within the last two years that these problems have been recognized and dealt with. As a result, a fairly clear picture of the laser damage process up to 1.06 μm has been developed. Bass and Barrett[5] observed statistics in the optical strength of surfaces and interpreted their results in terms of an electron avalanche model. Yablonovitch[6] measured the optical damage properties in the bulk of ten alkali halides at 10.6 μm and found that the damaging process appeared to be identical to dc avalanche breakdown. These measurements were extended to 1.06 μm by Fradin et al.[7] and it was found that the avalanche still appeared to be in its dc limit at these high frequencies. Subsequent work has reported statistics in bulk damage[8] and confirmed the equivalence of intrinsic optical damage processes on the surface and in the bulk for a number of materials.[9]

In this letter we report measurements of intrinsic bulk breakdown in nine single crystal alkali halides using a TEM_{00}, single-longitudinal mode ruby laser. Self-focusing was absent in these studies, and damage from inclusion absorption was distinguished from intrinsic damage. It was found that at 0.69 μm the relative breakdown strengths of the alkali halides have begun to differ from values obtained at 1.06 and 10.6 μm and at dc. The onset of this frequency dispersion in the avalanche breakdown process enables one to estimate the high-field electron-phonon collision frequency.

The laser system and techniques for avoiding and confirming the absence of self-focusing have been described in detail elsewhere.[7,8]

Damage from inclusions was distinguished from intrinsic damage by examining both the morphology of the damage sites[6,7] and the temporal shape of light pulses transmitted through the sample.[8] The latter technique employed the fact that a damaging light pulse is attenuated in a manner which is characteristic of the cause of damage. Only data obtained from intrinsic damage events were considered in the present work.

To measure the breakdown strengths of the alkali halides, we focused the laser beam inside the sample about 1.5 mm from the front surface. The focal spot diameter was about 15 μm. When the incident power was sufficiently high, a bright white spark was produced and a small volume of the material ($\lesssim 10^{-5}$ mm^3) was melted. Because a well-defined threshold could not be found,[5,8] we defined the damage field as that value of rms electric field inside the material which was necessary in order to induce damage on a single pulse with a probability of 0.5. The incident power necessary to reach this field in NaF under our conditions of focusing was 146 KW. For the other crystals, the input power was between 20 KW (for NaCl) and 9.2 KW (for RbI).

A large number of data points were taken for each sample (40 to 100), but normally less than half of these damage sites could be unambiguously identified as resulting from intrinsic processes. The remainder were apparently caused by the presence of absorbing inclusions.

As in Ref. 7, the rms on-axis damage field was determined for NaCl using the measured intensity distribution at the focus of the 13-mm-focal-length lens. This measurement was the basic calibration, and in order to avoid errors from possible alignment changes, damage fields for the other materials were measured relative to E_{NaCl}. The same sample of NaCl was tested with each alkali halide.

Figure 1 and Table I summarize the results of this study, the 1.06 μm data from Ref. 7, and accepted dc results.[10] In Fig. 1 the

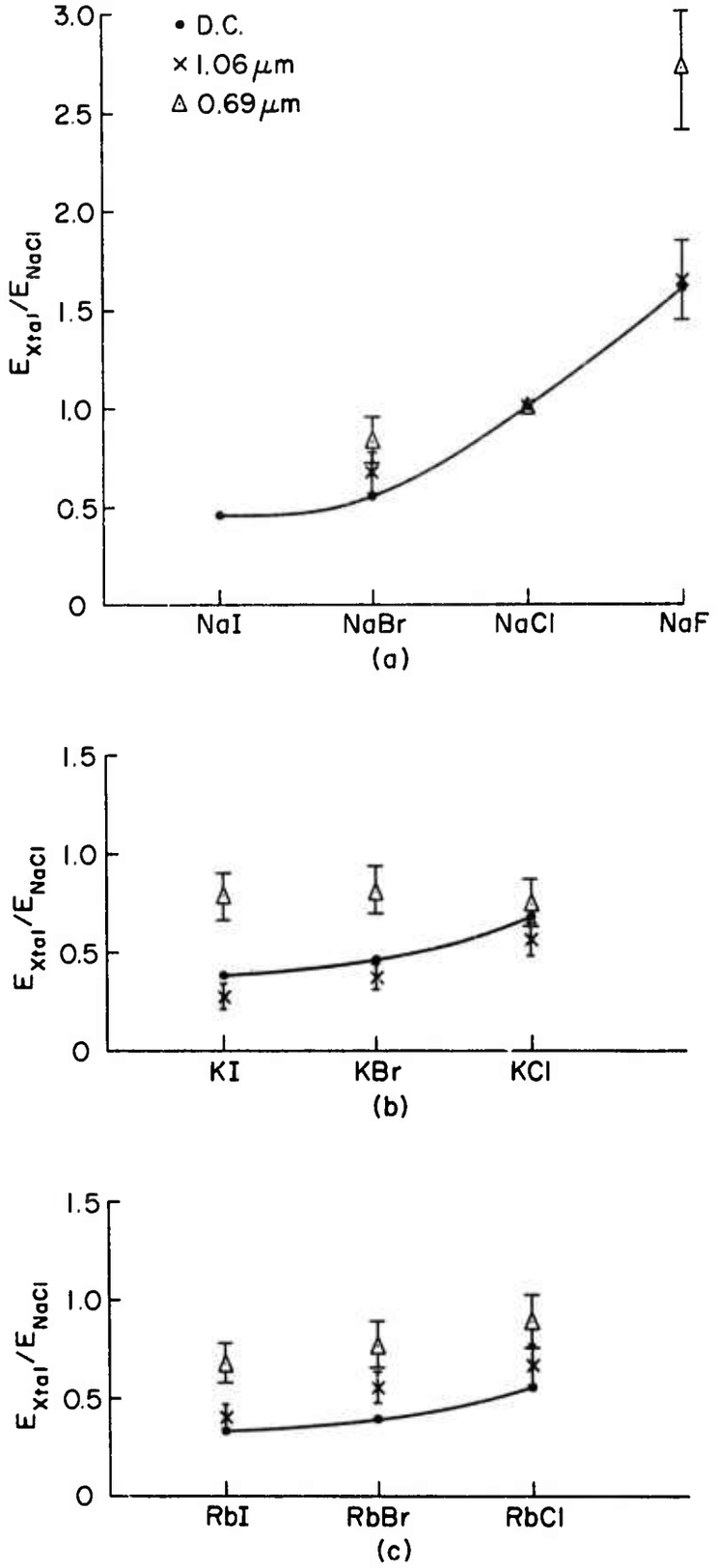

Fig. 1 RMS Electric Fields Necessary to Induce Damage in Nine Alkali Halides Normalized to the Damaging Field for NaCl. The dc data is taken from Ref. 10 and 1.06 μm is taken from Ref. 7.

TABLE I

ABSOLUTE BREAKDOWN STRENGTH
OF NaCl

E_{peak} (dc)*	1.50×10^6 V/cm
E_{rms} (10.6 μm)*	$(1.95 \pm 0.20) \times 10^6$ V/cm
E_{rms} (1.06 μm)*	$(2.3 \pm 0.46) \times 10^6$ V/cm
E_{rms} (0.69 μm)	$(2.2 \pm 0.44) \times 10^6$ V/cm

*These values are taken from Refs. 10, 6, and 7 respectively.

damage fields of the various alkali halides are normalized to that of NaCl at the appropriate frequency. This makes the variation in trends between the 1.06 μm and the 0.69 μm measurements more easily seen. The relative breakdown strengths at 1.06 μm are virtually identical to those measured at dc. Although the corresponding data at 10.6 μm[3] are not displayed, they too follow the same trend. This is not the case at 0.69 μm, however, even when the 10 to 15 percent measurement errors are considered.

Table I lists the rms damage fields of NaCl for these experiments. The agreement found in the four experiments is heartening because there are particular difficulties in determining the absolute damage fields in dc measurements.[12] Root-mean-square values of the electric field strength are given because for laser pulses of this intensity, the build-up time of an electron avalanche to damaging levels is on the order of 10^3 to 10^4 cycles of the optical field.[11, 12] Heating of the electron population is thus effectively averaged over many cycles.

A complete theoretical description of avalanche breakdown has not been developed. The onset of frequency dispersion can be qualitatively understood, however, by using the results of models based on relaxation time approximations.[12, 13] These models predict that the damage field will scale with frequency as

$$E_{rms}(\omega_L) = (1 + (\omega_L)^2\tau^2)^{1/2} E_{dc} \qquad (1)$$

where $\omega_L = 2\pi\nu_L$ is the laser radian frequency and τ it an effective, high-field, electron-phonon collision time. Since each material has a different value of τ, the relative breakdown fields for the alkali halides should begin to change at high frequencies. Data such as shown in Figure 1 can be used to infer approximate relative values of τ for a variety of theoretical models.

Perturbation calculations of τ have been performed which are applicable for electron energies greater than the longitudinal optical photon energies.[14, 15] If $\omega_L \tau \approx 0.5$ for NaCl, then the results of these calculations can explain qualitatively the change in relative breakdown strengths observed at ruby frequencies for most of the alkali halides. The collision time for NaCl under this assumption is about 2×10^{-16} sec and agrees with independent estimates of τ.[11] For NaF these calculations predict that the relative breakdown field (E_{NaF}/E_{NaCl} in Fig. 1) will decrease at ruby frequencies, contrary to the change which is experimentally observed. This discrepancy may be the result of the inadequacy of the perturbation calculations or it may indicate that the frequency dependence of the electron avalanche is not determined by the electron-phonon collision frequency alone.

Seitz[16] has suggested that the presence of deep-lying exciton bands may influence the dielectric strength of alkali halide crystals. If this is the case, then as the field frequency, ν_L, is increased, direct excitation out of these bands becomes possible and the damage field will decrease. NaF, which has the deepest lying bands (1.5 - 2.0 eV) of the materials studied,[17] will experience this effect at a higher frequency than the other alkali halides. Such considerations of the relative importance of the exciton bands may explain the observed large increase in the NaF damage field at 0.69 μm.

Multiphoton absorption directly across the bandgap cannot explain the changes in relative breakdown strength which have been observed. In addition, theoretical calculations of the fields at 0.69 μm necessary to induce damage from multiphoton ionization or from its low-frequency limit, tunnel ionization, give damage fields which are about an order of magnitude larger than those measured.[16]

In conclusion, we have measured the intrinsic optical breakdown fields of nine alkali halides using a ruby laser. Although the absolute and relative thresholds fields are comparable to the thresholds observed at 1.06 μm

and at dc, differences are observed which suggest that at $\nu_L = 4.3 \times 10^{14}$ sec^{-1}, avalanche breakdown is no longer identical to dc dielectric breakdown. Current theories of avalanche breakdown do not appear tc explain this observed difference and so additional theoretical studies are called for.

The authors wish to thank D. Bua and S. Maurici for their skillful assistance and M. Adlerstein for helpful discussions.

2. References

1. C. R. Giuliano, Appl. Phys. Lett. 5, 137 (1964).

2. Michael Bass, Damage in Laser Materials, NBS Special Publication 341, p. 90 (1970).

3. R. W. Hopper and D. R. Uhlman, J. Appl. Phys. 41, 4023 (1970).

4. C. R. Giuliano and J. H. Marburger, Phys. Rev. Lett. 27, 905 (1971).

5. M. Bass and H. H. Barrett, IEEE J. Quantum Elec. QE-8, 338 (1972).

6. E. Yablonovitch, Appl. Phys. Lett. 19, 495 (1971).

7. D. W. Fradin, E. Yablonovitch, and M. Bass, "Confirmation of an Electron Avalanche Causing Laser-Induced Bulk Damage at 1.06 Microns," to be published Appl. Optics (April 1973).

8. M. Bass and D. W. Fradin, "Surface and Bulk Laser Damage Statistics and the Identification of Intrinsic Breakdown Processes," submitted for publication IEEE J. Quantum Elec.

9. D. W. Fradin and M. Bass, "A Comparison of Laser-Induced Surface and Bulk Damage," to be published in Appl. Phys. Lett. (15 February 1973).

10. A. von Hippel, J. Appl. Phys. 8, 815 (1937).

11. E. Yablonovitch and N. Bloembergen, Phys. Rev. Letters 29, 907 (1972).

12. For a review of dc breakdown in insulators, see J. J. O' Dwyer, The Theory of the Dielectric Breakdown of Solids (Oxford Univ. Press, London, 1964).

13. L. Hollway, Phys. Rev. Lett. 28, 280 (1972).

14. G. M. Zverev, T. N. Mikhailova, V. A. Pashkov, and N. M. Solov' eva, Sov. Phys. JETP 26, 1053 (1968). (Zh. Theor. Fiz. 53, 1849 (1967)).

15. H. Frohlich, Proc. Roy. Soc. (A) 160, 230 (1937).

16. F. Seitz, Phys. Rev. 76, 1376 (1949).

17. K. Teegarden and G. Baldini, Phys. Rev. 155, 896 (1967).

VI. A COMPARISON OF LASER INDUCED SURFACE AND BULK DAMAGE

A. Introduction

A comparison of laser induced damage on the surfaces and in the volume of transparent media is reported in this section in which the role of surface finish quality is demonstrated. This comparison is made possible by the use of TEM_{00} mode beams and focusing optics which can produce internal breakdown but no self-focusing. The data show that if the field E can cause bulk damage with a probability p_B or entrance surface damage with probability p_S then

$p_B = p_S$ for surfaces free of polishing imperfections

and

$p_B < p_S$ for conventionally finished surfaces.

The ratios of the applied fields which cause equal bulk and surface damage probability for three different materials with conventionally finished surfaces were determined. Electric field enhancement at certain types of polishing imperfections can explain the measured ratios.

B. A Comparison of Laser Induced Surface and Bulk Damage

D. W. Fradin†
Gordon McKay Laboratory, Harvard University
Cambridge, Mass. 02138

and

Michael Bass*
Raytheon Research Division
Waltham, Mass. 02154

ABSTRACT

Data is presented which shows that the optical field required to produce damage on a conventionally polished surface of a transparent medium is less than that required to damage an imperfection-free surface. Electric field enhancement at imperfections can explain this result. In addition, the bulk damage field at 1.06 μm is reported for three materials and is found to be the same as the surface damage field on imperfection-free surfaces.

---

† Supported by the Joint Services Electronics Program at Harvard University under Contract No. N00014-67-A-0298-0006.

* Supported by the Advanced Research Projects Agency of the Department of Defense and was monitored by the Air Force Cambridge Research Laboratories under Contract No. F19628-70-0223.

1. Experiments and discussion

A comparison of laser induced damage on the surfaces and in the volume of transparent media is reported in which the role of surface finish quality is demonstrated. This comparison is made possible by the use of TEM_{00} mode beams and focusing optics which can produce internal breakdown but no self-focusing. The data show that if the field E can cause bulk damage with a probability p_B or entrance surface damage with probability p_S then

$p_B = p_S$ for surfaces free of polishing imperfections

and

$p_B < p_S$ for conventionally finished surfaces.

The ratios of the applied fields which cause equal bulk and surface damage probability for three different materials with conventionally finished surfaces were determined. Electric field enhancement at certain types of polishing imperfections[1] can explain the measured ratios.

The experimental procedure employed in this work to obtain laser induced bulk damage fields was described by Fradin et al.[2] It was shown that by restricting the total peak power in the laser beam to no more than one tenth of the critical power for catastrophic self-focusing, bulk damage could be studied unambiguously. The low power TEM_{00} mode, Q switched Nd:YAG laser beams were made to have power densities high enough to cause damage by focusing with an aberration-free lens to a very small spot ($\sim 20\,\mu m$ dia.). Tests confirming the absence of catastrophic self focusing in fused quartz and BSC-2 glass were performed as in Ref. 1. The value of bulk damage field for sapphire was corrected for beam distortion due to the index nonlinearity using measured self-focusing parameters.[3,4] Surface damage measurements were obtained using the lens above and the experimental procedure described by Bass and Barrett.[5] The same sample was used for both bulk and surface damage measurements to eliminate any question of sample to sample differences causing the measured ratios of damage fields.

We were able to eliminate absorbing inclusion induced damage from our data by examining the damage morphology[2] and/or by monitoring the manner in which the occurrence of damage attenuated the transmitted laser pulse. The essential point in the latter procedure[6] was that a very rapid and well-defined attenuation was always correlated with residual damage having a morphology characteristic of damage caused by an intrinsic process. Thus, any other form of attenuation was suspect and such events not included in our data.

Since the same statistical properties are observed for both bulk[6] and surface damage[5,6] a threshold field for either process cannot be defined in the conventional manner. Instead, we call the damage field, that field which results in a probability for damage by a single laser pulse equal to 0.5. Using this definition we measured the ratios of bulk to surface damage fields, E_B/E_S, listed in Table I. These data show that the clean but conventionally polished surface (Fig. 1a) of a transparent medium is generally more easily damaged than the bulk. On the other hand when care is taken to achieve imperfection-free surface finishes such as shown in Fig. 1b, the bulk and surface breakdown fields are equal.

The morphology of the residual entrance surface damage gives additional evidence to the preceding conclusions. When a spark is observed during laser irradiation, very small pit damage usually identified as entrance surface damage [7] is found on a conventionally finished surface. Imperfection-free surfaces show more extensive damage including a region of cracks surrounding the irradiated volume. In addition, damage to such surfaces generally extends into the material much further than the 0.25 μm depth characteristic of damage to conventionally finished surfaces. In fact, damage to an imperfection-free surface is very similar to a cut through a bulk damage in a plane perpendicular to its long axis.[2]

Since the region where the light intensity is high extends into the medium even when the focal plane is exactly at the surface, it is possible for the light to cause internal or bulk damage. A conventionally finished

Material	Finishing Procedure Finish Quality[a]	Predicted Ratio E_B/E_S Spherical Void	 Cylindrical Groove	 "Vee" Groove	Measured E_B/E_S	Surface Damage Morphology
Fused Quartz	Conventional #1 Standard 0-0 (see Fig. 1a)	1.21	1.35	2.1	1.3 ± 0.1	b
	Conventional #2 Standard 0-0	"	"	"	1.5 ± 0.1	b
	"Bowl" feed finish See Fig. 1b	"	"	"	1.0 ± 0.1	c
	Ion beam polish Standard 0-0 with final 1.25 μm removed by Ar ion beam	"	"	"	1.0 ± 0.1	c
Sapphire	Conventional Many scratches and digs with 50X mag and dark field	1.29	1.50	3.00	2.0 ± 0.2	b
BSC-2 Glass	Conventional Standard 0-0	1.23	1.39	2.25	1.3 ± 0.1	b
	"Bowl" feed finish See Fig. 1c	"	"	"	1.0 ± 0.1	b, c

a. All surfaces were cleaned with collodion

b. Very faint pit ~ 20 μm in dia. and ~ 0.25 μm deep

c. Extensive cracking out to ~ 150 μm with central hole ~ 20 μm dia. and ~ 3-10 μm deep

TABLE I

Comparison of Bulk and Surface Damage Fields for Different Samples and Surface Finishes

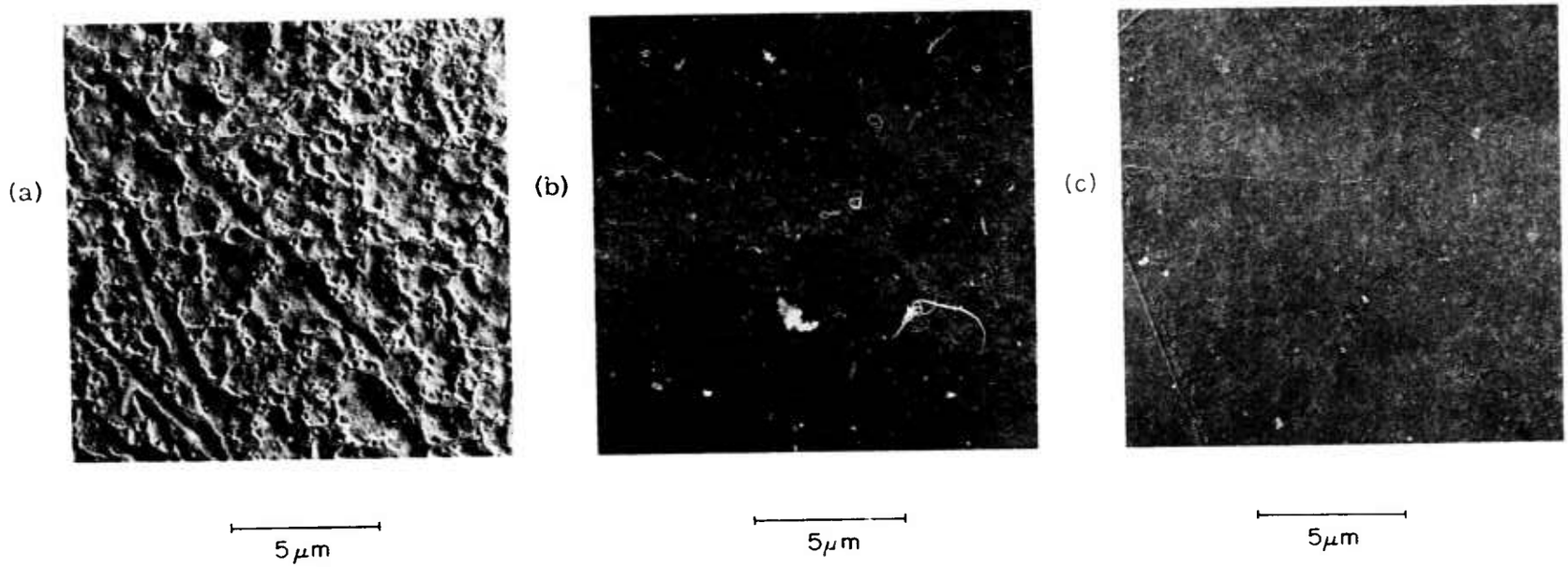

Fig. 1

a. Electron Micrograph of Conventionally Polished Fused Quartz (No. 1)

b. Electron Micrograph of a Bowl Feed Finished Fused Quartz

c. Electron Micrograph of the Bowl Feed Finished Surface of BSC-2 Glass

surface, however, damages more easily than the bulk and so, since the onset of damage is accompanied by a strong attenuation of the transmitted beam, light of intensity sufficient to cause bulk damage never gets into the medium. The resulting damage then is localized in the surface. If, on the other hand, a more highly finished surface does not damage any more easily than the volume of the medium, it is possible for intense light to reach the bulk. When bulk damage occurs just below and breaks out of the entrance surface, the observed morphology is to be expected. These morphological observations, which are valid only when inclusion induced damage is absent show, that if very small pit damage, localized in the surface of a medium, is normally produced, then that surface is more easily damaged than the bulk. The observation that damage on imperfection-free surfaces appears to be bulk damage which erupted from within the medium might explain Guilliano's report of more extensive surface damage on ion beam polished sapphire than on a conventionally polished sample[8]

The morphology of damage on the "bowl" feed finished surface of BSC-2 glass was generally of the small pit type though more extensive damage was detected occasionally. The measured ratio of bulk to surface damage fields, 1.0 ± 0.1, implied a perfect surface, but based on the damage morphology we decided that the surface was in fact not as uniformly imperfection-free as possible. Not long after we had reached this conclusion we received the electron micrograph shown in Fig. 1c which confirmed this interpretation of the surface quality. Note the sensitivity of the damage morphology test to surface quality. In addition recall that, morphology aside, the results in Table I demonstrate that a carefully finished surface, even though not perfect, is still measurably harder to damage than one conventionally finished.

Bloembergen[1] has demonstrated that certain structural defects created by polishing a surface enhance the local optical electric field over that which would be present in the absence of the defect. The ratio of

externally measured bulk to surface damage fields should be equal to this enhancement assuming the same damage mechanism and that there are no defects in the bulk.[1] We note that the field which actually causes surface or bulk damage is the same as viewed by the electrons in the medium. Due to field enhancement near defects, the surface damage field as measured by the experimenter seems lower than the bulk.

Bloembergen's treatment predicts the following ratios:

	Type of Defect	
Spherical Void	Cylindrical groove	"Vee" groove
$\frac{3\epsilon}{2\epsilon + 1}$	$\frac{2\epsilon}{\epsilon + 1}$	ϵ

where ϵ = optical frequency dielectric constant. These expressions were used to obtain the predicted ratios in Table I. It is clear that there are no sharp "Vee" grooves present on conventionally finished surfaces (see also Fig. 1a) though there might very well be grooves which are neither cylindrical nor "Vee" shaped.

Another point of interest in Table I is the fact that the first and third fused quartz samples were purchased from the same manufacturer at the same time. These were described as "1/20 wave interferometer flats." We note the improvement in surface damage field which can be achieved by finer finishing. Similarly, the second and fourth fused quartz samples were both obtained from another manufacturer with his best "1/20 wave" finish. This time ion beam polishing to a depth greater than 3 times the smallest grit size used in the mechanical polishing process achieved an increase in surface damage field. The ion beam polisher employed Ar^+ ions at 10 kV and incident at 60° to the surface normal to remove 1.25 μm of material.

Table II gives the measured bulk damage fields for the samples in Table I.

The incident laser fields for entrance surface and bulk damage to transparent media are the same for imperfection-free surfaces. When imperfections are present, they enhance the optical field locally so that the surface damages more easily than the bulk. Improved surface finish quality is recognized as essential to minimizing the problem of scattering in optical systems. The results of this work show that it is also critical in the problem of laser induced surface damage.

We wish to thank L. Solomon and R. Hills of the Optical Systems Division of Itek Corp. for providing the "bowl" feed finishing so essential to these experiments. Similarly J. Gale of Ion Optics Corp. for the ion beam polishing. We also thank D. Bua for the design of the unusually stable, stable laser which was used.

TABLE II

Measured Bulk Damage Fields at 1.06 μm

Material		E_B(MV/cm)[a]
Fused Quartz	Conventional #1 Conventional #2 Bowl feed finish Ion beam polished	5.2 ± 1.3
Sapphire		6.3 ± 1.6
BSC-2 Glass		4.7 ± 1.2

(a) RMS field values are listed
Measurements were made relative to E_B in NaCl

2. References

1. N. Bloembergen, "The Role of Cracks, Pores and Absorbing Inclusions on Laser Induced Damage Threshold at Surfaces of Transparent Dielectrics" to be published, Applied Optics 12, (April 1973).

2. D. W. Fradin, E. Yablonovitch and M. Bass, "Confirmation of an Electron Avalanche Causing Laser-Induced Bulk Damage at 1.06 Microns" to be published, Applied Optics 12 (April 1973).

3. R. M. Zverev and V. A. Pashkov, Zh. Eksp. Theor. Fiz., 57, 1128 (1969).[Sov. Phys. JETP 30, 616 (1970).]

4. C. R. Guiliano and J. H. Marburger, Phys. Rev. Lett., 27, 905 (1971).

5. M. Bass and H. H. Barrett in Damage in Laser Materials NBS Special Publication 356, p. 76 and IEEE J. of Quantum Elect. QE-8 338 (1972).

6. M. Bass and D. W. Fradin, "Statistics in Laser Breakdown Dynamics" to be published.

7. M. Bass, IEEE J. of Quantum Elect. QE-7, 350 (1971).

8. C. R. Guiliano, Appl. Phys. Letters 21, 39 (1972).

VII. HIGH FREQUENCY BREAKDOWN IN IONIC CRYSTALS

A. Introduction

The growth of an electron avalanche is a time-dependent phenomena and, for a constant field, we expect the number of electrons to increase as $e^{-t/\tau}$ where τ is the e-folding time. In the following discussion we give a procedure for calculating values of τ from a Fokker-Planck equation in energy space. One of the important conclusions is that the "diffusion" term in the F-P equation plays a more important role than the average rate of energy loss which is the quantity used in the "average electron" theory of Zverev et al.[1] Based on this F-P equation we have calculated numerical results for sapphire using the parameters given by Zverev. The e-folding time is a rapidly decreasing function of field which has the value of 0.25 nanoseconds for an rms field E = 23 megavolts/cm. This value of E might be considered as a theoretical "breakdown field" since it would allow 20 generations to occur during a pulse length of 5 nanoseconds. This theoretical prediction is higher than the experimental result by a factor of about 3 (see Sec. VI for the damage field in sapphire), which Zverev reported on the basis of an average electron theory. At 50 Mv/cm our model predicts an e-folding time of 1.4×10^{-3} nanoseconds, so that a pulse length of only .028 nanoseconds would correspond to 20 generations.

B. HIGH FREQUENCY BREAKDOWN IN IONIC CRYSTALS

by

Lowell H. Holway, Jr.
Raytheon Research Division
Waltham, Massachusetts 02154

ABSTRACT

A Fokker-Planck formulation is used to describe electron avalanche breakdown in a high frequency field. It is shown that the dispersion term dominates the "average electron" term. The effect of the statistical fluctuations is to reduce the breakdown field and increase the rate of buildup of the electron population compared to the "average electron" theory. The F-P coefficients are also useful for obtaining energy distributions in the theory of gaseous discharges. Numerical results are obtained for the e-folding time in sapphire based on coefficients which were previously given by Zverev et al. in the context of "average electron" theory.

1. INTRODUCTION

In this paper a Fokker-Planck equation will be applied to the theory of avalanche breakdown in a solid. This approach predicts lower breakdown fields than those obtained by the average-electron theory of avalanche breakdown which has been applied to high frequency electric fields by Zverev et al.[1] who adopted a theory originally devised by Frolich[2] to treat the electrical breakdown caused by d.c. fields in a solid dielectric. The coefficients in our Fokker-Planck equation are given in terms of certain functions which appear in the average-electron theory,[1] which assumes the electron loses energy by collisions with longitudinal optical phonons. The crucial difference between our approach and the average electron approach is that we find that the electron dynamics in the avalanche are dominated by the dispersion rather than the average rate of energy charge.[3-6] This is considerably different from the case of energetic electrons losing energy by elastic collision in a neutral gas. These cases differ because an energetic electron is almost sure to lose energy in a collision with the cooler background gas so that the dispersion represents a small spread about this average energy loss. In contrast, when an electron emerges from a collision into an electric field, it is just as likely to gain energy as it is to lose energy, depending upon whether its velocity is directed parallel or antiparallel to the field. Thus the average energy change is the small energy change left after we subtract nearly cancelling terms from the electrons travelling in opposite directions; the dispersion is obtained by adding up the squares of these energy charges.

To see this more clearly, compare two electrons which rebound from a collision with the same speed V_o in a constant electric field of magnitude E. Let the first electron rebound in a direction antiparallel to the field so that it gains at a rate proportional to V_oE, while the second electron travels parallel to the field and loses energy at the same rate. Although the energy changes cancel at the early stages of a "free flight", the first electron has an increasing speed so that it will be gaining energy at the rate V(t) E which, at the later stages of the flight, is faster than the rate at which the second electron is losing energy. Moreover, if the collision frequency is a decreasing function of energy, the probable duration

of the flight of the first electron will be slightly greater than that of the second electron. Although both of these effects are second-order in E, they determine the average rate of energy change since the first-order terms cancel. There is no such cancellation when we calculate the dispersion. More precise results, including the effects of a high frequency electric field are calculated below.

This paper begins with a review of the "average electron" theory in Section 2 which defines the coefficients A and B which determine the F-P coefficients as discussed later. The Fokker-Planck equation is introduced in Section 3 and the contribution of the energy loss which occurs at collisions is discussed. The electric field or "free flight" contributions to the Fokker-Planck coefficients are given in Section 4, and are related to the terms A and B in the "average-electron" version of the high frequency theory. Numerical results for the e-folding times and the distribution functions which were obtained by a finite-difference solution of the Fokker-Planck equation are given in Section 5, and concluding arguments are given in the final section.

2. "AVERAGE ELECTRON" THEORY

The average electron theory as used by Zverev et al.[1] takes the average rate of energy gain from the field to be

$$A(u,E) = \left(\frac{e^2 E^2}{m^* \omega^2} \right) \nu(u) \qquad (1)$$

where they have assumed $\omega >> \nu$. Frolich's contribution to the theory was the determination of $\nu(u)$, the collision frequency for momentum transfer, by assuming that ν results from the interaction of the electron with longitudinal optical phonons. Frolich[2] obtains

$$\nu(u) = b\, u^{-3/2} \quad . \qquad (2)$$

In the last two equations, E is the rms intensity of the electric field of the laser beam, ω is the angular frequency of the laser field, e and m^* are

the charge and effective mass of the electron, u is the electron energy, and b, a parameter depending on the temperature and physical characteristics of the ionic crystal is:

$$b = (1 + \frac{2}{\exp(\hbar\omega_t / kT) - 1}) \, 2^{1/6} \pi^3 e^4 h / 4m^{*1/2} Ma^5 \omega_t \quad , \qquad (3)$$

where M is the reduced mass of the ions, a is the lattice constant and ω_t is the (Reststrahlen) frequency of the optical phonons.

The average rate at which an electron loses energy to the longitudinal optical phonons was given by Frohlich[2] as

$$B = d_1 u^{-1/2} \ln (d_2 u^{1/2}) \qquad (4)$$

where d_1 and d_2 depend on the material parameters

$$d_1 = \pi e^4 \sqrt{2m^*} / Ma^3 \qquad (5)$$

and

$$d_2 = 2^{5/6} \pi / a \omega_t \quad m^* \quad . \qquad (6)$$

We will consider in detail the numerical example considered by Zverev et al.,[1] in which sapphire was exposed to 0.694 μm laser wavelength. For this example they assumed T = 300°K, the ionization energy I = 6 ev, the lattice spacing a = 5.13 Angstroms, the angular frequency of the longitudinal optical phonons is $\omega_t = 3.77 \times 10^{13}$ sec^{-1} and the effective mass is $m^* = 9.107 = 10^{-28}$ gm. In addition, we assume reduced mass M is 10.05 atomic mass units, where $M = M_+ M_- / (M_+ + M_-)$.

In Fig. 1, the average rate of energy loss (B) to the optical phonons is shown in electron-volts per picosecond as a function of energy as well as the average rate of gain (A) for applied rms fields of 2×10^7 v/cm, 3×10^7 v/cm and 5×10^7 v/cm. Low energy electrons will gain energy until they reach u_{crit}, the energy at which curve B intersects the appropriate curve A. For example, if the applied field is $3 = 10^7$ v/cm, electrons with energy less than about 2.05 ev gain energy on the average while electrons

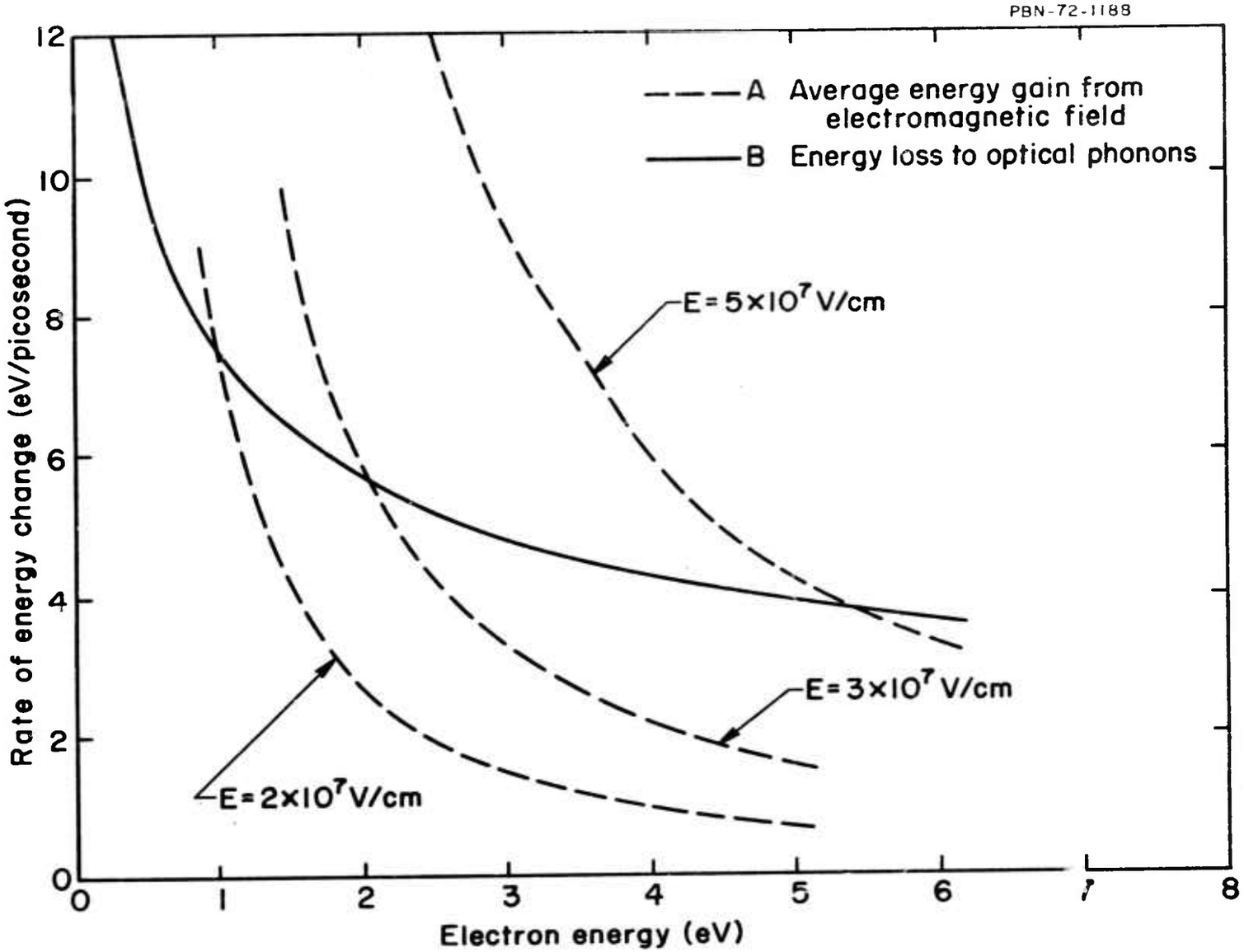

Fig. 1 Average Ratios of Energy Change in Sapphire. The solid curve gives the rate of energy loss according to Frohlich. The dashed curves give rates of energy gain for different electric fields according to Zverev et al. The intersection of a dashed curve with the solid curve defines u_{crit} where the average electron neither gains or loses energy.

with energy greater than 2.05 ev lose energy on the average. The breakdown criterion is therefore defined by Zverev et al.[1] as the field for which u_{crit} equals the ionization energy I, which is 6 ev for sapphire. This corresponds to an applied field slightly greater than $5 = 10^7$ v/cm, as can be seen from Fig. 1.

The high frequency limit for A, given by Eq. (1) assumes that $\omega >> \nu$, but, in view of the energy dependence given by Eq. (2), it is clear that this form is incorrect for sufficiently low energy electrons. We will consider Zverev's parameters and radiation frequency, for which the high frequency limit can be safely used since it is only violated below 0.1 ev. However, this may no longer be true for other crystals or for laser radiation with a longer wavelength.

It is interesting to compare the high frequency formula for energy gain with the low frequency or d.c. solution for which

$$A = \frac{e^2 E^2}{m^* \nu(u)} \quad , \qquad \nu >> \omega \quad . \tag{7}$$

For Eq. (7) the average rate of energy gain increases with increasing energy. In this event, although a u_{crit} is still defined by the intersection of curves A and B, now all electrons with energies above u_{crit} gain energy on the average while electrons with energy below u_{crit} lose energy. This led to two criterion for breakdown. Frohlich took $u_{crit} = I$ as defining breakdown[2] as it does in the high frequency case; according to Seitz[7] this implies that electrons reach the ionization energy by some unexplained method and the breakdown criterion only requires that electrons with energies on the order of the ionization energy I will continue to gain energy on the average. On the other hand, Von Hippel[8] applied the more stringent requirement that the electric field must be so strong that all electrons above thermal energy will gain energy from the field. This somewhat paradoxial situation no longer occurs in the following derivation in which we will show that the fluctuations in electron energy play a more important role than the average rate of energy change.

3. FOKKER-PLANCK EQUATION

Let f(u,t) du be the number of electrons with energy between u and u + du at time t. The distribution function has been shown to satisfy[9] the kinetic equation

$$\frac{\partial f}{\partial t} = -\frac{\partial}{\partial u}\left(\frac{<\Delta u>}{\Delta t} f\right) + \frac{1}{2}\frac{\partial^2}{\partial u^2}\left(\frac{<(\Delta u)^2>}{\Delta t} f\right) \tag{8}$$

where $<\Delta u>/\Delta t$ is the average rate of energy change and $<(\Delta u)^2>/\Delta t$ is the dispersion. If the dispersion is taken to be zero, Eq. (8) is essentially equivalent to the "average electron" theory since Eq. (8) would then describe the behavior of a distribution of electrons in which every electron was following the same trajectory as the average electron.

The basic assumption made in deriving Eq. (8) is that it is possible to choose a time increment Δt which is long compared to the time between collisions but is short compared to the time in which a significant change occurs in the electron energy. This will always be possible if the fractional energy change between two collisions is small, i.e., if

$$e^2 \frac{E^2}{\nu^2} \ll mu \quad , \tag{9}$$

a condition which is generally obeyed unless the electric field is much larger than typical breakdown fields.

In computing these coefficients it is convenient to separate the energy-changing mechanisms into two parts: first, the electric field accelerations which occur during free flights between two collisions; secondly, energy transfer which occurs at a collision. For the case of elastic collision of electrons in a gas composed of heavy molecules which have a Maxwell-Boltzmann distribution, expressions have been obtained for these coefficients by assuming that both free-flight and collisional energy-changes were statistically independent.[3-6] When the average rate of energy loss is calculated it is seen that A from Eq. (1) should be identified with the free-flight energy change caused by the electric field while the energy loss which occurs at a collision is associated with -B in Eq. (4).

In order to estimate the variance associated with the energy loss which occurs at a collision, we consider an analogous case for electrons colliding elastically with a cold background gas; i.e., a gas in which $kT << u$. The central limit theorem has been used to obtain expressions for an arbitrarily long time t, which are given by Eq. (32) of Ref. 6 for the collisional energy loss due to contact collision-frequency and isotropic scattering. For short times Δt, such that Eq. (17) of the same reference is satisfied, the equation holds for energy-dependent collision frequencies. According to Eq. (32) the mean rate of change of the energy and the dispersion in a time Δt are

$$< \Delta u > = < u - u_o > = - \epsilon \nu u \Delta t \tag{10}$$

and

$$< (\Delta u)^2 > = < (u - u_o)^2 > = \frac{4}{3} \nu u^2 \epsilon^2 \Delta t \tag{11}$$

where ϵ is the small parameter $\epsilon = 2mM/(m + M)^2$, m is the mass of the electron and M is the mass of a background gas. Equations (10) and (11), which are correct to order ϵ^2, show that the ratio of the variance to the average rate of change of the energy is

$$< (\Delta u)^2 > / < \Delta u > = - \frac{4}{3} \epsilon u \quad . \tag{12}$$

Thus, the variance is small compared with the mean energy loss and it is not a bad approximation to neglect the dispersion in Eq. (8). Since the energy loss in collision with optical phonons will be a process similar to the loss in an elastic collision with gas molecules we will assume that the collision process contributes the term -B to the term $< \Delta u > / \Delta t$ in Eq. (8), but makes a negligible contribution to the term $< (\Delta u)^2 > / \Delta t$. An equation similar to Eq. (10) is given by Braglia and Ferrari,[4] but since they neglect terms of order ϵ^2 they would not obtain Eq. (11).

4. ELECTRIC FIELD CONTRIBUTIONS TO THE F-P COEFFICIENTS

For the electric field contribution, we will assume that the energy change during free flight between any two collisions is independent of the changes between any other two collisions. This result is assumed by Braglia and Ferrari[4] and, for energy-independent collision frequency, gives the same results as is obtained by giving the probability distribution for the collision times.[3] According to this assumption, the mean and variance of the sum of the energy changes during a time Δt is just n, the expected number of collisions, times the mean and variance due to a single free flight. However, since Braglia and Ferrari's results[4] were for a d.c. field, we must extend them to include radiation of an arbitrary frequency.

According to our assumption we have

$$< \Delta u > = n < \delta u > = \nu \Delta t < \delta u > \quad , \tag{13}$$

where $< \delta u >$ is the average energy change between any one flight. We assume that the electric field is along the z-axis with magnitude

$$E(t) = \sqrt{2}\, E \sin \omega t \tag{14}$$

so that E is the rms field. If a collision occurs at a time t_o and the electron emerges from the collision with a velocity making an angle θ with the z-axis, it is easily shown that, at a later time t, the energy of the electron will have changed by an amount u, where

$$\delta u = \frac{a}{\omega} \sqrt{2mu}\, (\cos \omega t_o - \cos \omega t) \cos \theta + \frac{ma^2}{2\omega^2} (\cos \omega t_o - \cos \omega t)^2 \quad , \tag{15}$$

where u is the original energy of the electron, and a is the peak acceleration $a = \sqrt{2}eE/m$. Because of the inequality in Eq. (9), we can show that the term $(a/\omega)(\cos \omega t_o - \cos \omega t)$ is a small quantity.

Now let $p_1(t)\, dt$ be the probability that the time between collisions will be between t and $t + dt$. In addition, define $p_2(\theta)\, d\theta$ as the probability

that the electron emerges from the collision at time t_o with its velocity vector making an angle between θ and $\theta + d\theta$. Then the average value of the energy change between collisions is

$$< \delta u > = \int_o^{\pi} p_2(\theta)\, d\theta \int_{t_o}^{\infty} p_1(t')\, \delta u\, dt' \quad . \tag{16}$$

Now $p_1 = \nu(u + \delta u)p_o$ where p_o, the probability that a collision has not occurred at time t, satisfies

$$\frac{dp_o}{dt} = -\nu(u + \delta u)p_o = -(\nu + \delta u \frac{\partial \nu}{\partial u})\, p_o \quad . \tag{17}$$

Then

$$p_1 = \nu(u + \delta u)\, e^{-\int_{t_o}^{t} \nu(u + \delta u)\, dt'}$$

$$\simeq (\nu + \frac{\partial \nu}{\partial u}\, \delta u)\, (1 - \frac{\partial \nu}{\partial u} \int_{t_o}^{t} \delta u\, dt')\, e^{-\nu(t-t_o)} \quad , \tag{18}$$

where we have used the fact that $\delta u << u$ to expand the collision frequency in a Taylor's series.

Now we assume that all directions are equally likely for the velocity vector when the electron emerges from collision at time t_o, so that

$$p_2 = (\frac{1}{2}) \sin \theta \quad . \tag{19}$$

Let Eqs. (15) and (16) be expanded in powers of a. The term proportional to a involves $\cos \theta$ so that it vanishes when integrated over θ. Physically, this indicates that while individual electrons either gain or lose energy at a rapid rate (proportional to a), there are as many electrons that gain energy as lose energy, so that the average rate of energy change is a small number which results from the near cancellation of large numbers.

For this reason, the dispersion is much more important in the "free flight" random walk process than it is in the process of energy transfer to heavy particles where a particle far above thermal energy is almost certain to lose energy at each collision. The term proportional to a^2 which are obtained from Eq. (15) - (18) are

$$\langle \delta u \rangle = \left(\frac{a}{\omega}\right)^2 \int_0^{\pi} p_2(\theta)\, d\theta \int_{t_o}^{\infty} \nu\, e^{-\nu(t-t_o)}\, H(\theta, t-t_o)\, dt \qquad (20)$$

where

$$H(\theta,t) = \frac{m}{2}[\cos\omega t_o - \cos\omega(t+t_o)]^2 \left(1+4\cos^2\theta \left(\frac{u}{\nu}\right)\frac{\partial\nu}{\partial u}\right)$$

$$- 2\,mu\cos^2\theta \frac{\partial\nu}{\partial u}[\cos\omega t_o - \cos\omega(t+t_o)]\left[t\cos\omega t_o + \frac{1}{\omega}(\sin\omega(t+t_o) - \sin\omega t_o)\right].$$

The time of collision t_o is equally likely to occur at any time between 0 and $2\pi/\omega$. Therefore we take $t-t_o = x$ in Eq. (20) and average over t_o to obtain

$$\langle \delta u \rangle = \frac{1}{2}\left(\frac{a}{\omega}\right)^2 m\nu \int_0^{\pi} p_2(\theta)\, d\theta \int_0^{\infty} e^{-\nu x}\left[(1-\cos\omega x)\left(1+4\cos^2\theta\left(\frac{u}{\nu}\right)\frac{\partial\nu}{\partial u}\right)\right.$$

$$\left. - 2\cos^2\theta\, x\,(1-\cos\omega x)\, u\frac{\partial\nu}{\partial u}\right] dx$$

$$= \frac{ma^2}{2(\omega^2+\nu^2)}\left(1+\frac{2}{3}\frac{\omega^2-\nu^2}{\omega^2+\nu^2}\left(\frac{u}{\nu}\right)\frac{\partial\nu}{\partial u}\right) . \qquad (21)$$

From Eq. (13) we have:

$$\frac{\langle \Delta u \rangle}{\Delta t} = \frac{e^2 E^2 \nu}{m(\omega^2+\nu^2)}\left(1+\frac{2}{3}\frac{\omega^2-\nu^2}{\omega^2+\nu^2}\left(\frac{u}{\nu}\right)\frac{\partial\nu}{\partial u}\right) . \qquad (22)$$

If $\omega = 0$, Eq. (22) is equivalent to the results of Braglia and Ferrari[4] and, if ν is independent of energy, it is identical in the limits $\omega >> \nu$ or $\nu >> \omega$, with Holway's results.[3]

In this paper we are interested in the high frequency limit $\omega >> \nu$ in which Eq. (22) becomes

$$\frac{\Delta u}{\Delta t} = A\left(1 + \left(\frac{2u}{3\nu}\right)\frac{\partial \nu}{\partial u}\right) \tag{23}$$

where A, defined in Eq. (1), is the standard form for the average rate of energy gain. The correction to the standard form given by Eq. (23) can be large for some force laws, and has the opposite sign from the d.c. correction given by Braglia and Ferrari.[4]

The dispersion of the energy, which is most important to our theory, is

$$< (\delta u)^2 > = \int_0^{\pi} p_2(\theta) \int_{t_o}^{\infty} p_1(t)\, (\delta u)^2\, dt \quad . \tag{24}$$

In this case the calculations are much simpler because the lowest order term does not vanish, and Eqs. (15) and (24) give

$$< (\delta u)^2 > = \left(\frac{2mu}{3}\right)\left(\frac{a}{\omega}\right)^2 \nu \int_{t_o}^{\infty} e^{-\nu(t-t_o)} (\cos \omega t_o - \cos \omega t)^2\, dt$$

$$= \frac{4mu\, a^2}{3(\nu^2+4\omega^2)} \left[\frac{2\omega^2 - \nu^2}{\nu^2 + \omega^2} \cos^2 \omega t_o + \frac{3\omega\nu}{\nu^2+\omega^2} \sin \omega t_o \cos \omega t_o + 1 \right] . \tag{25}$$

After averaging over t_o, Eq. (25) yields

$$\frac{< (\Delta u)^2 >}{\Delta t} = \frac{4}{3} \frac{e^2 E^2 \nu}{m(\nu^2 + \omega^2)} u \quad , \tag{26}$$

where the relationship $< (\Delta u)^2 > \doteq \nu \Delta t < (\delta u)^2 >$ has been used. The result in Eq. (26) was given earlier[3] in the limits $\omega >> \nu$ and $\nu >> \omega$.

The ratio $< (\Delta u)^2 > / < \Delta u > = \frac{4}{3} u \left(1 + \frac{2}{3} \frac{u}{\nu} \frac{\partial \nu}{\partial u}\right)^{-1}$ for the electric field contribution to the F-P coefficients; this demonstrates that dispersion is much more important for the electric field energy exchange process than it is for the collisional energy exchange, which has the ratio given by Eq. (12).

When f is independent of time, the coefficients derived here are in agreement with those given by Brown[10] for F_o^o with the appropriate change in variable.

5. APPLICATION TO A SAPPHIRE CRYSTAL

The application of our derivation can be illustrated by considering high frequency breakdown in sapphire, where we continue to use the parameters of Zverev et al. given in Section 2.

From Eq. (23), the average rate of energy gain from the electric field for the high frequency limit when $\nu = b\, u^k$, is

$$\frac{\Delta u}{\Delta t} = A\left(1 + \frac{2}{3} k\right) \tag{27}$$

and, since k is - 3/2 in Frohlich's model the contribution vanishes. Thus the only contribution to the average rate of energy change is a loss due to energy transfer at collisions which is given by Eq. (4)

$$\frac{< \Delta u >}{\Delta t} = - B \quad , \tag{28}$$

which means that the average rate of energy loss is independent of the electric field.

On the contrary, we assume that electric field and not the collisional loss contributes significantly to the dispersion, which according to Eq. (26) with $\omega >> \nu$ is just

$$\frac{< (\Delta u)^2 >}{\Delta t} = \frac{4}{3} A\, u \quad . \tag{29}$$

In this way we are able to get both the dispersion and the average rate of energy loss while using only the same quantities which Zverev et al. used.[1]

The number of electrons whose energies increase from a value less than u to a value greater than u per unit time is the "current.

$$J(u) = f \frac{<\Delta u>}{\Delta t} - \frac{1}{2} \frac{\partial}{\partial u} \left(\frac{<\Delta u^2>}{\Delta t} f \right) \tag{30}$$

so that the number of electrons reaching ionization energy is J(I) and we assume that two electrons appear at zero energy for each ionization. Thus our boundary conditions are

$$J(0) = 2\, J(I)$$

$$f(I) = 0 \tag{31}$$

and the F-P equation is

$$\frac{\partial f}{\partial t} = - \frac{\partial J}{\partial u} \quad . \tag{32}$$

A finite-difference computer program was written to integrate Eq. (31) and (32) with the coefficient defined by Eqs. (28) - (30). Anticipating that the solution will have the form

$$f = \sum_m a_m \phi_m(u)\, e^{t/\tau_m} \tag{33}$$

where the ϕ_m are eigenfunctions and $1/\tau_m$ are the eigenvalues, we find that the solution behaves as if these were a single eigenvalue τ_o such that $1/\tau_o > 1/\tau_m$ for $m \neq 0$. Then, for late times, the distribution function has the form

$$f = a_o \phi_o(u)\, e^{+ t/\tau_o} \quad , \tag{34}$$

where we define τ_o as the e-folding time, and ϕ_o is the asymptotic shape of the distribution function.

In Fig. 2, the e-folding times are plotted as a function of electric field. The dashed line shows the results which we would have obtained if A-B had been used as the average rate of energy change, following Zverev et al., instead of using -B as was derived above. The small difference between the two results verifies that the solution is dominated by the dispersion term. It is fortunate that $< \Delta u > / \Delta t$ is not important, since the vanishing of the electric field contribution is an artifact of the -3/2 power law for ν obtained by Frohlich[2] and requires $\omega >> \nu$.

The evolution of a distribution function which is assumed to be a constant at t = 0 is shown in Fig. 3 for 50 Mv/cm rms field. At each time, the distribution functions were renormalized before they were plotted so that

$$\int_o^I f\,du = 1 \quad .$$

The distribution function is found to approach its asymptotic form of Eq. (34) when $\bar{t}$ is of the order of one or two, where $\bar{t}$ is a nondimensional time defined by $t/\bar{t} = 1.6 \times 10^{-12}/A$, which is inversely proportional to the square of the field. These times are much less than the e-folding times.

Figure 4 shows the evolution of a Gaussian function which was initially centered near 2 ev, for the same field as in the previous figure. By the time $\bar{t} = 1$ the influence of the initial condition has almost disappeared as each function approaches its asymptotic value. Figure 5 shows the evolution under the influence of a weaker field, E = 20 Mv/cm. In all of these cases, J(u) is positive everywhere for the asymptotic distribution. At very low energies this is achieved because $< (\Delta u)^2 > / \Delta t$ increases as $u^{-1/2}$ as $u \to 0$; at high energies the steep slope of f causes electrons to diffuse towards higher energies.

Once we have obtained a solution for the distribution function, we can define an e-folding time as $\tau(t) = n/(dn/dt)$, where $n = \int f\,du$ is the

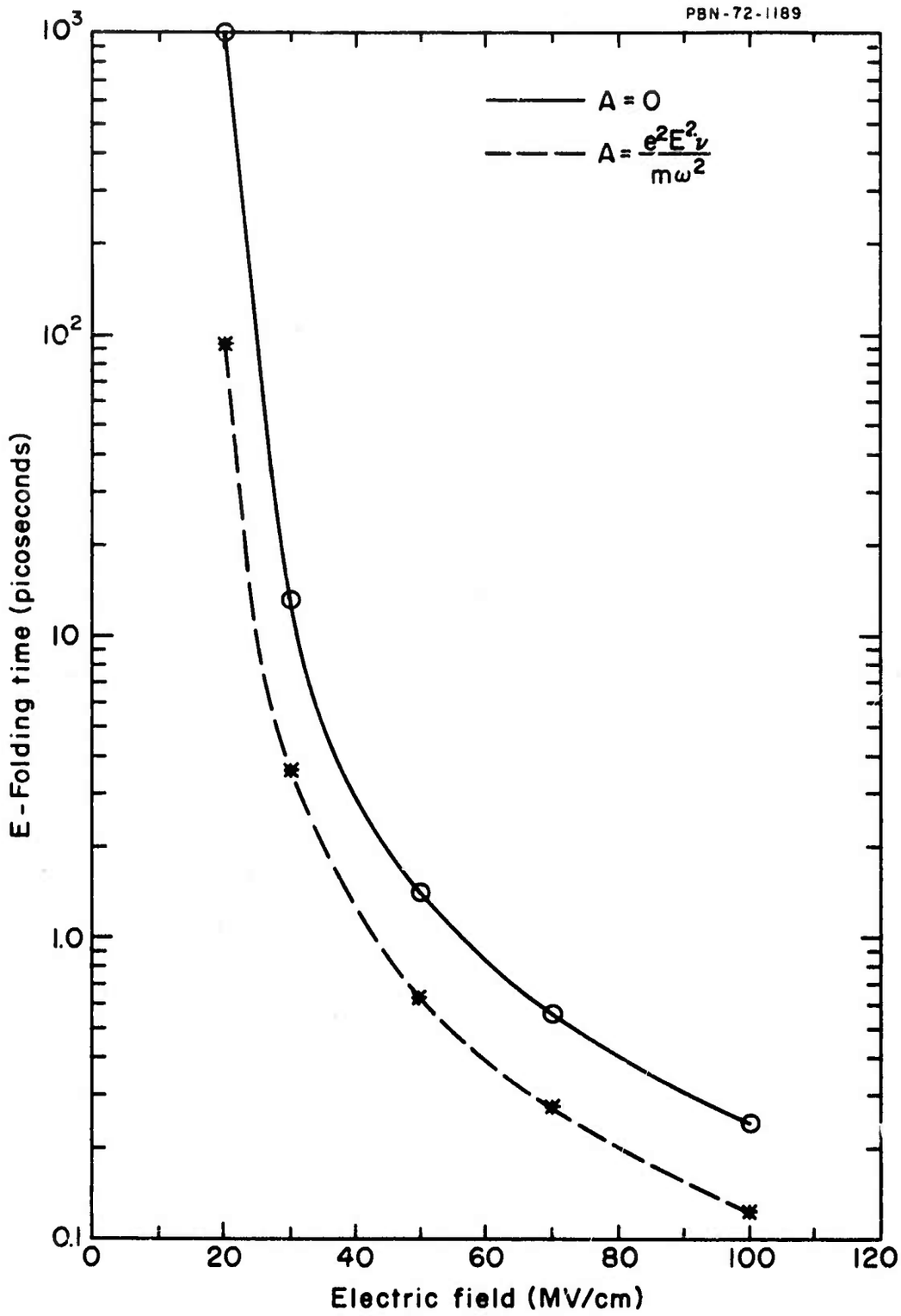

Fig. 2 The e-folding Time as a Function of Electric Field in Sapphire. The dashed curve uses Zverev's A as average rate of energy gain from the field. The solid curve takes zero for the average energy gain from the field. There is little difference because the behavior of the distribution function is controlled by the dispersion, not the average rate of gain.

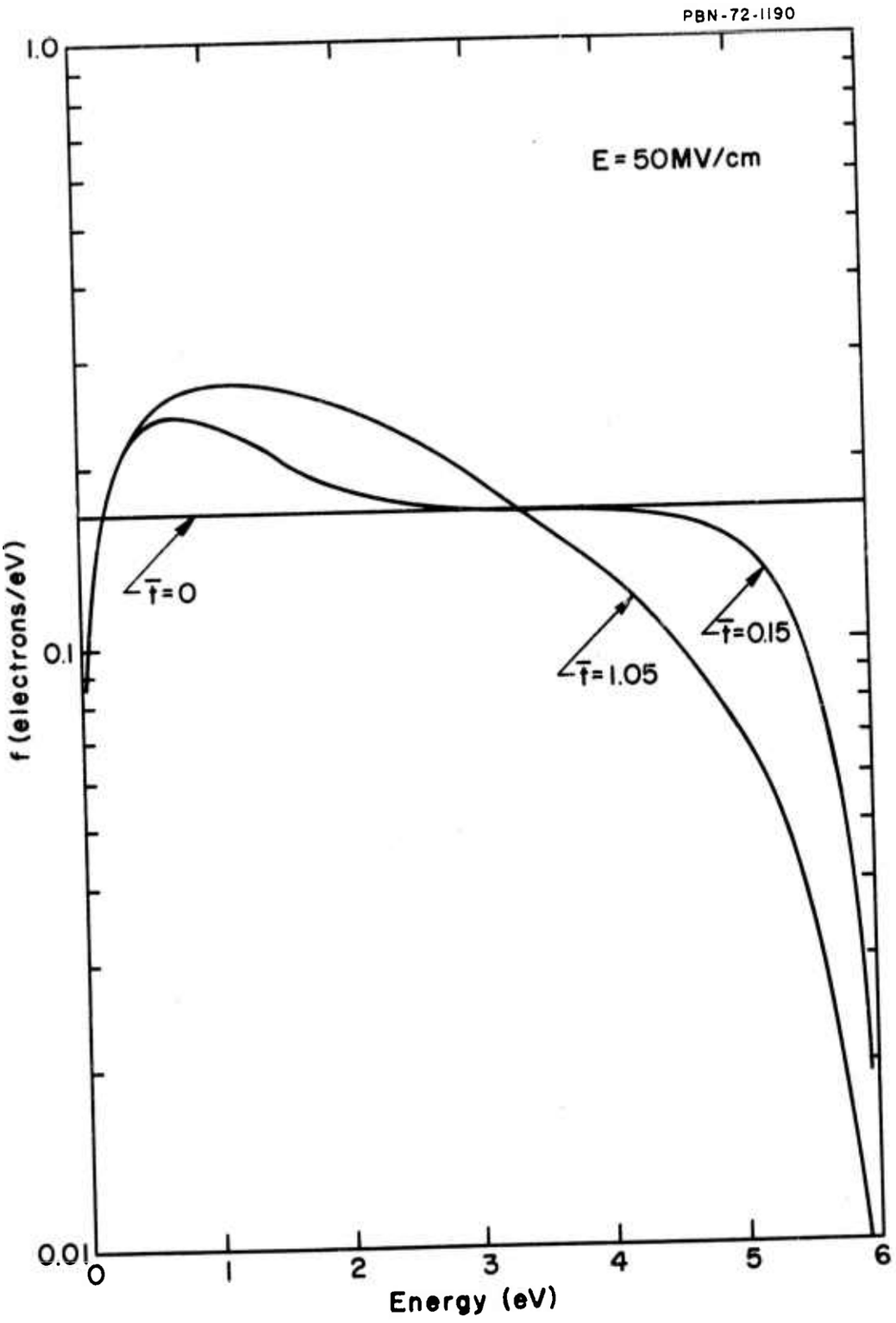

Fig. 3 Distribution Function for a 50 MV/cm rms Field When the Original Distribution Function is a Constant. The function changes until a steady state is reached near $\bar{t}$= 1. Here $(t/\bar{t})$ = .104 picoseconds.

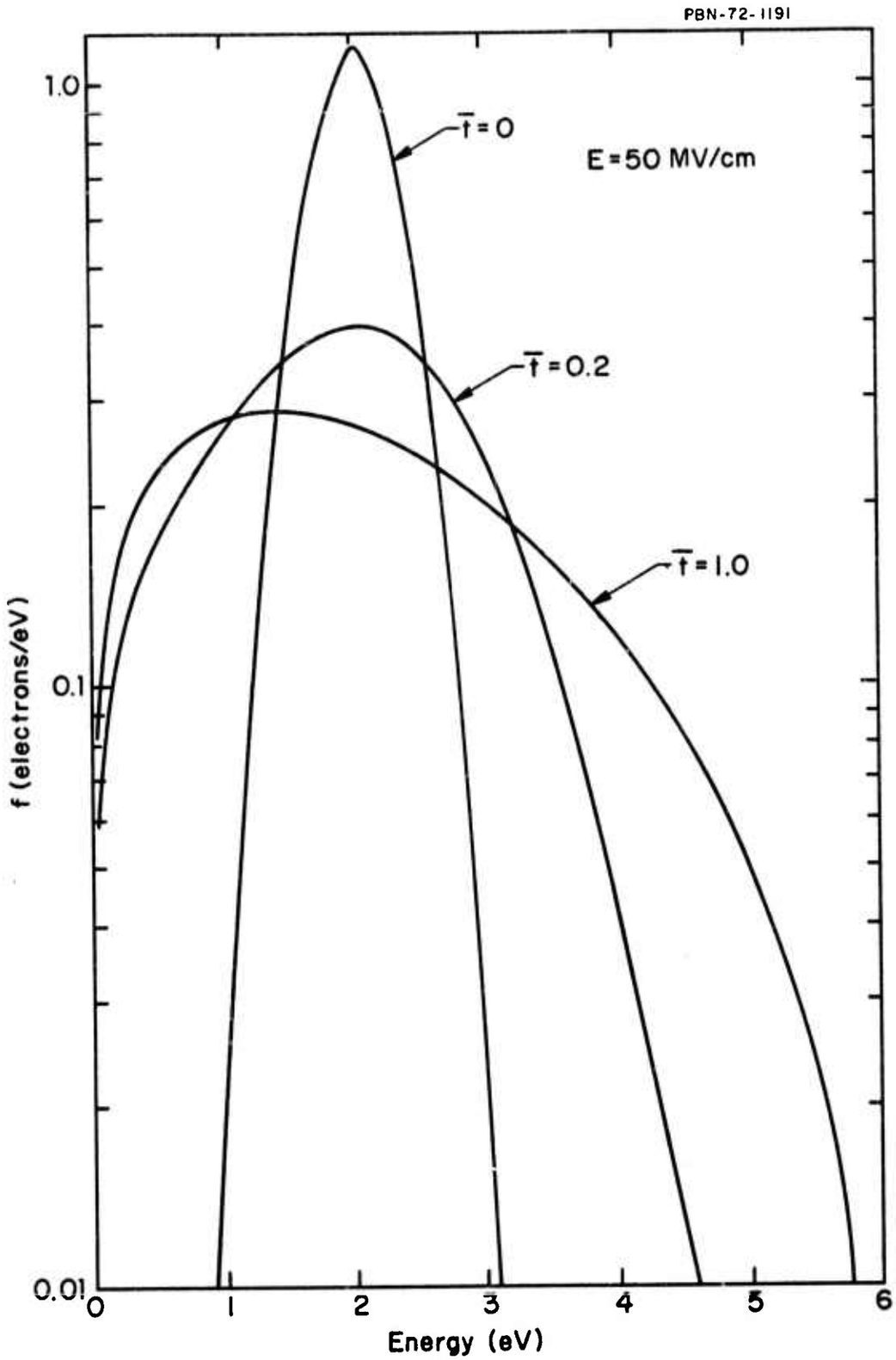

Fig. 4 Distribution Function for a 50 MV/cm Field When the Original Distribution is a Gaussian Ceneter ed at 2.05 eV. The steady-state distribution is independent of the original distribution.

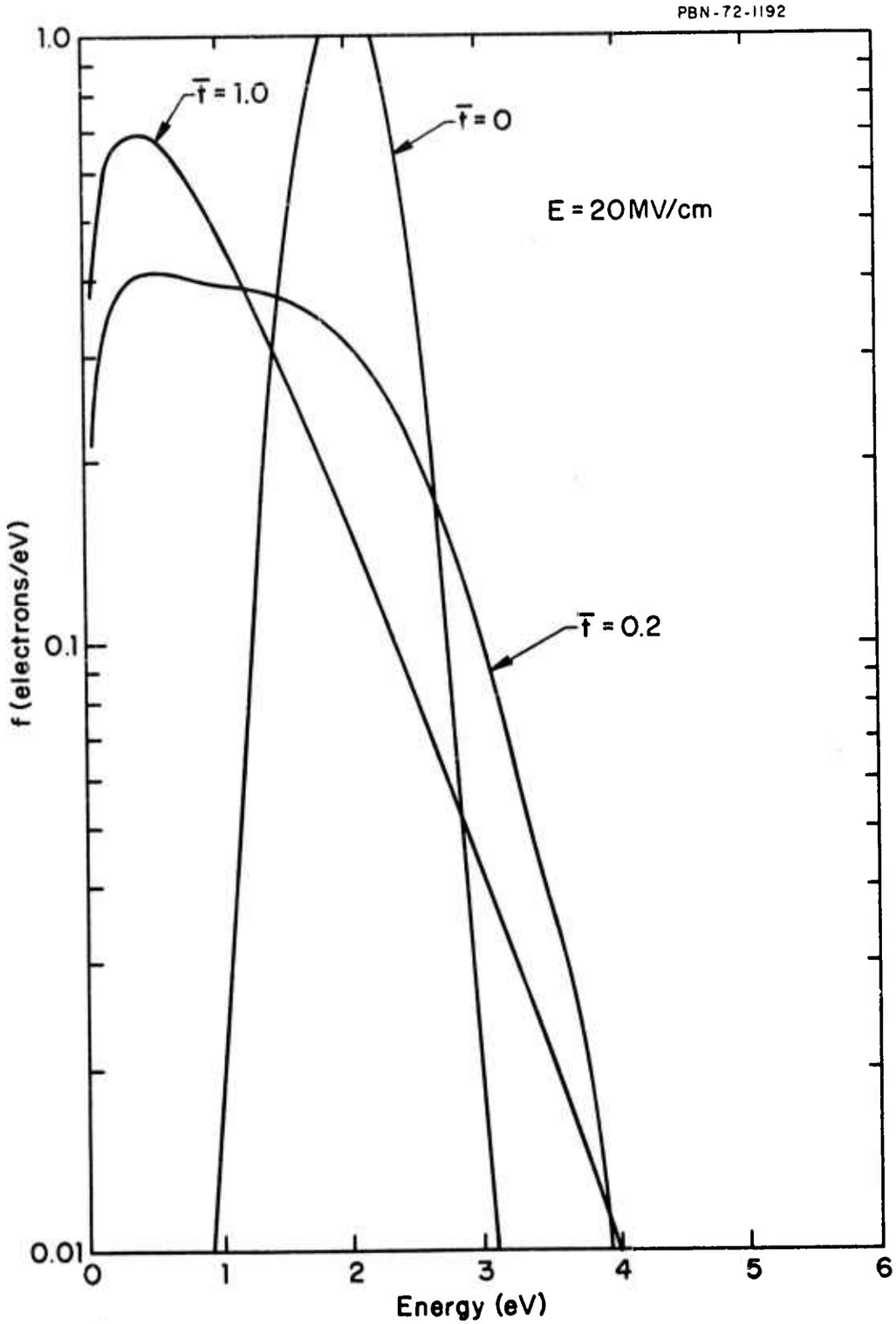

Fig. 5 Distribution Function for a 20 MV/cm rms Field When the Initial Distribution is a Gaussian Centered at 2.05 eV. Here $(t/\bar{t})$ = .649 picoseconds.

total number of electrons present. Assuming Eq. (34) to hold at late times, this definition of an e-folding time yields

$$\lim_{t \to \infty} \tau(t) = \tau_o$$

where τ_o is the constant e-folding time. This time-dependent e-folding time is plotted in Fig. 6 where the fact that τ approaches a constant for $\bar{t}$ greater than about two verifies Eq. (34). The solid curves are for a Gaussian initial distribution and the dashed curve for a uniform initial distribution function. As usual, the form of the initial distribution becomes irrelevant in a time short compared to the e-folding time.

6. CONCLUSIONS

If the laser pulse is 5 nanoseconds long and we require 20 e-folding times for the breakdown process, the breakdown field would be reached when $\tau_o = 0.25$ nanoseconds which, according to Fig. 2, corresponds to an rms field of 23 Mv/cm in sapphire. There will be only a small increase in breakdown field if we require 40 e-folding times as suggested by Seitz.[7] This theoretical breakdown field is reasonably close to a recent experimental result[11] of 6.3 ± 1.6 Mv/cm, which was obtained by taking great care to avoid self-focussing and defined the damage field as that field which results in a probability for damage by a single laser pulse equal to 0.5. The present result is considerably smaller than the "average electron" theoretical prediction which was 50 Mv/cm. There was excellent agreement with the temperature dependence of the destruction threshold shown by Zverev et al.[1] Since the electric field dependence of the present theory appears only in A, the present theory will give the same temperature dependence, i.e., $E_{thr}^2 \sim (1 + \frac{2}{\exp(h\omega/kT) - 1})^{-1}$.

It would be useful to extend the finite-difference program to include the effects of a finite ionization cross section in which case the new electrons would be born at non-zero energies. It was convenient to illustrate our approach by using the example Zverev et al.,[1] since our Fokker-Planck coefficients were completely determined by their coefficients A and B.

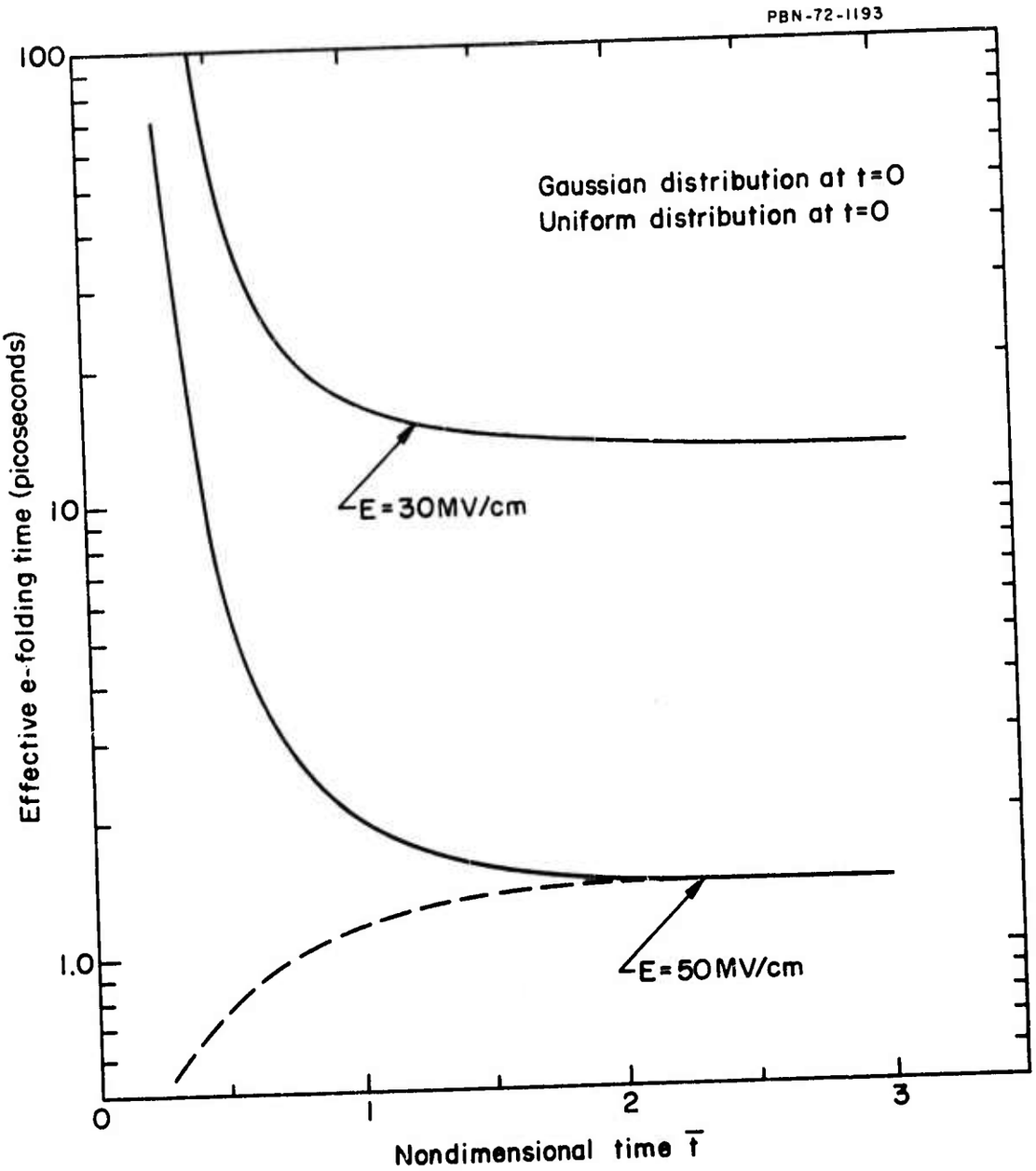

Fig. 6 Effective e-folding Times $\tau = n/(dn/dt)$. This e-folding time reaches its constant value characteristic of the applied electric field after the distribution function reaches its steady-state value. Here $(t/\bar{t})$ equals 0.289 picoseconds for 30 MV/cm and equals 0.104 picoseconds for 50 MV/cm.

However, these calculations can be extended to other materials and to lower laser frequencies where d.c. effects begin to become important.

Our formulation of breakdown in terms of e-folding times does not lead to a precise value of the breakdown field until we introduce some relevant time scale such as the pulse duration. The e-folding time which we calculate remains positive as E decreases although it becomes much longer. This is because we have ignored dissipative processes which become more important when τ_o becomes large. For example, diffusion should be included when the diffusion time (which is about 1 nanosecond for a 10 um beam, if we accept Frohlich's collision frequency) is of the order of the e-folding time.

ACKNOWLEDGEMENT

This research was partly supported by the Raytheon Independent Research Program and partly under Contract No. F19628-70-C-0223 sponsored by the Advanced Research Projects Agency. The author is grateful for the advice and encouragement supplied by M. Bass and D. Fradin.

7. REFERENCES

1. G. M. Zverev, T. N. Mikhailova, V. A. Pashkov, and N. M. Soloveva, Sov. Phys. (JETP) 26, 1053 (1968).
2. H. Frohlich, Proc. Roy. Soc. (A) 160, 230 (1937).
3. L. H. Holway, Jr., Phys. Rev. Letts. 28, 280 (1972).
4. G. L. Braglia and L. Ferrari, Lett. Nuovo Cimento 4, 537 (1972).
5. G. L. Braglia, Nuovo Cimento 70B, 169 (1970).
6. C. F. Eaton and L. H. Holway, Jr., Phys. Rev. 143, 48 (1966).
7. F. Seitz, Phys. Rev. 76, 1376 (1949).
8. A. von Hippel, Ergeb. d. exakt. Naturwiss. 14, 79 (1935).
9. G. E. Uhlenbeck and L. S. Ornstein, Phys. Rev. 36, 823 (1930).
10. S. C. Brown, "Introduction to Electrical Discharges in Gases," p. 177, John Wiley and Sons, Inc., New York (1966).
11. D. Fradin and M. Bass, "A Comparison of Laser-Induced Surface and Bulk Damage," Raytheon Memo M-2736, to be published. (Section VI of this report.)

VIII. ADDITIONAL OBSERVATIONS

A. Introduction

In this section several observations, speculations, and experimental techniques are presented which are useful but not discussed elsewhere in the report. These include: 1) A discussion of entrance and exit surface damage morphology, 2) The observation of a sharp, well-defined transmitted pulse attenuation for intrinsic surface damage, 3) a possible reason for the few, very hard to damage places on $LiNbO_3$ surfaces described previously, 4) Some comments on the occurrence of inclusion damage, and 5) A new technique for determining the laser beam mode pattern using a video camera-TV monitor system.

B. Comments on Entrance and Exit Surface Damage Morphology

In Scientific Report No. 1[1] scanning electron micrographs of entrance and exit surface damage to conventionally polished $LiNbO_3$ were presented. These showed the former to be small, shallow regions on the surface while the latter was larger and deeper and was surrounded by a region of cracked material. Figure VIII-1 and 2 show that the same is true for conventionally finished KDP. The difference can be understood by reasoning along the same lines as in the discussion of damage morphology in Sec. VI.

a) Unirradiated, polished KDP surface.

0.0005 cm

e⁻ Beam incident at 45°

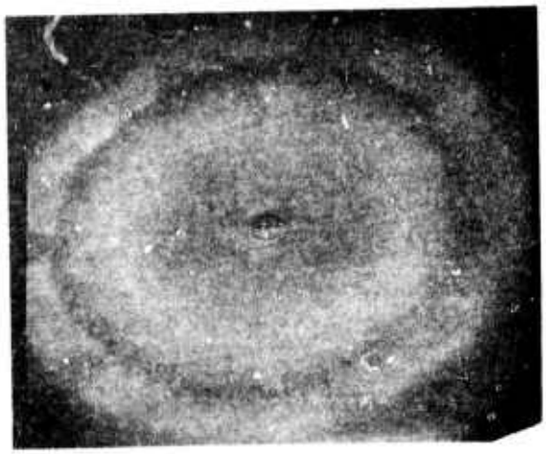

b) Entrance surface damage on KDP due to a TEM_{00} mode 1.06μm pulse with 0.003 cm diameter.

0.002 cm

e⁻ Beam incident at 45°

c) Detail of area in (b) directly exposed to laser beam.

0.0005 cm

e⁻ Beam incident at 45°

FIGURE 1

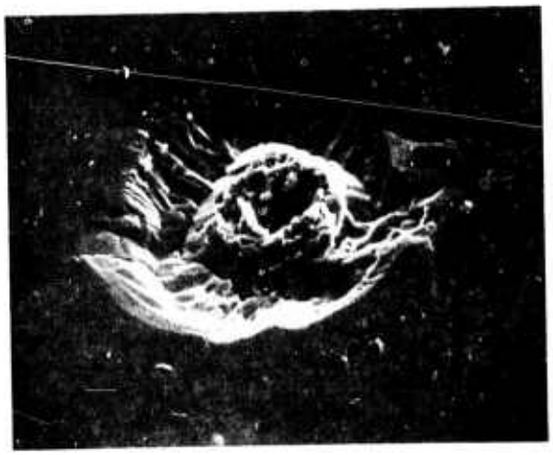

a) Exit surface damage on KDP due to a TEM_{00} mode 1.06μm pulse with 0.003 cm diameter.

0.002 cm

e⁻ Beam incident at 45°

b) Same as (a) but showing height of central region. Approximate profile:

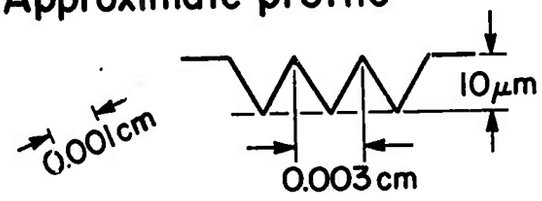

e⁻ Beam incident at 80°

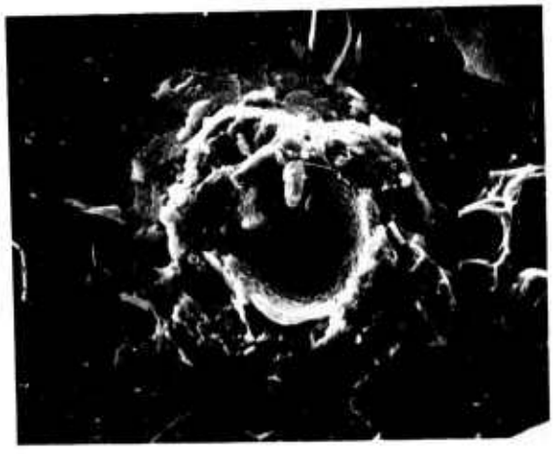

c) Detail of area directly exposed to laser beam. Note the only material which might have been molten is in this area.

0.001 cm

e⁻ Beam incident at 17.5°

FIGURE 2

When entrance damage occurs on a conventionally finished surface, it prevents light from getting inside the medium and so only a small region near the surface can be damaged. By focusing at an exit surface, the conditions of irradiation are similar to those which produce entrance surface damage just below an imperfection-free surface. The conventionally finished exit surface breaks down first, but is down stream from the region just below the exit surface. This materials is then intensely irradiated and breaks down. Thus, more extensive damage, including a region of cracked material, is formed.

C. The Sharp, Well-Defined Transmitted Pulse Attenuation for Surface Damage

The technique for identifying damage events caused by intrinsic processes described in Section III was applied to entrance surface damage to serveral of the materials studied in Scientific Report No. 1 and not discussed elsewhere in this report. In all cases using the Nd:YAG laser the sharp, well-defined attenuation characteristic of damage due to an intrinsic process was observed.

D. Comments on the "Hard-to-Damage Areas" of a $LiNbO_3$ Crystal Surface

In Scientific Report No. 1 we pointed out that one sample of $LiNbO_3$ showed areas which were much more resistant to damage than

the rest of the surface. On the basis of the results in Sec. VI, we now feel that these small areas may have been imperfection-free and so the field for damage could have been ~ 2-3 times higher than at places which contained polishing imperfections.

E. Inclusion Damage

In the present work, we have treated damage from absorbing inclusion as a dirt effect to be avoided. An interesting observation concerning inclusion damage was made, however, which may reveal the nature of damaging impurities. It was found that Nd:YAG laser pulses seldom induce inclusion damage under the conditions of our measurements, but they were the major cause of damage in these same crystals at ruby wavelength. The duration of the ruby pulses was about three times as long as that of the Nd:YAG pulses. If the intrinsic damage field was the same at both ruby and Nd:YAG wavelengths, then the input energy was three times greater at 0.69 μm. Since damage can be energy-dependent for inclusions having dimensions larger than about 0.1 μm, the difference in importance of inclusion damage may be explained. On the other hand, energy is absorbed at the same rate from both laser pulses, and it is the rate of energy deposition which is important for the smallest and presumably most frequently occurring inclusions.

Another more likely source of this difference may be the absorption characteristics of the inclusions. Previous calculations have assumed that the absorption of radiation by inclusions does not depend on frequency. For metallic inclusions, such approximations may be justified. If, on on the other hand, inclusions are composed of nonmetallic materials, then their absorption may increase strongly with frequencies in the visible, As the wavelength of the input laser light is decreased, therefore, dirt particles which did not damage at longer wavelengths become able to cause damage. Because inclusions normally determine the breakdown strength of materials, this frequency dependence of inclusion damage may be a major limitation on the use of high-power, short-wavelength, lasers.

F. TV Monitor for Laser Beam Mode

A new scheme for monitoring the laser beam mode pattern was developed following the suggestion of C.F. Luck of Raytheon's Laser Advanced Development Center. In this we take advantage of the persistence of an image in a TV vidicon tube. Thus if the tube views the laser beam, say as the beam strikes a ground glass plate, the video signal out of the TV camera will be a plot of the laser beam mode.

The envelope of horizontal traces which compose one vertical scan of the TV camera gives the mode structure in the vertical direction and a single horizontal trace gives the mode structure in the horizontal direction. Such a map of the laser pattern is shown for a TEM_{00} mode in Fig. 3 where on one trace of a dual trace oscilloscope we display the many horizontal sweeps constituting one vertical scan of the camera and on the other a single horizontal scan. Since the latter is intensified in the former, we know which horizontal section of the laser mode was monitored.

This procedure allows one to record the laser mode pattern for each pulse so that complete documentation of the experimental conditions is possible. Since TV monitoring of the laser mode was not developed until late in our program it was not generally used. We have described it here, however, because of its many potential applications.

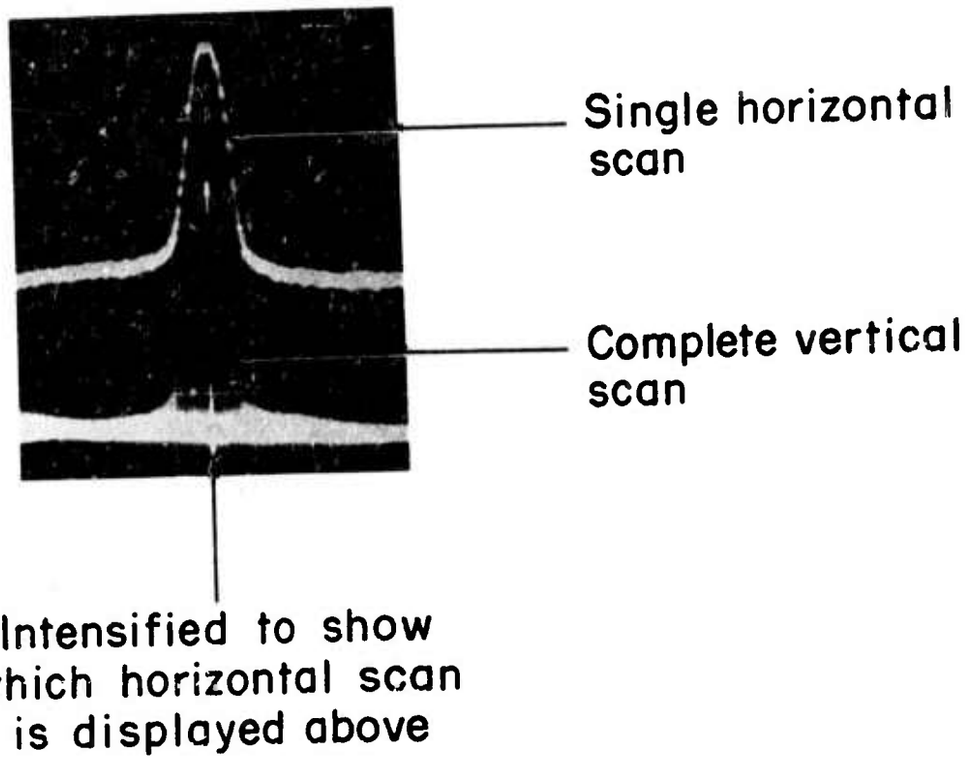

Fig. 3 TV Monitor Traces of a 1.06 μm TEM_{00} Mode Laser Beam in the Far Field.

G. References

1. M. Bass, H.H. Barrett, and L.H. Holway, Jr., Scientific Report No. 1 for Contract No. F19628-70-C-0223 (Feb. 1972).

2. R.W. Hopper and D.R. Uhlman, "Mechanisms of Inclusion Damage in Laser Glass," J. Appl. Phys. 41, 4023(Sept. 1970).

IX. CONCLUSIONS

The objective of this program was to find out how and why permanent damage is produced in transparent media by intense light beams. If possible means to minimize or avoid the deleterious effects of such damage on laser system performance were to be identified.

During the first part of the work (see Scientific Report No. 1) the importance of the laser's transverse mode, the focusing conditions and the pulse waveform in determining both the morphology of the residual damage and the dynamics of damage formation was demonstrated. The statistical nature of the intrinsic damage process was identified and a model for the damaging interaction based on an electron avalanche breakdown with statistical starting properties was suggested.

The major results obtained during the last year's effort are summarized below:

1. The first unambiguous comparison of laser damage induced at 0.69 μm and at 1.06 μm showed that in general it is harder to produce intrinsic damage at 0.69 μm. On the other hand, damage due to absorbing inclusions is more of a problem at 0.69 μm than it is at 1.06 μm. This suggests that the presence of absorbing inclusions will severely limit the performance of optical materials at short wavelengths.

2. The statistical nature of both bulk and surface intrinsic damage was demonstrated. When the surface is free of polishing imperfections it damages with the same probability as the bulk when exposed to the same field. A conventionally finished surface breaks down more easily then the bulk.

3. The damage field (i.e., the field which resulted in a damage probability of 0.5) at different wavelengths and at dc were compared for several alkali-halide crystals. These comparisons showed that the damage process is an electron avalanche breakdown essentially in its dc limit up to 1.06 μm. At 0.69 μm the first signs of a dependence of damage field on the field frequency were noted.

4. Measurements of the distributions of breakdown starting times for both surface and bulk intrinsic breakdown supported the statistical intepretation of the damage process. Computations of these distributions based on the statistical-electron avalanche breakdown model were found to be consistent with the experimental data.

5. Experimental techniques for avoiding self-focusing in damage experiments and for identifying the occurrence of an intrinsic damage event were developed. As part of a discussion of the compatibility of the probabilistic and threshold-like points of view we showed how certain experimental procedures can lead one to conclude erroniously that a well-defined damage threshold exists.

6. A Fokker-Planck equation in energy space was used to calculate the rate of avalanche growth and thus estimate the damage field. The results for sapphire are in better agreement with experiment than those obtained using "average electron" theories.

A SIMPLE TECHNIQUE FOR LONGITUDINAL MODE SELECTION*

D. Bua, D. Fradin+ and M. Bass
Raytheon Research Division
Waltham, Massachusetts 02154

ABSTRACT

Single longitudinal mode operation of pulse pumped Q-switched Nd:YAG and ruby lasers has been achieved by providing an intracavity mode selecting resonator which contains the laser's active medium.

* This research was supported by the Advanced Research Projects Agency of the Department of Defense and was monitored by the Air Force Cambridge Research Laboratories under Contract No. F19628-70-C-0223.

+ Also at Harvard University, Div. of Engineering and Applied Physics, Cambridge, Mass.

Temporally smooth Q-switched laser pulses are desirable for a number of scientific applications, particularly in nonlinear optics. Smooth pulse operation is most often obtained by restricting the lasing bandwidth to a single longitudinal mode through use of a spectrum narrowing device such as a tilted intracavity etalon or a resonant reflector output coupler.[1]

We have developed a particularly simple technique for mode selection which does not require any special optical cavity components. The technique consists of aligning the front surface of a plane cut laser rod parallel to the 100 percent reflecting mirror. Fig. 1 indicates the resulting intracavity resonator M_1-A. The anti-reflection coating on each end of the laser rod has a residual reflectivity of about 0.25 percent and so the passive finesse of resonator M_1-A is very low. When lasing occurs, however, M_1-A contains a medium with gain and its effective finesse can be very high. In our ruby laser with a 10 cm rod, for example, the combination of a 0.25 percent reflection surface, A, a laser gain coefficient of $\approx 0.25\ cm^{-1}$, and the 99.9 percent cavity reflector, M_1, results in a steady-state reflectivity finesse of about 6. All other intracavity elements are placed between surfaces A and M_2 to minimize reflection and scattering losses in the subcavity M_1-A.

In figures 2 and 3 the effects of rod alignment on the temporal outputs of a Nd:YAG and a ruby laser are illustrated as measured by a photodiode-oscilloscope combination having a measured risetime of 0.5 nsec. These lasers were used in optical damage studies [2,3]. For the ruby laser, additional mode selection was achieved by using a single sapphire etalon as the output mirror, M_2.

The detection of a smooth pulse by a limited bandwidth detector may be the result of either single-frequency output or the simultaneous oscillation of many randomly phased modes. In order to resolve this question the laser's output spectra were studied with a Fabry-Perot interferometer. The

lasing bandwidth narrowed significantly as the rod was aligned to achieve smoother pulses. Unfortunately, our interferometers lacked sufficient finesse to resolve individual laser cavity modes ($\Delta\nu \approx 300$ MHz). The longitudinal mode content of a perfectly smooth laser pulse can be inferred, however, by combining the interferometer and pulse waveform data. The observed interferometer limited bandwidth of a smooth ruby laser pulse was ≈ 1.2 GHz, implying that a maximum of 4 adjacent modes could have been oscillating. Since the photodiode-oscilloscope combination could detect frequencies as high as ~ 3 GHz, the presence of four adjacent oscillating modes would have been detected through the observation of mode beating as in Fig. 3b. Therefore, our smooth ruby laser pulses, as shown in Fig. 3c, were caused by single longitudinal mode lasing. In support of this conclusion we note that Giuliano et al. [4] reported that perfectly smooth pulses correspond to single mode oscillation while non-smooth waveforms were always associated with two or more oscillating modes. Replacing the sapphire etalon with a wedged output mirror did not qualitatively change the results.

We have found that slight misalignment of a multi-component resonant reflector or of one which employs high reflectivity mirrors often causes transverse mode distortion. The simple technique for obtaining smooth pulses described above does not have this problem and is quite compatible with TEM_{00} mode operation.

When the product of the double-pass gain and the output reflector is less than about 40 percent, it is no longer possible to operate the laser in a single longitudinal mode. A simple modification of the present technique is to misalign the rod and to insert a coated optical flat parallel to the cavity mirrors. One surface of the flat functions as the rod face M_1 above, and its reflectivity can be chosen to be high enough to give high mode discrimination while still low enough so that there is no lasing from that surface. This configuration is identical in basic form to conventional resonant reflectors except that the first surface has a low reflectivity to minimize degradation of the transverse structure. As in the previous technique, mode discrimination is achieved by providing a subcavity containing an active medium.

In summary, we have found that the alignment of a plane-cut anti-reflection coated laser rod parallel to the output mirrors creates an intracavity resonator with sufficient finesse to restrict the laser output to a single longitudinal mode.

References

1. D. A. Kleinman and P. P. Kisliuk, "Discrimination Against Unwanted Orders in the Fabry-Perot Resonator," Bell Sys. Tech. J. 41, 453 (1962).

2. M. Bass and H. H. Barrett, "Avalanche Breakdown and the Probabilistic Nature of Laser-Induced Damage," QE-8, 338 (1972).

3. D. W. Fradin, E. Yablonovitch, and M. Bass, "Comparison of Laser Induced Bulk Damage in Alkali Halides," 4th ASTM-NBS Symposium on Damage in Laser Materials (1972).

4. C. R. Guiliano, R. W. Hellwarth, L. D. Hess, and G. R. Rickel, "Damage Threshold Studies in Laser Crystals," Semiannual Report No. 2 for Contract No. F19628-69-C-0277 (July 1970).

Figure Captions

Fig. 1 Schematic Diagram of a Laser Cavity Showing Mode Selecting Intracavity Resonator

Fig. 2 Effect of Rod Alignment on Output Pulses for Q-Switched YAG:Nd^{+3}

(a) Rod misaligned
(b) Four successive shots with rod aligned

Fig. 3 Effects of Rod Alignment on Output Pulses for Q-Switched Ruby

(a) Rod badly misaligned
(b) Rod coarsely aligned
(c) Cavity finely tuned

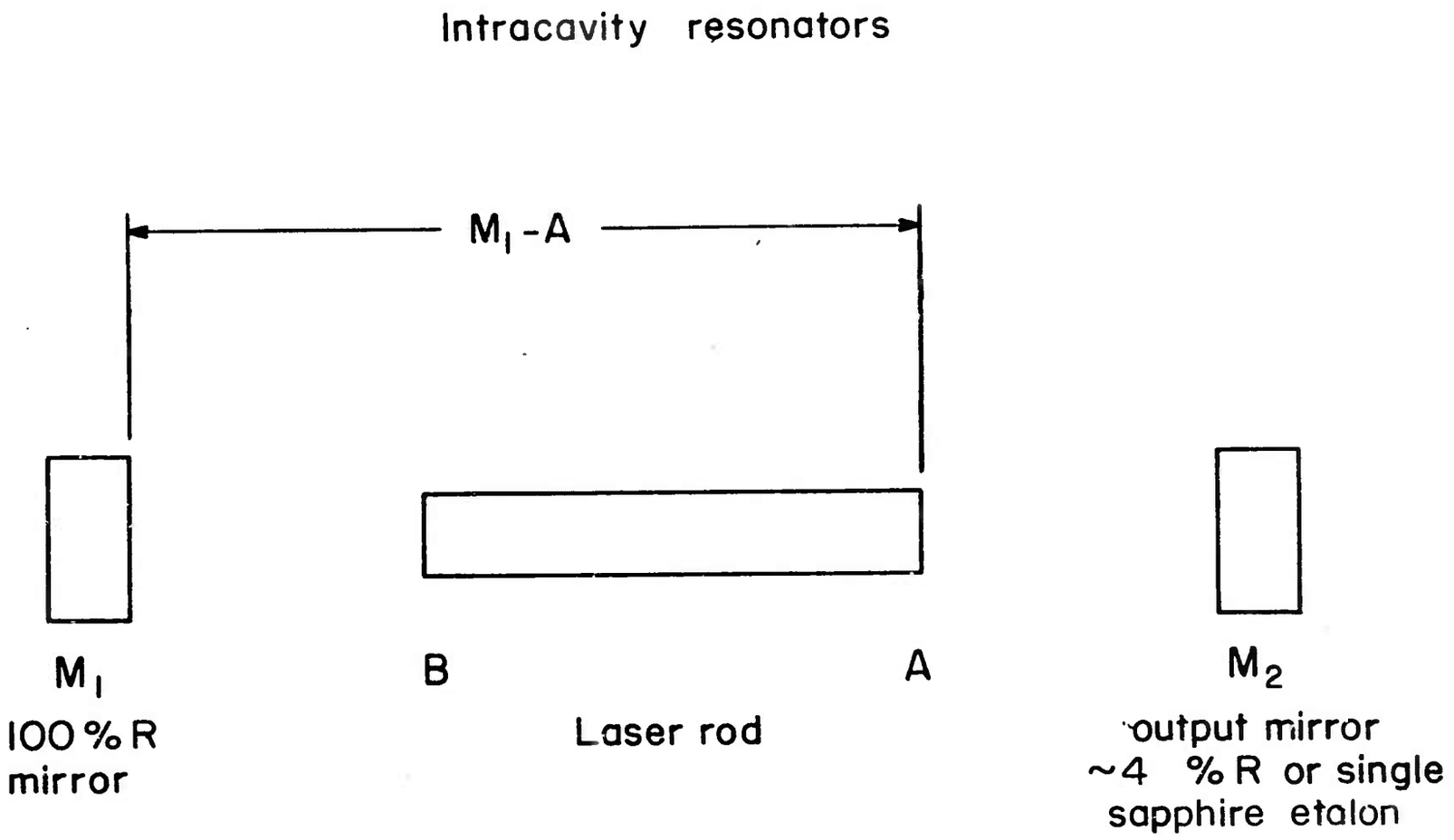

Fig. 1 Schematic Diagram of a Laser Cavity Showing Mode Selecting Intracavity Resonator.

(a)

(b)

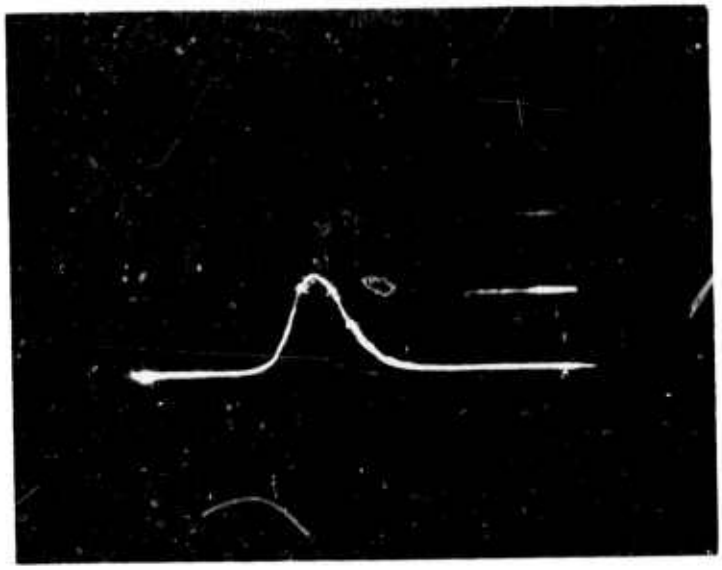

5 ns

Fig. 2 Effect of Rod Alignment on Output Pulses for Q-Switched YAG:Nd^{+3}.
(a) Rod misaligned
(b) Four successive shots with rod aligned

(a)

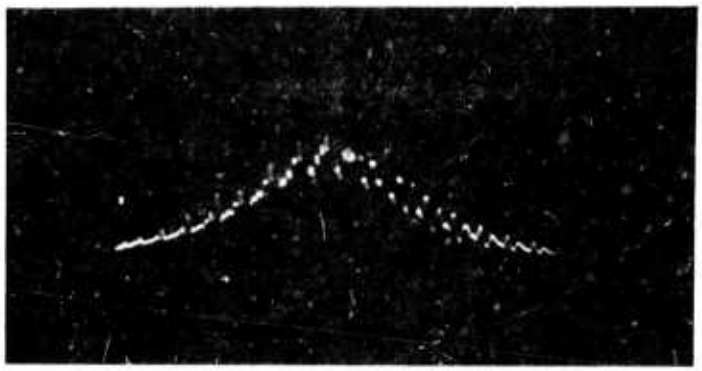

(b)

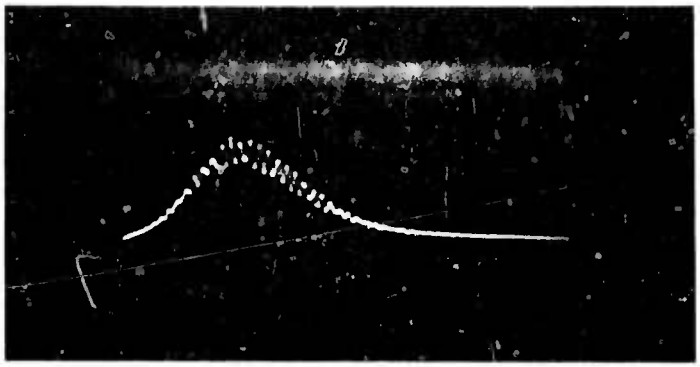

(c)

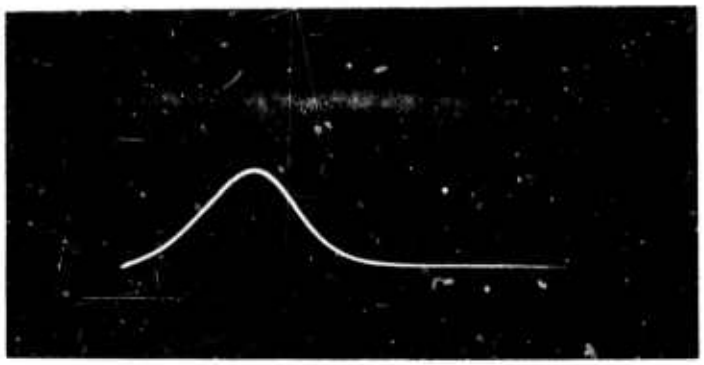

10 ns

Fig. 3 Effects of Rod Alignment on Output Pulses for Q-Switched Ruby.
(a) Rod badly misaligned
(b) Rod coarsely aligned
(c) Cavity finely tuned